



Transportation Consortium of South-Central States

*Solving Emerging Transportation Resiliency, Sustainability, and Economic Challenges through the Use of Innovative Materials and Construction Methods: From Research to Implementation*

# Evaluation of Alternative Sources of Supplementary Cementitious Materials (SCMs) for Concrete Materials in Transportation Infrastructure

---

Project No. 20CLSU07

Lead University: Louisiana State University

**Final Report**

**September 2021**

### **Disclaimer**

The contents of this report reflect the views of the authors, who are responsible for the facts and the accuracy of the information presented herein. This document is disseminated in the interest of information exchange. The report is funded, partially or entirely, by a grant from the U.S. Department of Transportation's University Transportation Centers Program. However, the U.S. Government assumes no liability for the contents or use thereof.

### **Acknowledgements**

The authors would like to acknowledge the financial support for this study by the Transportation Consortium of South-Central States (Tran-SET) and the Louisiana Transportation Research Center (LTRC). The authors also acknowledge the assistance of NEAR Ready Mix Concrete for providing raw materials for this study.

## TECHNICAL DOCUMENTATION PAGE

<b>1. Project No.</b> 20CLSU07	<b>2. Government Accession No.</b>	<b>3. Recipient's Catalog No.</b>	
<b>4. Title and Subtitle</b>  Evaluation of Alternative Sources of Supplementary Cementitious Materials (SCMs) for Concrete Materials in Transportation Infrastructure		<b>5. Report Date</b> Sept. 2021	
<b>7. Author(s)</b> PI: Gabriel A. Arce <a href="https://orcid.org/0000-0002-3610-8238">https://orcid.org/0000-0002-3610-8238</a> PI: Miladin Radovic <a href="https://orcid.org/0000-003-4571-2848">https://orcid.org/0000-003-4571-2848</a> PI: Zahid Hossain <a href="https://orcid.org/0000-003-3395-564X">https://orcid.org/0000-003-3395-564X</a> Co-PI: Marwa M. Hassan <a href="https://orcid.org/0000-0001-8087-8232">https://orcid.org/0000-0001-8087-8232</a> GRA: Sujata Subedi; GRA: Oscar Huang; GRA: Raiyan Chowdhury		<b>6. Performing Organization Code</b>	
<b>9. Performing Organization Name and Address</b> Transportation Consortium of South-Central States (Tran-SET) University Transportation Center for Region 6 3319 Patrick F. Taylor Hall, LSU, Baton Rouge, LA 70803		<b>8. Performing Organization Report No.</b>	
<b>12. Sponsoring Agency Name and Address</b> United States of America, Department of Transportation, Research and Innovative Technology Administration		<b>10. Work Unit No. (TR AIS)</b>	
<b>15. Supplementary Notes</b> Report uploaded and accessible at Tran-SET's website ( <a href="http://transet.lsu.edu/">http://transet.lsu.edu/</a> ).		<b>11. Contract or Grant No.</b> 69A3551747106	
<b>16. Abstract</b> <p>Fly ash is the most utilized supplementary cementitious material (SCM) in the US. Nonetheless, rapid decline in coal-fired power generation threatens its supply. The objective of this study was to evaluate alternative SCMs for concrete transportation infrastructure in Region 6. SCMs investigated included reclaimed fly ash (RFA), reclaimed ground bottom ash (GBA), metakaolin (MK), and conventional Class F fly ash (FA) as a reference. SCMs were characterized and the fresh and hardened properties of concrete incorporating different dosages (i.e., 10, 20, and 30% cement replacement by mass) of the individual SCMs (i.e., binary systems) and blended SCM systems of RFA-MK and GBA-MK (i.e., ternary systems) were assessed. All the coal ashes met the requirements for pozzolanic component, CaO, SO<sub>3</sub>, moisture content, LOI, SAI, and water requirement to be classified as Class F pozzolan according to ASTM C618. MK met all the but the water requirement. Concrete using FA generally exhibited better workability than the control mixture (i.e., without SCMs), whereas concrete incorporating RFA, GBA, and MK presented decrements in workability. Mixtures implementing ternary systems also displayed decrements in workability. Air content of fresh concrete mixtures incorporating binary and ternary systems generally decreased. Relative to the control mixture, decrements in 28-day compressive strength (f'c) were reported when incorporating FA and RFA, yet this was generally not the case for the 90-day f'c. In the case of GBA mixtures, significant differences in f'c were not observed after 28 days nor 90 days. MK mixtures as well as RFA-MK and GBA-MK mixtures generally presented increments in 28-day and 90-day f'c. Concrete mixtures implementing coal ashes did not produce significant differences in 28-day surface resistivity (SR) at any cement replacement levels; yet after 90 days of curing, significant improvements in SR were reported. MK, RFA-MK, and GBA-MK mixtures exhibited significant increments in SR at all dosages after 28 and 90 days of curing. Notably, while the control mixture and mixtures incorporating coal ashes did not meet the 28-day SR requirement for class A1 concrete according to LaDOTD, mixtures implementing MK and ternary systems did in almost all cases. All SCMs were effective at reducing drying shrinkage. Binary systems reduced drying shrinkage by 24.2-69.1%, whereas ternary systems reduced drying shrinkage by 55.2-75.3%. With regards ASR, mixtures implementing SCMs presented significantly lower expansion and the increment in SCMs content further reduced the expansion; thus, signaling a positive effect in suppressing ASR related expansion, specially at high dosages.</p>		<b>13. Type of Report and Period Covered</b> Final Research Report: Aug. 2020 – Nov. 2021	
<b>17. Key Words</b> Concrete, Durability, Supplementary Cementitious Materials, Fly ash, Reclaimed fly ash, Bottom Ash		<b>14. Sponsoring Agency Code</b>	
<b>18. Distribution Statement</b> No restrictions. This document is available through the National Technical Information Service, Springfield, VA 22161.		<b>19. Security Classif. (of this report)</b> Unclassified	
<b>20. Security Classif. (of this page)</b> Unclassified		<b>21. No. of Pages</b> 74	<b>22. Price</b>

# SI\* (MODERN METRIC) CONVERSION FACTORS

## APPROXIMATE CONVERSIONS TO SI UNITS

Symbol	When You Know	Multiply By	To Find	Symbol
<b>LENGTH</b>				
in	inches	25.4	millimeters	mm
ft	feet	0.305	meters	m
yd	yards	0.914	meters	m
mi	miles	1.61	kilometers	km
<b>AREA</b>				
in <sup>2</sup>	square inches	645.2	square millimeters	mm <sup>2</sup>
ft <sup>2</sup>	square feet	0.093	square meters	m <sup>2</sup>
yd <sup>2</sup>	square yard	0.836	square meters	m <sup>2</sup>
ac	acres	0.405	hectares	ha
mi <sup>2</sup>	square miles	2.59	square kilometers	km <sup>2</sup>
<b>VOLUME</b>				
fl oz	fluid ounces	29.57	milliliters	mL
gal	gallons	3.785	liters	L
ft <sup>3</sup>	cubic feet	0.028	cubic meters	m <sup>3</sup>
yd <sup>3</sup>	cubic yards	0.765	cubic meters	m <sup>3</sup>
NOTE: volumes greater than 1000 L shall be shown in m <sup>3</sup>				
<b>MASS</b>				
oz	ounces	28.35	grams	g
lb	pounds	0.454	kilograms	kg
T	short tons (2000 lb)	0.907	megagrams (or "metric ton")	Mg (or "t")
<b>TEMPERATURE (exact degrees)</b>				
°F	Fahrenheit	5 (F-32)/9 or (F-32)/1.8	Celsius	°C
<b>ILLUMINATION</b>				
fc	foot-candles	10.76	lux	lx
fl	foot-Lamberts	3.426	candela/m <sup>2</sup>	cd/m <sup>2</sup>
<b>FORCE and PRESSURE or STRESS</b>				
lbf	poundforce	4.45	newtons	N
lbf/in <sup>2</sup>	poundforce per square inch	6.89	kilopascals	kPa

## APPROXIMATE CONVERSIONS FROM SI UNITS

Symbol	When You Know	Multiply By	To Find	Symbol
<b>LENGTH</b>				
mm	millimeters	0.039	inches	in
m	meters	3.28	feet	ft
m	meters	1.09	yards	yd
km	kilometers	0.621	miles	mi
<b>AREA</b>				
mm <sup>2</sup>	square millimeters	0.0016	square inches	in <sup>2</sup>
m <sup>2</sup>	square meters	10.764	square feet	ft <sup>2</sup>
m <sup>2</sup>	square meters	1.195	square yards	yd <sup>2</sup>
ha	hectares	2.47	acres	ac
km <sup>2</sup>	square kilometers	0.386	square miles	mi <sup>2</sup>
<b>VOLUME</b>				
mL	milliliters	0.034	fluid ounces	fl oz
L	liters	0.264	gallons	gal
m <sup>3</sup>	cubic meters	35.314	cubic feet	ft <sup>3</sup>
m <sup>3</sup>	cubic meters	1.307	cubic yards	yd <sup>3</sup>
<b>MASS</b>				
g	grams	0.035	ounces	oz
kg	kilograms	2.202	pounds	lb
Mg (or "t")	megagrams (or "metric ton")	1.103	short tons (2000 lb)	T
<b>TEMPERATURE (exact degrees)</b>				
°C	Celsius	1.8C+32	Fahrenheit	°F
<b>ILLUMINATION</b>				
lx	lux	0.0929	foot-candles	fc
cd/m <sup>2</sup>	candela/m <sup>2</sup>	0.2919	foot-Lamberts	fl
<b>FORCE and PRESSURE or STRESS</b>				
N	newtons	0.225	poundforce	lbf
kPa	kilopascals	0.145	poundforce per square inch	lbf/in <sup>2</sup>

**TABLE OF CONTENTS**

TECHNICAL DOCUMENTATION PAGE ..... ii

LIST OF FIGURES ..... vii

LIST OF TABLES ..... x

ACRONYMS, ABBREVIATIONS, AND SYMBOLS ..... xii

1. INTRODUCTION ..... 1

2. OBJECTIVES ..... 3

3. LITERATURE REVIEW ..... 4

    3.1. Reclaimed Fly Ash (RFA) ..... 4

    3.2. Bottom Ash ..... 5

    3.3. Calcined Clays..... 6

    3.4. Influence of SCMs on Concrete Durability..... 7

        3.4.1. Shrinkage ..... 7

        3.4.2. Alkali-silica reaction (ASR) ..... 8

    3.5. Texas DOT Research on Alternative Sources of SCMs ..... 10

4. METHODOLOGY ..... 13

    4.1. Materials..... 13

        4.1.1. Alternative SCMs..... 13

        4.1.2. Cement ..... 14

        4.1.3. Aggregates ..... 14

        4.1.4. Superplasticizer and Air-Entraining Admixture ..... 14

4.2.	Characterization of Alternative SCMs .....	14
4.2.1.	Microstructure.....	14
4.2.2.	X-Ray Diffraction (XRD).....	15
4.2.3.	Chemical Composition.....	16
4.2.4.	Particle Size Analysis .....	16
4.2.5.	Moisture Content and Loss on Ignition .....	17
4.2.6.	Strength Activity Index.....	18
4.2.7.	Thermogravimetric Analysis .....	18
4.3.	Concrete Testing .....	19
4.3.1.	Mixture Proportions .....	19
4.3.2.	Specimen Preparation .....	21
4.3.3.	Compressive Strength Test .....	22
4.3.4.	Surface Resistivity .....	22
4.3.5.	Drying Shrinkage .....	23
4.3.6.	Alkali-Silica Reactivity.....	25
5.	ANALYSIS AND FINDINGS .....	27
5.1.	Characterization and Pozzolanic Activity of SCMs.....	27
5.1.1.	Microstructure.....	27
5.1.2.	X-ray Diffraction (XRD) and X-ray Fluorescence (XRF).....	29
5.1.3.	Particle Size Analysis .....	30
5.1.4.	Moisture Content (MC) and Loss on Ignition (LOI) .....	31
5.1.5.	Thermogravimetric Analysis .....	31

5.1.6.	Strength Activity Index (SAI).....	33
5.2.	Testing of SCMs Admixed Concrete Mixtures.....	36
5.2.1.	Slump .....	36
5.2.2.	Air Content and Unit Weight.....	38
5.2.3.	Compressive Strength .....	41
5.2.4.	Surface Resistivity .....	46
5.2.1.	Drying Shrinkage .....	50
5.2.2.	Alkali-Silica Reactivity.....	52
6.	CONCLUSIONS.....	54
7.	REFERENCES .....	58
APPENDIX A: STATISTICAL ANALYSIS OF CONCRETE CYLINDERS COMPRESSIVE STRENGTH (BINARY SYSTEM).....		66
APPENDIX B: STATISTICAL ANALYSIS OF CONCRETE CYLINDERS COMPRESSIVE STRENGTH (TERNARY SYSTEM) .....		68
APPENDIX C: STATISTICAL ANALYSIS OF CONCRETE CYLINDERS SURFACE RESISTIVITY (BINARY SYSTEM).....		70
APPENDIX D: STATISTICAL ANALYSIS OF CONCRETE CYLINDERS SURFACE RESISTIVITY (TERNARY SYSTEM).....		73

## LIST OF FIGURES

Figure 1. Fly ash production and consumption: (a) concrete industry consumption relative to total consumption (b) total fly ash production and consumption, and percentage of fly ash utilization from total available production [6] .....	2
Figure 2. Materials: (a) FA, (b) RFA, (c) GBA, and (d) MK .....	13
Figure 3. JEOL JSM-7500F for SEM imaging .....	15
Figure 4. Bruker-AXS D8 advanced for XRD analysis.....	16
Figure 5. Partica LA-960 for particle size analysis.....	17
Figure 6. Compressive strength testing setup for 50.8-mm (2-in) mortar cubes. ....	18
Figure 7. Q600 SDT for TGA.....	19
Figure 8. Fresh properties testing: (a) slump and (b) air content.....	21
Figure 9. Compression test setup.....	22
Figure 10. Surface resistivity setup.....	23
Figure 11. Drying shrinkage test: (a) lime-saturated water curing of the specimens, (b) taking of reading, and (c) specimens in air storage.....	24
Figure 12. ASR test: (a) crushed and sieved aggregates, (b) casting of mortar bar, (c) curing of specimen at 1N NaOH solution at 80°C .....	26
Figure 13. SEM images: a) FA at 2000x, b) FA at 5000x, (c) RFA at 2000x, (d) RFA at 5000x, (e) GBA at 2000x, (f) GBA at 5000x, (g) MK at 2000x, and (h) MK at 5000x .....	28
Figure 14. XRD spectra of SCMs.....	29
Figure 15. Particle size distribution of SCMs.....	30
Figure 16. TGA curves: (a) FA, (b) RFA, (c) GBA, and (d) MK.. <b>Error! Bookmark not defined.</b>	
Figure 17. CH consumption of SCMs.....	32
Figure 18. 7- and 28-day SAI results for binary mixtures: (a) compressive strength and (b) SAI34	



Figure 19. 7- and 28-day SAI results for ternary mixtures: (a) compressive strength and (b) SAI .....	35
Figure 20. Slump of fresh concrete mixtures (binary systems) .....	37
Figure 21. Slump of fresh concrete mixtures (ternary systems) .....	37
Figure 22. Air content for of fresh concrete mixtures (binary systems).....	39
Figure 23. Air Content of fresh concrete mixtures (ternary systems).....	39
Figure 24. Unit Weight of fresh concrete mixtures (binary systems).....	40
Figure 25. Unit Weight of fresh concrete mixtures (ternary systems).....	41
Figure 26. Compressive strength of binary concrete mixtures after 28 and 90 days: (a) FA, (b) RFA, (c) GBA, and (d) MK .....	43
Figure 27. Relative strength gain (%) of binary concrete mixtures .....	44
Figure 28. Compressive strength for ternary concrete mixtures: (a) RFA-MK, (b) GBA-MK, and (c) Relative strength gain .....	45
Figure 29. 28- and 90-day surface resistivity of binary concrete mixtures: (a) FA, (b) RFA, (c) GBA, and (d) MK .....	47
Figure 30. Relative SR Gain (%) of binary concrete mixtures .....	48
Figure 31. Surface resistivity of ternary concrete mixtures: (a) RFA and MK, (b) GBA and MK, and (c) relative surface resistivity gain .....	49
Figure 32. Drying shrinkage of binary concrete mixtures: (a) FA, (b) RFA, (c) GBA, and (d) MK .....	51
Figure 33. Drying shrinkage of ternary concrete mixtures: (a) RFA and MK, and (b) GBA and MK .....	52
Figure 34. ASR with sandstone for binary mortar mixtures: (a) FA, (b) RFA, (c) GBA, and (d) MK .....	53
Figure 35. ASR with sandstone for ternary mortar mixtures: (a) RFA and MK, and (b) GBA and MK .....	53

Figure A1. Binary concrete mixtures cylinders 28 days compressive strength Tukey grouping for means of index ( $\alpha=0.05$ ) .....	66
Figure A2. Binary concrete mixtures cylinders 90 days compressive strength Tukey grouping for means of index ( $\alpha=0.05$ ) .....	67
Figure B1. Ternary concrete mixtures cylinders 28 days compressive strength Tukey grouping for means of index ( $\alpha=0.05$ ) .....	68
Figure B2. Ternary concrete mixtures cylinders 90 days compressive strength Tukey grouping for means of index ( $\alpha=0.05$ ) .....	69
Figure C1. Binary concrete mixtures cylinders 28 days surface resistivity Tukey grouping for means of index ( $\alpha=0.05$ ) .....	70
Figure C2. Binary concrete mixtures cylinders 90 days surface resistivity Tukey grouping for means of index ( $\alpha=0.05$ ) .....	71
Figure D1. Ternary concrete mixtures cylinders 28 days surface resistivity Tukey grouping for means of index ( $\alpha=0.05$ ) .....	73
Figure D2. Ternary concrete mixtures cylinders 90 days surface resistivity Tukey grouping for means of index ( $\alpha=0.05$ ) .....	74

## **LIST OF TABLES**

Table 1. U.S. concrete industry fly ash and GGBFS consumption.....	4
Table 2. Alternative SCMs evaluated in [64] .....	10
Table 3. Summary of SCM performance at different replacement dosages [64] .....	10
Table 4. Alternative SCMs evaluated [14] .....	11
Table 5. Summary of SCMs effect on cementitious mixture performance [14].....	12
Table 6. Chemical composition (by weight) of cement used in the study.....	14
Table 7. Binary system concrete mixture proportions.....	20
Table 8. Ternary system concrete mixture proportions. ....	21
Table 9. Chloride ion penetrability based. ....	23
Table 10. Chemical composition of SCM from XRF.....	30
Table 11. Moisture content and LOI of coal ashes and MK.....	31
Table 12. Water requirement for binary and ternary mortar mixtures.....	33
Table 13. Summary of alternative SCMs properties.....	36
Table 14. Summary of SCMs effect on concrete properties.....	57
Table A1. Binary concrete mixtures cylinders 28 days compressive strength one-way ANOVA results	66
Table A2. Binary concrete mixtures cylinders 90 days compressive strength one-way ANOVA results .....	67
Table B1. Ternary concrete mixture cylinders 28 days compressive strength one-way ANOVA results	68
Table B2. Ternary concrete mixture cylinders 90 days compressive strength one-way ANOVA results .....	69

Table C1. Binary concrete mixtures cylinders 28 days surface resistivity one-way ANOVA results.....70

Table C2. Binary concrete mixtures cylinders 90 days surface resistivity one-way ANOVA results ..... 71

Table D1. Ternary concrete mixtures cylinders 28 days surface resistivity one-way ANOVA results 73

Table D2. Ternary concrete mixtures cylinders 90 days surface resistivity one-way ANOVA results ..... 74

## **ACRONYMS, ABBREVIATIONS, AND SYMBOLS**

ANOVA	Analysis of Variance
ASR	Alkali-Silica Reactivity
ASTM	American Society for Testing and Materials
DOTD	Department of Transportation and Development
FA	Fly Ash
GBA	Ground Bottom Ash
HRWR	High Range Water Reducer
LSU	Louisiana State University
LaDOTD	Louisiana Department of Transportation and Development
LTRC	Louisiana Transportation Research Center
OPC	Ordinary Portland cement
RFA	Reclaimed Fly Ash
SAI	Strength Activity Index
SCM	Supplementary Cementitious Material
SEM	Scanning Electron Microscopy
TGA	Thermogravimetric Analysis
XRD	X-ray Diffraction
XRF	X-ray Fluorescence

## EXECUTIVE SUMMARY

In the U.S., fly ash is the most utilized supplementary cementitious material (SCM) for the manufacture of concrete due to its historical wide availability, cost-effectiveness, and beneficial effects to the fresh and hardened properties of concrete. However, the sharp decline in coal-fired power generation in recent years is jeopardizing fly ash supply. Consequently, there is an urgent need to find alternative sources of SCMs that are high-quality, cost-effective, and readily available. As a response to the expected shortage of fly ash, this study focused on evaluating the use of alternative sources of SCMs for the manufacture of concrete for transportation infrastructure in Region 6. SCMs investigated included: (1) reclaimed fly ash (RFA), (2) reclaimed ground bottom ash (GBA), (3) metakaolin (MK), and (4) conventional Class F fly ash (FA) as a reference. SCMs were comprehensively characterized to determine their microstructure, mineralogical composition, and physical and chemical properties. Characterization techniques utilized included scanning electron microscopy (SEM), X-ray fluorescence (XRF), X-ray diffraction (XRD), laser diffraction particle size analysis, and thermogravimetric analysis (TGA). Furthermore, according to ASTM C311, moisture content, loss on ignition (LOI), water requirement, and strength activity index (SAI) were evaluated. Beyond the characterization of SCMs, the fresh and hardened properties of concrete incorporating different dosages of the SCMs (i.e., 10, 20, and 30% cement replacement by mass) were studied. In addition, the feasibility of implementing blended SCM systems of unconventional coal ashes (i.e., RFA and GBA) and MK using a 70/30 coal ash to MK proportion (by mass) was evaluated. Tests conducted on concrete mixtures included slump (ASTM C143), air content (ASTM C231), compressive strength (ASTM C39), surface resistivity (AASHTO T358), drying shrinkage (ASTM C157), and alkali-silica reactivity potential (ASTM C1567).

Characterization of SCMs revealed that similar to FA, RFA consisted of mostly spherical particles whereas GBA presented a prismatic morphology with sharp edges. Furthermore, MK consisted of small plate-like particles. Among the SCMs evaluated, RFA exhibited the largest particles followed by GBA and FA, which presented similar particle size, and finally MK, which presented the smallest particles. All the SCMs presented silica ( $\text{SiO}_2$ ) and alumina ( $\text{Al}_2\text{O}_3$ ) as their main constituents, yet coal ashes did also exhibit some calcium oxide (CaO) content. RFA exhibited the lowest CaO content, whereas GBA presented the highest content. From XRD results, crystalline and amorphous phases were identified in all SCMs. Notably, MK presented the largest amorphous hump, while GBA presented the smallest one. Calcium hydroxide (CH) consumption of all SCMs exceeded the threshold to be classified as pozzolanic. Moreover, MK presented the highest CH consumption followed by RFA, GBA, and finally FA. All the coal ashes evaluated met the requirements for pozzolanic component, CaO,  $\text{SO}_3$ , moisture content, LOI, and SAI (after 7 and 28 days of curing), and water requirement to be classified as Class F pozzolan according to ASTM C618. Except for the water requirement, MK did also meet the requirements.

While concrete using FA exhibited similar or better workability than the control mixture (i.e., without SCMs), concrete implementing RFA, GBA, and MK presented a progressive decrease in slump with the increase in cement replacement. MK produced by far the greatest decrease in slump

followed by GBA and finally RFA. For mixtures implementing ternary systems (i.e., RFA-MK and GBA-MK), workability did also reduce with the increment in cement replacement, with the GBA-MK system producing the largest decrease in slump. The air content of fresh concrete mixtures incorporating SCMs decreased in almost all cases (relative to the control mixture), where RFA generally produced the lowest decrease in air content among the coal ashes, followed by FA and GBA. Mixtures implementing ternary systems did also exhibit a reduction in air content and air content decreased with the increase in cement replacement.

Relative to the control mixture, negligible decrements in 28-day compressive strength were reported when incorporating FA and RFA at 10% cement replacement, whereas statistically significant decrements were reported at 20 and 30% cement replacement. In the case of the 90-day compressive strength, concrete mixtures incorporating FA did only present statistically significant decrements in strength at 30% cement replacement, while mixtures implementing RFA presented statistically similar strengths than the control mixture at all cement replacement levels. Importantly, relative to control, mixtures incorporating GBA did not exhibit statistically significant differences in 28-day and 90-day compressive strength at any of the cement replacement levels evaluated. In contrast to the mixtures incorporating coal ashes, mixtures implementing MK exhibited statistically significant increments in compressive strength after 28 and 90 days of curing at all cement replacement levels evaluated (excepting MK-10 after 90 days of curing) and strength increased with increments in MK content. For concrete mixtures implementing ternary systems, the 28-day compressive strength generally improved with the increase in cement replacement level. Nonetheless, a statistically significant difference in 28-day compressive strength was only encountered at 20% cement replacement for RFA-MK mixtures, whereas for GBA-MK mixtures, improvements in strength were statistically significant at all cement replacement levels evaluated. After 90 of curing, statistically significant differences in compressive strength were not encountered for ternary mixtures relative to the control mixture.

Concrete mixtures implementing coal ashes did not produce statistically significant differences in 28-day surface resistivity (compared to the control mixture) at any of the cement replacement levels evaluated. Furthermore, neither the control mixture nor mixtures implementing coal ashes met the minimum 28-day surface resistivity requirement for class A1 concrete according to LaDOTD (i.e.,  $>22 \text{ k}\Omega\text{-cm}$ ). Notwithstanding, after 90-days of curing, mixtures implementing coal ashes produced statistically significant improvements in surface resistivity relative to control (excepting FA-10 and RFA-10), and the surface resistivity increased with the increase in coal ash content. Mixtures incorporating MK exhibited statistically significant increments in surface resistivity at all cement replacement levels after 28 and 90 days of curing (relative to the control mixture and mixtures implementing coal ashes); and increments in MK dosage improved both the 28-day and 90-day surface resistivity. Importantly, all mixtures incorporating MK exceeded LaDOTD's minimum surface resistivity requirement of  $22 \text{ k}\Omega\text{-cm}$  after 28 days of curing. For mixtures incorporating ternary systems, statistically significant improvements in surface resistivity relative to the control mixture were also observed after 28 and 90 days of curing at all cement replacement levels and surface resistivity improved with the increase in cement replacement.

Notably, while mixtures incorporating coal ashes did not meet minimum surface resistivity requirement of 22 k $\Omega$ -cm after 28 days of curing according to LaDOTD, mixtures implementing ternary systems did (excepting the RFA-MK mixture at 10% cement replacement level).

Relative to the control mixture, all SCMs evaluated were effective at reducing drying shrinkage. Binary systems reduced drying shrinkage by 24.2-69.1%, whereas ternary systems reduced drying shrinkage by 55.2-75.3%. Regarding ASR, mortar mixtures implementing SCMs presented significantly lower expansion than the control mixture and the increment in the dosage of SCMs further reduced the expansion. These findings suggest that the incorporation of the SCMs evaluated may be effective in suppressing ASR related expansion, specially at high dosages. Nonetheless, after 16 days, all mortar mixtures evaluated including the control mixture exhibited lower expansion than the maximum limit according to ASTM C1567.

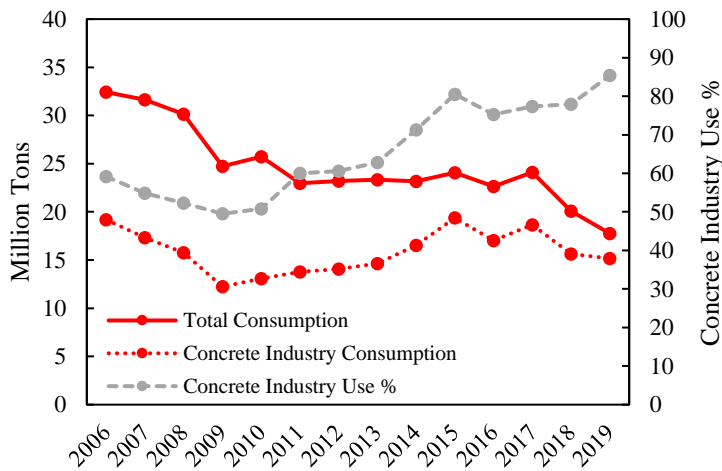
Based on the findings of this study, any of the evaluated SCMs (i.e., binary systems) and coal ash-MK combined SCM systems (i.e., ternary systems) provides a promising source of alternative SCMs. Generally, 20% of cement (by mass) can be replaced in concrete mixtures with RFA and GBA, and 30% of cement can be replaced with MK or a combination of RFA-MK and GBA-MK without compromising their long-term mechanical and durability properties. Nonetheless, it is relevant to mention that slight adjustments in mixture design and/or admixture dosage may be necessary to meet specified performance depending on the SCM and dosage selected. Furthermore, it is important to notice that while the alternative SCMs evaluated in this study generally presented a satisfactory performance, the source and processing of these SCMs can have significant effects on their properties. Consequently, verification of SCMs' performance should be conducted on a supplier and source basis prior to implementation in concrete mixtures. The use of the alternative sources of SCMs evaluated in concrete mixtures provides environmental benefits due to lower cement consumption (i.e., an overall reduction of CO<sub>2</sub> emission). In addition, the use of RFA and GBA also solves the challenges attributed to their disposal.



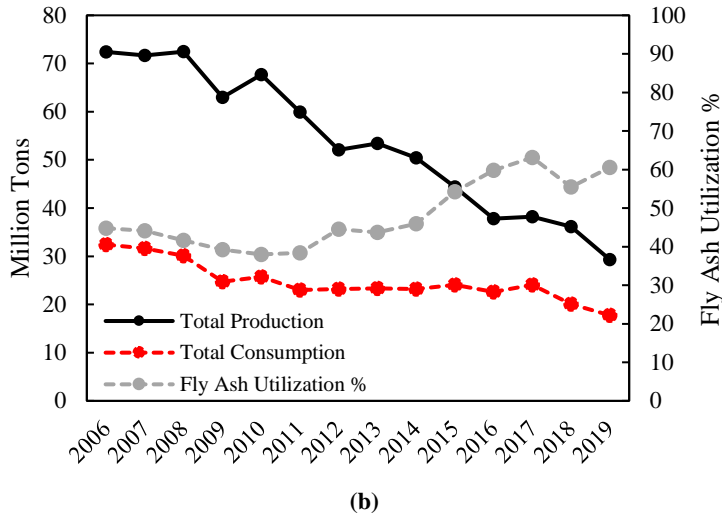
# 1. INTRODUCTION

Rapid urbanization and construction of structures have a significant impact on natural resources, which affect the natural ecosystem adversely. In recent years, the overall construction cost of a project has been increased due to the huge demand for raw materials. After the 2008 recession, the utilization of cement in the United States has increased steadily and reached approximately 102 million metric tons in 2020 [1]. The prices of cement in the U.S. have also been increased as well in recent years, and in the same year, it reached 124 U.S. dollars per metric ton. [1]. To improve this condition, modern sustainable construction technologies and materials have been evolved. Thus, supplementary cementitious materials (SCMs) have been included in the cement and concrete industry. ASTM International had defined an SCM as an inorganic material that influences the properties of a cementitious mixture by its hydraulic or pozzolanic activity, or both [2].

Fly ash from coal-burning power production is the most widely utilized SCM in the US. Its implementation enhances the durability and long-term mechanical properties of concrete while reducing its carbon footprint. Furthermore, fly ash has proven effective to improve workability, reduce bleeding, improve pumpability, and mitigate alkali-silica reactivity in concrete materials [3,4]. While the implementation of fly ash as a partial cement replacement in concrete has become a common practice in the US, the increasing demand for this resource by the concrete industry (Figure 1a) combined with the decline in coal-fired power generation and stricter environmental regulations has led to complications in finding high quality and economical fly ash [3]. In fact, in a recent AASHTO survey (including the participation of 46 State DOTs), 80% of respondents indicated issues with fly ash supply [5].



(a)



(b)  
**Figure 1. Fly ash production and consumption: (a) concrete industry consumption relative to total consumption (b) total fly ash production and consumption, and percentage of fly ash utilization from total available production [6]**

While the energy produced from coal-burning power plants has reduced sharply over the past decade, coal remains an important source of energy in the US, with 28% of US electricity being produced from this resource [7]. Based on the most recent Coal Combustion Product (CCP) Production & Use Survey Report from the American Coal Ash Association (ACAA), in 2019, the amount of fly ash produced in the US was 29.3 million tons while only 17.8 million tons (i.e., about 60.8%) were utilized (as shown in Figure 1b). Furthermore, from the 17.8 million tons of fly ash utilized, 15.2 million tons were consumed by the concrete and cement industries (i.e., 85.4%). It is important to notice that a significant amount of fly ash produced is currently not being utilized (i.e., 39.2%). This is mainly attributed to market disparities (e.g., excessive seasonal supply) and logistical challenges (e.g., storage space constrains); however, the utilization of fly ash is growing rapidly as shown in Figure 1b [3]. Furthermore, electricity generated from coal is expected to decline in the coming years (e.g., due to lower natural gas prices and declining costs of renewable electricity generation) to approximately 17% of the total US energy by 2050 [4]. In the case of fly ash consumption, according to a study conducted by the American Road & Transportation Builders Association (ARTBA), the expected fly ash demand in the year 2033 will be approximately 35.7 million tons (i.e., ~101% increase from 2019 levels); thus, exceeding 2019 total fly ash supply [8]. As such, the long-term supply of fly ash is a serious challenge for the future of concrete materials in the US and must be urgently addressed.

As a response to the expected shortage of fly ash, the main objective of this project was to evaluate the much-needed alternative sources of SCMs, which can include unconventional coal ash products (i.e., reclaimed fly ash and ground bottom ash), natural pozzolans, and calcined clays to provide with high-quality, cost-effective, and readily available SCM alternatives for the future of concrete production in Region 6.

## 2. OBJECTIVES

The objective of this study was to evaluate the use of alternative sources of SCMs for the manufacture of concrete for transportation infrastructure in Region 6. SCMs evaluated included (1) reclaimed fly ash (RFA), (2) reclaimed ground bottom ash (GBA), (3) metakaolin (MK), and (4) conventional Class F fly ash (FA) as a reference. Furthermore, this study also evaluated the feasibility of using blended system of unconventional coal ashes (i.e., RFA and GBA) and MK (i.e., ternary systems) as SCMs for concrete mixtures. Specific technical objectives are as follows:

- Characterize and evaluate the pozzolanic activity of the different SCMs
- Evaluate the effect of individual SCMs and blended SCM systems on the fresh and hardened properties of concrete.
- Evaluate the effect of SCMs and blended SCM systems on concrete's dimensional stability and ability to mitigate alkali-silica reaction (ASR).

### 3. LITERATURE REVIEW

Supplementary cementitious materials (SCMs) are widely used in concrete to partially replace clinker in cement (i.e., blended cement) or to partially replace cement in concrete (at the ready mix concrete plant) [9–11]. Since the clinker process is highly energy-intensive, the use of SCMs significantly reduces CO<sub>2</sub> emissions associated with concrete production by reducing the amount of clinker utilized [10]. SCMs can exhibit hydraulic (i.e., cementitious) and pozzolanic characteristics based on their composition [12]. SCMs with hydraulic properties (e.g., ground granulated blast furnace slag, i.e., GGBFS and Class C fly ash) can set and harden in contact with water through a hydration reaction; yet, its hydraulic activity is usually low compared to that of Portland cement [12]. On the other hand, pozzolanic SCMs (e.g., natural pozzolans, silica fume, and Class F fly ash) are siliceous or siliceous and aluminous materials that when admixed with water exhibit little or no cementitious activity; yet, in the presence of water and calcium hydroxide form compounds with cementitious properties [12].

SCMs can be classified into two broad groups, SCMs of natural origin and artificial SCMs [12]. Natural SCMs are pyroclastic rocks or sedimentary rocks with high silica content, such as pumice or diatomaceous earth, respectively [12]. Conversely, artificial SCMs are man-made materials that have been purposely manufactured (e.g., metakaolin from thermal activation of kaolin-clays) or formed as waste or by-products of high-temperature processes (e.g., GGBFS, fly ash, and silica fume) [12]. In the U.S., fly ash and GGBFS are the most utilized SCMs, with fly ash being largely the most utilized, as shown in Table 1. However, as the cement demand increases and the supply of widely used SCMs such as fly ash shrinks, concerns about SCMs availability are rising and encouraging the search for alternative sources of these materials [11]. Recently, unconventional sources of fly ash such as reclaimed fly ash (RFA) from landfills and calcined clays have been proposed as promising alternative sources of SCMs.

**Table 1. U.S. concrete industry fly ash and GGBFS consumption**

Year	Fly Ash [6] (Million Tons)	GGBFS [13] (Million Tons)
2015	24.1	2.7
2016	22.6	3.0
2017	24.1	3.4
2018	20.1	3.8

#### 3.1. Reclaimed Fly Ash (RFA)

Due to market disparities (e.g., excessive seasonal supply) and logistical challenges (e.g., storage space constraints) or failure to meet ASTM C 618, every year, significant amounts of fly ash (as shown in Figure 1b) are not utilized; and consequently, they are disposed of in landfills and surface impoundments [3,14]. When fly ash is ponded, it is mixed with water to form a slurry and pumped into ponds where it naturally settles [15]. Logistically, the utilization of impounded fly ash in concrete is challenging due to the necessity of significant processing [3,15]. However, it is important to mention that there is significant pressure to end fly ash impoundment due to concerns of groundwater contamination and possibly catastrophic failure of this type of storage, such as the dam failure at the Kingston power plant in Tennessee in 2008 [14]. As such, fly ash disposal in

landfills instead of ponds is expected to increase significantly. In contrast to impounded fly ash, landfill stored ash typically contain low amounts of moisture (i.e., 10 to 20% moisture content) which is added for optimum compaction and dust containment [15]. For its beneficial use in concrete, landfill fly ash can be dried and classified or further processed to meet specifications [3].

Recent studies have demonstrated that reclaimed fly ash (RFA) can perform similarly to production-grade Class F fly ash [3,15]. This is the case since landfill and surface impoundment environment do not provide with highly alkaline conditions required for the reaction of these ashes; and consequently, these remain pozzolanic [3,16]. However, to date, RFA has predominately been used for highway base material, subbase and subgrade stabilization, structural fill under Portland cement concrete (PCC), and railroad sub-ballast over soils [15,17,18].

### **3.2. Bottom Ash**

The combustion of pulverized coal produces two different kinds of ashes, namely, fly ash and bottom ash. Fly ash is the fine ash that exits the boiler suspended in the flue gas, whereas bottom ash is the coarse ash that settles at the bottom of the boiler [19,20]. In 2019, the annual production of fly ash in the US was 29.3 million tons, whereas the production of bottom ash was nearly 9.2 million tons [6]. Nonetheless, while the production of fly ash was approximately three times that of bottom ash, about 60.6% of the fly ash was utilized, whereas only 32.0% of the bottom ash found useful applications [6]. Consequently, nearly 11.5 million tons of fly ash and 6.3 million tons of bottom ash had to be disposed of in landfills or surface impoundments in 2019 alone. While fly ash is mainly consumed by the concrete and cement industry (i.e., representing about 85.4% of the total consumption), only about 42.7% of the utilized bottom ash is used by the concrete and cement industry [6]. Conversely, most of the bottom ash consumption comes from other applications, including structural fills/embankments, soil stabilization, blasting grit, roofing granules, and road base/subbase [6].

The particle size distribution of bottom ash typically ranges from 0.075 mm to 10 mm (i.e., comparable with natural sand), and its main constituents are silica, iron oxide, and alumina [21,22]. Even though bottom ash consists of large amounts of pozzolanic components (i.e.,  $\text{SiO}_2$ ,  $\text{Al}_2\text{O}_3$ ,  $\text{Fe}_2\text{O}_3$ ), it cannot be used directly as an SCM due to their coarse particles, high porosity compared to fly ash, and high carbon content [23]. While many studies have investigated the influence of bottom ash on concrete properties when used as a partial or complete replacement to fine aggregate [24–31], limited studies have investigated the feasibility of using bottom ash as SCMs [20,21,32–35]. Different studies showed that the replacement of fine aggregate with bottom ash is feasible and that it can produce concrete with similar or higher strength than conventional concrete [26,30,31]. The primary benefit of using bottom ash as fine aggregate is the density reduction of the concrete (due to bottom ash low specific gravity), reduction in cost, and reduction in the environmental impact (by using a waste product) [36,37]. Different studies have investigated the possibility of using coal bottom ash as an SCM in concrete mixtures [20,23,32–34]. These concluded that, when processed by grinding to a particle size similar to that of fly ash, bottom ash exhibits SCM quality and can be used in concrete materials [20,23,32]. The use of ground bottom ash as SCM in concrete mixtures has two primary environmental benefits, (1) substantial reduction of greenhouse gasses emissions due to lower cement consumption, and (2) utilization of solid

waste produced from the coal-fired thermal power plants. While studies in the literature have investigated the use of production-grade bottom ash, to our knowledge, no study has evaluated the use of reclaimed bottom ash for its beneficial use in concrete. As previously mentioned, most of the bottom ash produced every year is disposed of in landfills and surface impoundments. In turn, massive amounts of potentially reclaimable bottom ash exist in the US, which is currently not been utilized. Consequently, along with RFA, this study aims to evaluate the use of GBA as an alternative source of SCMs for concrete application.

### 3.3. Calcined Clays

Thermal activation (calcination) of many clay minerals at 600-900°C in the air by dihydroxylation leads to a complete and/or partial breakdown of their crystal structure and formation of the transition phase with high reactivity. This process is well known since the 19<sup>th</sup> century and is widely used for processing aluminosilicate ceramics. A typical example of this is the calcination of kaolinite clay ( $\text{Al}_2(\text{OH})_4\text{Si}_2\text{O}_5$ ) or lateritic soils rich in kaolinite to produce highly reactive metakaolin ( $\text{Al}_2\text{Si}_2\text{O}_7$ ) phase with  $\text{Al}_2\text{O}_3:\text{SiO}_2$  ratios around 1:2 which exhibit pozzolanic activity [38].

The pozzolanic activation of metakaolin (MK) by various activators (calcium hydroxide (CH) as well as alkali hydroxide) and the properties of these binders have been previously reported elsewhere [39]. The principal reaction between MK and CH from Portland cement hydration in the presence of water results in the formation of additional cementitious CSH gel, together with crystalline products, which include calcium aluminate hydrate and aluminosilicate hydrates ( $\text{C}_2\text{ASH}_8$ ,  $\text{C}_4\text{AH}_{13}$ , and  $\text{C}_3\text{AH}_6$ ) [39]. The type and amount of the crystalline products depend principally on the MK/CH ratio and reaction temperature [39]. This reaction between MK and CH is slower than the hydration of plain Portland cement, but it improves the binding properties of blended cement when compared to Portland cement [40].

It is well established by now that the addition of MK in blended cement not only provides an effective way to protect the environment but also leads to better performance of the final product, as it is reviewed in [38]. It has been reported that the replacement of 30 wt% of Portland cement with MK leads to substantial improvement in strength and transport properties of blended concrete when compared to that of unblended concrete [41]. Partial replacement of Portland cement with MK also enhances the compressive strength of concrete, with the highest strength reported for mixtures with approximately 20 wt% of MK [42]. However, a very few publications report on combined effects of fly ash and MK as SCMs, and they show that the use of two types of SCMs as a ternary blend (i.e., OPC, MK, and fly ash) has the potential to synergistically optimize the contributions of each, considering factors such as early and late-age strength, workability, durability, and economy [43,44]. For example, Sujjavanich et al. [45] showed that the relative amount of added MK and fly ash to OPC concrete strongly influenced the reaction and the products obtained in the concrete, and claimed that synergistic action of MK and FA helped to improve long-term strength and durability, most likely due to the fact that produced mono carboaluminate fills voids providing a denser and more uniform microstructure. In addition, some reports showed that adding MK and fly ash to OPC improves workability and rheological properties of the concrete mixture [46] when compared to two-component cementitious mixtures (i.e., fly ash + OPC or MK+OPC). At the same time, other studies [47] demonstrated significantly lower drying shrinkage

of three-component (MK+ fly ash + OPC) cementitious mixtures. However, to the best of our knowledge, studies using reclaimed fly ash and MK as components in ternary cementitious systems has not been published in the open literature.

### **3.4. Influence of SCMs on Concrete Durability**

#### **3.4.1. Shrinkage**

Shrinkage is generally defined as the volume reduction of concrete because of changes in moisture, chemical reactions, and temperature reduction [48,49]. The main contributors to concrete shrinkage are commonly autogenous shrinkage, drying shrinkage, and thermal shrinkage, which act through different mechanisms [49]. Nonetheless, carbonation shrinkage can also be meaningful over long periods of time [49]. Research shows that the relationship between concrete's mixture proportions, shrinkage, strength, and workability is complex [48]. Autogenous shrinkage, also known as self-desiccation shrinkage, is driven by chemical shrinkage occurring from the cement hydration reaction, which results in lower volume in contrast to the initial components (i.e., water and cement). On the other hand, drying shrinkage is caused by the withdrawal of capillary water from the cementitious matrix due to evaporation in the hardened state and its occurrence is lengthy relative to the autogenous shrinkage (which occurs mostly within the first 24 hours) [49,50]. Both types of shrinkage take place in the cement paste, while aggregates in concrete restrain these volumetric contractions [50]. The amount of cement can be lowered by partial replacement with fly ash, which can be beneficial to reduce both autogenous and drying shrinkage [50].

Ghafari et al. [51] studied the feasibility of replacing silica fume with different SCMs (i.e., fly ash and GGBFS) in ultra-high performance concrete (UHPC) to reduce autogenous shrinkage. The influence of partial and/or complete replacement of SF by fly ash and GGBFS was investigated on compressive strength, autogenous shrinkage, and porosity. The experimental results revealed that the addition of fly ash or GGBFS to be effective in reducing the amount of fine pores in UHPC; thus, leading to a reduction of the autogenous shrinkage.

Cheng et al. [52] evaluated the compressive strength and durability performance of concrete mixtures utilizing two different SCMs, i.e., blast furnace slag (BFS) and metakaolin, and porous coral sand aggregate (CSC) as a complete replacement to river sand. The durability performance of concrete mixtures was assessed in terms of accelerated carbonation, drying shrinkage, chloride penetrability, sulfate drying-wetting cycle, and capillary water absorption. In addition, the study also evaluated the influence of CSC and SCMs on concrete microstructure through SEM imaging and measuring porosity and pore size distribution. The experimental results revealed that CSC admixed concrete exhibited higher 28 days capillary water absorption, drying shrinkage, 28 days carbonation depths, and a marginally lower 28 days compressive strength compared to the river sand concrete (RSC). However, the addition of SCMs (i.e., 5% MK and 15% BFS as cement replacement by mass) in CSC admixed concrete resulted in an increase in compressive strength, reduction in drying shrinkage, and enhancement in durability properties in comparison to RSC (i.e., reduction in capillary water absorption, and carbonation depths). These improvements were likely attributed to the combined effect of the pozzolanic reaction of SCMs and internal curing by porous coral sand.

Guo et al. [53] studied the mechanical and durability properties of self-compacting concrete (SCC) by replacing high volumes of natural aggregate with recycled concrete aggregate, i.e., RCA (75% and 100% by weight) and cement with SCMs (50% and 75% by weight). The influence of SCMs in SCC was investigated by using a combination of fly ash, slag, and silica fume, where binary mixtures were prepared with fly ash, ternary mixes with the equal proportions of fly ash and slag, and quaternary mixes were blended with the equal proportions of fly ash, slag, silica fume. The results exhibited a progressive decrease in the cube and axial compressive strength and an increase in drying shrinkage with the increase in the aggregate replacement ratio with RCA. While a decrease in the compressive strength of binary mixtures was observed, quaternary RCA-SCC mixtures exhibited similar strength and durability properties to that of control mixtures without SCMs and RCA. Overall, quaternary RCA-SCC (i.e., using a combination of fly ash, silica fume, and slag as a high-volume replacement to cement) exhibited lower drying shrinkage, improvement in freezing and thawing resistance, and improvement in mechanical properties.

Hu et al. [54] measured early age autogenous and chemical shrinkage of fly ash and slag admixed mortars. The experimental results showed a significant increase in the autogenous shrinkage with the decrease in the water to binder (w/b) ratio for all mortar mixtures. However, the predominant influence of w/b ratio on autogenous shrinkage was observed in fly ash and slag admixed mortars than in the control mixture without SCMs.

Cheng et al. [55] evaluated the mechanical properties and durability of lightweight aggregate concrete utilizing metakaolin and GGBFS mixed with artificial seawater. The study determined the compressive strength, chloride penetration, drying shrinkage, and hydration products of concrete mixtures. The combination of internal curing of lightweight aggregate, the pozzolanic reaction of metakaolin and GGBFS, and accelerated cement hydration by seawater led to the reduction of Ca/Si ratio in the interfacial transition zone (ITZ) and denser hydration products. As a result, this led to the decrease in drying shrinkage and mobility of chloride ion in lightweight aggregate concrete.

### 3.4.2. *Alkali-silica reaction (ASR)*

The alkali-silica reaction (ASR) is an important durability-related problem of concrete caused by aggregates comprising reactive siliceous minerals and the alkaline pore solution of the cementitious matrix [56,57]. The reaction between reactive silica in the aggregate and alkali in the cementitious matrix forms a gel in the ITZ or aggregate micro-crack [57]. This gel soaks water from the environment or the surrounding cement paste and swells. The swelling of this gel generates internal stresses and damages the concrete [57]. There are various sources of alkali in concrete including the cement, water, and aggregates; however, the primary source is the cement. Concerning ASR, aggregates used in concrete can be categorized into reactive and non-reactive aggregates. Reactive aggregates consist of high contents of amorphous silica, while non-reactive aggregates contain crystalline silica [56]. It has been observed that a higher amount of amorphous silica content in aggregates increases ASR expansion [56]. Furthermore, particle size also impacts the ASR expansion. Research demonstrated that particle size larger than 1 mm causes higher ASR expansion [58]. In addition, temperature and humidity also influence ASR as the reaction accelerates with higher temperatures and its occurrence potential increases in high moisture environments [58].



Cassiani et al. [59] investigated the effectiveness of the chemical index model in determining the minimum content of various types of SCMs to eliminate the ASR related expansion in mortar mixtures. The study produced mortar bars with four different natural aggregates and two recycled aggregates. Furthermore, the study utilized four different SCMs in mortar mixtures (i.e., two different types of fly ash at 15, 20, and 25% cement replacement level, GGBFS at 20, 40, and 60% cement replacement level, and silica fume at 5, 8, and 10% cement replacement level by mass). The experimental results revealed that appropriate proportions of SCMs could mitigate the ASR expansion effectively. Overall, silica fume presented the most effective SCM to reduce ASR expansion at 10% cement replacement level, followed by Class F fly ash and slag at all cement replacement levels investigated in the study. Additionally, the study concluded the chemical index model to give good results to predict the minimum replacement of SCMs to suppress ASR.

Xuan et al. [60] investigated the influence of different SCMs (i.e., fly ash, GGBS, and waste glass powder) and different mixing methods (i.e., wet-mixed and dry-mixed method) on ASR related expansion of mortar mixtures using fine municipal solid waste incineration bottom ash (MSWIBA) as sand. All SCMs were used at a 30% of replacement level of cement by mass. The experimental data revealed that fly ash was the most effective SCM in mitigating both alkali-silica reaction and alkaline-AL reaction of mortars prepared with MSWIBA, followed by GGBS and glass powder. On the other hand, dry-mixing was more effective in mitigating the expansion of MSWIBA mortars in comparison to wet-mixing.

Oruji et al. [61] assessed the efficiency of pulverized ultra-fine bottom ash as SCM in reducing the ASR expansion in mortar mixtures. Two ultrafine bottom ash with different particle sizes were used as SCMs by replacing 9, 23, 33, and 41% of cement by mass. In addition, the study also produced mortars using Class F fly ash as SCM at the same replacement level as bottom ash. The experimental results showed that bottom ash with the finer particle size (at a 41% cement replacement level) decreased the expansion by a factor of ten compared to the control mixture. However, comparatively, both types of pulverized bottom ash admixed mortars exhibited slightly higher expansion than fly ash mortar bars. This is likely due to the lower reactivity and less solubility of alumina and silica in bottom ash mixtures.

Mahyar et al. [62] utilized three different natural pozzolans, GGBFS, six different types of fly ashes, two types of Portland cement, and reactive aggregate to assess the effectiveness of the chemical index model to estimate 14-day ASR expansion as per ASTM C1567. All SCMs admixed mortars were produced by replacing 12, 20, 30, 40, 50, and 60% of cement by mass. The experimental results revealed that 15-27% of cement replacement with most of the fly ashes or natural pozzolans and 27-32% of cement replacement with GBBS was required to reduce ASR to 0.1%. While a strong relationship was observed between total CaO and SiO<sub>2</sub> contents of cement/SCM blends with ASR expansion (i.e., a decrease in CaO and increase in SO<sub>2</sub> decreases ASR expansion), a relatively weaker influence of Al<sub>2</sub>O<sub>3</sub> in reducing the ASR expansion was observed. Na<sub>2</sub>O<sub>eq</sub>, Fe<sub>2</sub>O<sub>3</sub>, MgO, or SO<sub>3</sub> exhibited an expansion-increasing and expansion-decreasing effect depending on the Portland cement/SCM combination, i.e., if the amount of the oxides in SCM is greater than in the Portland cement, the ASR related expansion will decrease with the SCM addition. In contrast, if the amount of the oxides in SCM are less than in the Portland cement, the expansion increases with SCM addition. Since fly ashes had higher, and slags had

lower  $\text{Fe}_2\text{O}_3$  than Portland cement, ASR related expansion decreased in cement/fly ash and increased in a cement/slag blend.

Wei et al. [63] investigated the influence of the combined system of metakaolin (MK) and bentonite as SCMs in mitigating ASR related expansion of mortar mixtures. The study adopted three cement replacement levels, 10%, 30%, and 50% with MK for binary mixtures. For ternary mixtures, the substitution of MK by bentonite increased from 0% to 5% with increasing cement replacement. The experimental results showed that replacing 10% and 30% cement by SCMs in both ternary and binary mortar mixtures decreased ASR expansion from deleterious to innocuous level. Furthermore, no ASR expansion and no crack were observed at the 50% cement replacement level by SCMs for both ternary and binary mixtures. The authors suggested that this is likely attributed to the aluminum from minerals, which decelerated the  $\text{SiO}_2$  dissolution process, formation of gel, and, thus, its swelling capacity. Furthermore, the consumption of Ca, in tandem with, reduced alkalinity also contributed to the reduction of the ASR related expansion.

### 3.5. Texas DOT Research on Alternative Sources of SCMs

In recent years, Texas DOT has funded extensive research related to the evaluation of alternative sources of SCMs for the state of Texas. Texas DOT study TxDOT 0-6717 by Seraj et al. [64] investigated eight different types of alternative SCMs, including pumice, perlite, vitric ash, metakaolin, shale, and three different zeolites (Zeolite-A, Zeolite-T, and Zeolite-Z). These SCMs were obtained from the states of Texas, Idaho, Nevada, Missouri, and Indiana, as shown in Table 2.

**Table 2. Alternative SCMs evaluated in [64]**

Material	Source	Passes ASTM C618
Pumice (Pumice-D)	Idaho	Yes
Perlite (Perlite-I)	Idaho	Yes
Vitric Ash (Vitric Ash-S)	Nevada	Yes
Metakaolin (Metakaolin-D)	Missouri and Indiana	Yes
Shale (Shale-T)	Texas	Yes
Zeolites (Zeolite-A, Zeolite-T, and Zeolite-Z)	Texas and Idaho	No

Based on experimental findings as shown in Table 3, this study concluded that the best SCMs in terms of strength and durability were metakaolin and Zeolite-Z. Furthermore, pumice and perlite showed good durability performance; yet strength development was compromised. As such, pumice and perlite were recommended where high early strength is not a requirement. Shale, on the other hand, performed well in terms of strength and ASR resistance; yet it was not recommended for concrete requiring high resistance to sulfate attack.

**Table 3. Summary of SCM performance at different replacement dosages [64]**

Material	Min. SCM Replacement for ASR	Sulfate Exposure Level		Strength Relative to OPC Control at 28 Days		Approximate Price per Ton	Workability Problems at High Dosages?
		15%	25%	15%	25%		

Pumice-D	15%	Class 3	Class 3	90%	91%	\$116	NO
Perlite-I	15%	Class 3	Class 3	77%	78%	\$124	NO
Metakaolin-D	15%	UN	Class 2	100%	111%	\$325 (w/o shipping)	NO
Zeolite-Z	15%	Class 3	Class 3	126%	105%	\$100	YES
Shale-T	25%	-	Class 1	-	96%	\$49-51	NO
Vitric Ash-S	25%	-	UN	-	75%	\$100-\$160	NO
Zeolite-T	25%	-	UN	-	86%	\$200 (w/o shipping)	YES
Zeolite-A	35%	-	UN	-	72%	\$150	No

\*UN=Unsuitable

A subsequent Texas DOT study, TxDOT 5-6717-01 by Al-Shmaisani et al. [14], investigated 15 types of alternative SCMs from 3 different suppliers including. These SCMs were obtained from Texas, West Virginia, California, Arkansas, Wisconsin, Colorado, Oklahoma, and New Mexico, as shown in Table 4.

**Table 4. Alternative SCMs evaluated [14]**

Supplier	Material	Source	Passes ASTM C618
A	Dacite (D-L and D-S)	California	Yes
	Nepheline Syenite (NS-I, NS-L, and NS-S)	Arkansas	Yes
	Rhyolite (R-O)	Wisconsin	Yes
B	Remediated Fly Ash (RM-C, RM-L, and RM-S)	Colorado, Texas, and Oklahoma	Yes
	Pumice (P-B and P-W)	New Mexico	Yes
C	Reclaimed Fly Ash (RC-G, RC-M, and RC-P)	Texas	Yes (RC-M) No (RC-G and RC-P)
	Remediated Fly Ash (RM-M)	Texas	Yes

TxDOT 5-6717-01 results showed that all-natural minerals provided by supplier A (i.e., Dacite, Nepheline Synite, and Rhyolite) were determined to be inert fillers with no capability to increase long-term compressive strength and reduce ASR or sulfate attack. As such, these materials were not recommended as alternative SCMs. On the other hand, all the natural minerals provided by supplier B exhibited pozzolanic properties, improved concrete performance, and passed ASTM C 618 requirements for natural pozzolans. In the case of reclaimed and remediated fly ashes studied, excepting reclaimed fly ash RC-G (which marginally exceeded ASTM C618 moisture content criteria), all fly ashes investigated in the study met ASTM C618 requirements for Class F fly ash. Table 5 presents a qualitative summary of the effects of the different SCMs evaluated on the properties of cementitious materials.

**Table 5. Summary of SCMs effect on cementitious mixture performance [14]**

Test	Supplier A				Supplier B				Supplier C			
	D-S	NS-I	NS-S	R-O	RM-C	RM-L	RM-S	P-B	P-W	RC-G	RC-M	RM-M
<b>Yield Stress</b>	*	*	*	*	X	X	X	*	*	✓	✓	✓
<b>Viscosity</b>	*	*	*	*	X	X	X	*	*	✓	✓	✓
<b>WRA Interact</b>	*	*	*	*	--	*	--	*	*	--	--	*
<b>AEA Interact</b>	*	*	*	*	--	✓	--	*	*	✓	X	*
<b>CH Content</b>	X	✓	X	X	✓	✓	✓	--	✓	--	--	--
<b>Mortar Flow</b>	--	--	X	✓	✓	X	X	--	--	✓	✓	✓
<b>ASTM C109</b>	X	X	X	X	✓	--	--	--	✓	--	✓	✓
<b>ASR</b>	X	X	X	X	✓	✓	✓	✓	✓	✓	✓	✓
<b>Sulfate</b>	X	X	X	X	✓	✓	✓	X	✓	X	X	X
<b>Slump</b>	X	--	X	X	--	X	X	--	X	--	✓	✓
<b>Setting Time</b>	--	--	--	--	X	--	--	--	--	--	--	--
<b>ASTM C39</b>	X	X	X	X	✓	✓	✓	--	✓	--	✓	✓
<b>RCPT</b>	X	X	X	X	✓	✓	✓	✓	✓	✓	✓	✓

(\*) Not tested, (X) Did not perform well, (✓) Performed favorably, (--) Impact is neutral

From the reports presented above, it is important to notice that properties vary significantly depending on the supplier and source for the same type of SCM (e.g., zeolite, reclaimed fly ash, and remediated fly ash). As such, this highlights the importance of characterizing potential SCM materials on a supplier and source basis. Consequently, this project explores alternative SCM sources that will expand the current knowledge in the region with the goal to broaden the portfolio of alternative SCMs available in Region 6. This study concentrates particularly on reclaimed fly ash and bottom ash sources, which were not investigated in the studies presented above. Furthermore, this study expands the knowledge on the utilization of calcined clays as SCMs in the region. In particular, this study also intends to evaluate blends of reclaimed fly ash and calcined clays for optimum SCM performance.

## 4. METHODOLOGY

### 4.1. Materials

#### 4.1.1. *Alternative SCMs*

This study investigated three different coal ashes: (1) conventional ASTM C618 compliant Class F fly ash (FA) from Illinois, (2) reclaimed fly ash (RFA) from Georgia, and (3) reclaimed ground bottom ash (GBA) from Texas. All the ashes were used as received from the supplier without any further processing. In addition, the study evaluated calcined kaolinite clay or metakaolin (MK) as SCM in concrete mixtures. It is important to mention that metakaolin was used alone in binary mixtures (i.e., cement and MK) as well as with RFA and GBA in ternary mixtures (i.e., cement, coal ash, and MK). This was done to evaluate the potential synergic effects of the coal ashes with MK. Figure 2 presents photographic views of SCMs used in this study.

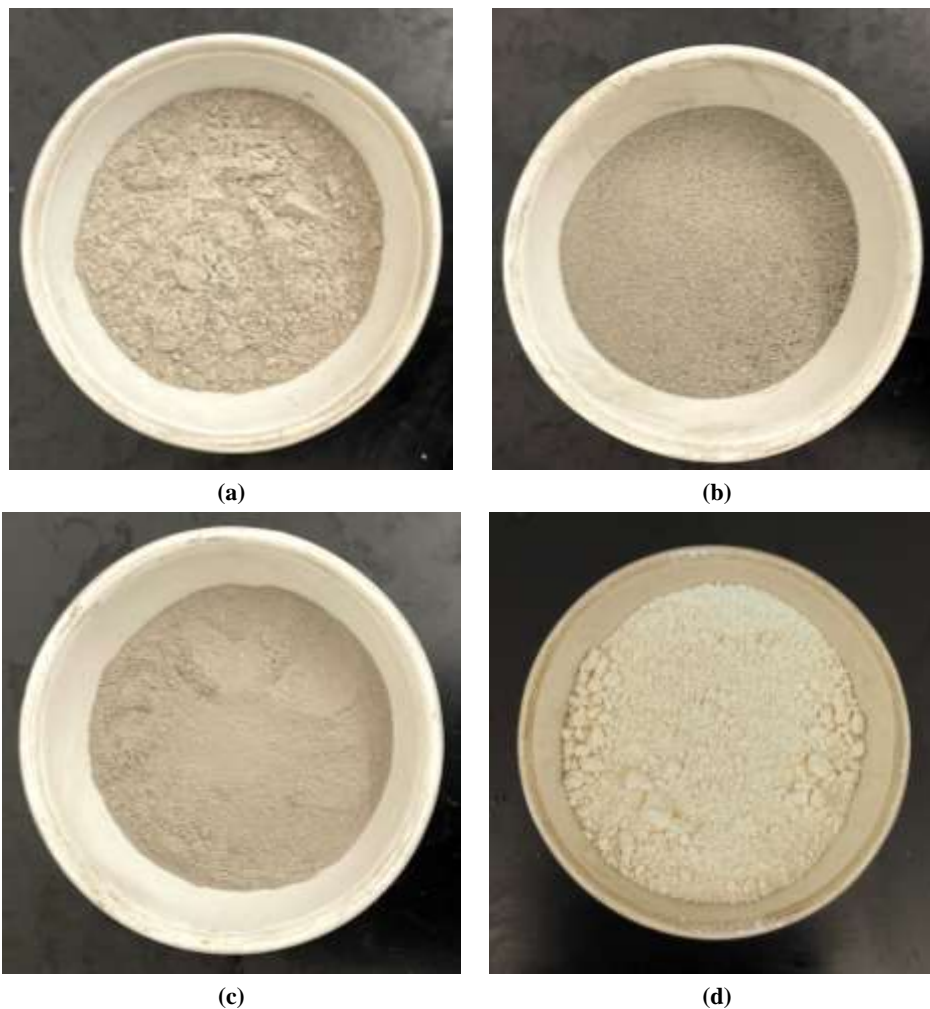


Figure 2. Materials: (a) FA, (b) RFA, (c) GBA, and (d) MK

#### 4.1.2. *Cement*

All mortars and concrete mixtures produced in this study utilized Ordinary Portland Cement (OPC) Type I conforming to the ASTM C150 standard [65]. The chemical composition of the cement, obtained from X-ray fluorescence, is presented in Table 6. The specific gravity of the cement was 3.15.

**Table 6. Chemical composition (by weight) of cement used in the study.**

SiO <sub>2</sub>	Al <sub>2</sub> O <sub>3</sub>	Fe <sub>2</sub> O <sub>3</sub>	CaO	Na <sub>2</sub> O	K <sub>2</sub> O	SO <sub>3</sub>	MgO
19.80	4.70	3.80	64.80	0.16	0.54	3.38	2.20

#### 4.1.3. *Aggregates*

For mortar specimens prepared for strength activity index (SAI) testing, standard-graded sand conforming to ASTM C778 was used. For the manufacture of concrete mixtures, limestone and concrete sand (silica sand) were used as coarse and fine aggregate, respectively. While the coarse aggregate had a maximum nominal particle size of 19 mm, the fine aggregate had a maximum nominal particle size of 4.75 mm. The aggregate size was determined from sieve analysis according to ASTM C136 [66]. The specific gravity and absorption (measured according to ASTM C127) were 2.68 and 0.8%, respectively, for the coarse aggregate [67]. Similarly, the specific gravity and absorption (measured according to ASTM C128) for fine aggregate were 2.65 and 0.4%, respectively [68].

#### 4.1.4. *Superplasticizer and Air-Entraining Admixture*

To produce a concrete mixture with the desired workability, a polycarboxylate-based High-Range Water Reducer (HRWR) was utilized for all concrete mixtures produced in this study. The air-entraining capabilities of air-entraining admixtures (AEA) in concrete mixtures can be disrupted by the carbon content and fineness of SCMs [69]. In turn, unintended reduction in air content can produce a negative impact on the durability of concrete exposed to freeze/thaw conditions. As such, to assess the effect of the different SCMs evaluated on AEA effectiveness, a constant dosage of AEA was used for all concrete mixtures. The AEA dosage used in concrete mixtures was 1.1 ml per kg of the binder.

### 4.2. **Characterization of Alternative SCMs**

A comprehensive characterization of the SCMs evaluated in this project was conducted to gain insight into the physical, chemical, and pozzolanic properties of these materials. The different analyses conducted are detailly described in the next sub-sections.

#### 4.2.1. *Microstructure*

The morphology (i.e., shape and size) of SCMs significantly influences essential properties of concrete, such as workability, strength, and durability. As such, Scanning Electron Microscopy (SEM) imaging was conducted with JEOL JSM-7500F equipment (JEOL USA Inc., MA, USA) to investigate the micro-morphology of the SCMs. To perform SEM imaging, a carbon tape was

initially attached to an aluminum stub, and a thin layer of material was placed on top of the carbon tape. Next, the sample was sputter-coated with 5nm of palladium-platinum alloy to avoid charging.



Figure 3. JEOL JSM-7500F for SEM imaging

#### 4.2.2. *X-Ray Diffraction (XRD)*

In blended systems of cement with SCMs, the amorphous phases of the SCMs participate exclusively in the pozzolanic reaction. As such, the mineralogical composition of SCMs has a significant influence on the strength and durability of concrete mixtures. This study conducted a mineralogical analysis of a powder sample using a Bruker-AXS D8 Advanced (Bruker Corporation, MA, USA) with Cu source (Cu  $K\alpha$  radiation,  $\lambda = 1.54178 \text{ \AA}$ ) a Lynxeye PSD detector. To analyze the XRD data, Profex software was used for all SCMs [70].



Figure 4. Bruker-AXS D8 advanced for XRD analysis.

#### 4.2.3. *Chemical Composition*

SCM materials should conform to the chemical composition requirement mentioned in ASTM C618 to be classified as a pozzolan [2]. As such, X-ray fluorescence (XRF) was conducted with a Rigaku Supermini200 (Rigaku Corporation, Japan) to identify the chemical compositions of the coal ashes and metakaolin. The XRF equipment was calibrated with three standard fly ash samples from the National Institute of Standards and Technology (NIST).

#### 4.2.4. *Particle Size Analysis*

The influence of SCMs particle size on concrete strength and durability is well documented in the existing literature [18]. The increase in the fineness of SCMs positively influences their reactivity, thus increasing the strength of concrete materials. As such, the particle size distributions of all coal ashes and metakaolin were assessed using the Partica LA-960 (HORIBA, Ltd., CA, USA). For the analysis, the dried powdered samples were fed into the measuring chamber with an air pressure of 0.3 MPa. The laser diffraction analyzer utilized had the capability of detecting particles from 0.01  $\mu\text{m}$  to 5000  $\mu\text{m}$  through light diffraction.





Figure 5. Partica LA-960 for particle size analysis.

#### 4.2.5. *Moisture Content and Loss on Ignition*

SCMs should meet the moisture content and loss on ignition (LOI) requirements prescribed in ASTM C618 [2]. Both moisture content and LOI of all coal ashes and metakaolin were determined according to ASTM C311. Moisture content was determined as a mass loss % due to drying (i.e., after keeping the sample inside the furnace at  $110^{\circ}\pm 5^{\circ}\text{C}$  for 24 hours). Next, the dried samples from the moisture content test were utilized for LOI determination. The sample of material remaining after the moisture content test was ignited at  $750^{\circ}\text{C}$  for 45 minutes and then allowed to cool at room temperature. The cooled sample was weighed, and LOI was calculated using Equation 1 [71].

$$\text{Loss on Ignition, \%} = \frac{A-C}{A-B} \times 100 \quad [1]$$

where:

A = mass of dried sample and crucible;

B = mass of empty crucible;

C = mass of ignited sample and crucible.

#### 4.2.6. *Strength Activity Index*

The strength activity index (SAI) of all the SCMs was evaluated after 7 and 28 days of curing [71]. The control mortar mixture (i.e., without SCMs) was prepared using sand to binder ratio of 2.75 and a water to binder ratio of 0.48. Subsequently, the flow value for the control mixture was determined per ASTM C1437 [72]. The test mixtures (i.e., mixture with SCMs) were prepared by replacing 20% of cement (by mass) with coal ashes or metakaolin. For the test mixtures, the amount of water required was determined such that the same flow value as the control mixture (within  $\pm 5\%$  tolerance) was achieved. For all mortar mixtures, twelve 50.8-mm (2-in) cubes were cast (i.e., six for each curing age). After 24 hours, the cubes were demolded and cured in a saturated lime water tank as per ASTM C511 [73]. At 7 and 28 days of curing, the compressive strength of mortars was measured following the ASTM C109 standard [74]. The test setup is presented in Figure 6. The strength activity index is the ratio of the strength of the test mixture cubes (i.e., SCMs admixed mortars) to the strength of the control mixture cubes (presented in %). It is important to mention that per ASTM C618 [71], a minimum SAI of 75% is required at both curing ages for a material to qualify as a pozzolan.

Apart from the SAI determination of coal ashes and metakaolin, this study also investigated the feasibility of using the combined system of coal ashes (RFA and GBA) with metakaolin as SCMs in concrete mixtures (ternary mixtures), i.e., RFA-MK or GBA-MK systems are used as the SCMs. The optimum replacement level of RFA or GBA by metakaolin in the ternary mixtures was determined from the SAI test (i.e., 20% of the cement was replaced by the combination of RFA and MK or GBA and MK). Specifically, 10, 20, and 30% of RFA or GBA (by mass) were replaced by MK in the mortar mixtures. The ternary mortar mixtures are designated as XRFA-YMK and XGBA-YMK, where X represents the % of the RFA or GBA of SCMs, and Y represents the % of MK of SCMs.



Figure 6. Compressive strength testing setup for 50.8-mm (2-in) mortar cubes.

#### 4.2.7. *Thermogravimetric Analysis*

To gain substantial insight into the pozzolanic activity of the evaluated materials, thermogravimetric analysis (TGA) was performed. A methodology described in a previous study was adopted to determine calcium hydroxide consumption for all coal ashes and metakaolin [75]. Initially, calcium hydroxide (ACS reagent grade) and SCMs, with a 3:1 mass ratio, were mixed with 0.5M potassium hydroxide (90% reagent grade) solutions. By maintaining a liquid-to-solid ratio at 0.9, the mixture was mixed using a spatula in a plastic container for 4 minutes. After completing the mixing procedure, nearly 6-7g of the mixture was placed in an oven at a temperature of  $50 \pm 0.05$  °C for ten days (i.e., 240 hours). After ten days, the sample was removed from the oven, and a TGA analysis was performed with the Q600 SDT (TA Instruments, DE, USA). Nearly 20–30 mg of material was heated from 23 to 600 °C, at a rate of 10 °C/ minute (Universal V4.5A) [75].



Figure 7. Q600 SDT for TGA.

### 4.3. Concrete Testing

In the first phase of this study, SCMs investigated were thoroughly characterized to determine their physical and chemical properties. In the subsequent phase, the properties of concrete using binary systems (i.e., cement and coal ash or metakaolin) as well as ternary systems (i.e., cement, coal ash, and metakaolin) are evaluated. Mechanical and physical properties of concrete replacing 10%, 20%, and 30% of cement (by mass) with SCMs were experimentally investigated. Properties evaluated included slump, air content, unit weight, compressive strength, surface resistivity, drying shrinkage, and ASR.

#### 4.3.1. *Mixture Proportions*

A total of thirteen binary concrete mixtures and six ternary concrete mixtures were prepared to assess the effect of the different systems on the properties of concrete. The control concrete mixture

used in this study (i.e., CO) was designed according to the Louisiana Department of Transportation and Development (LaDOTD) specifications for type A1 structural class concrete with a target compressive strength of 31 MPa (4500 psi) [76]. The control concrete mixture (i.e., without SCMs) was designated as CO. Similarly, concrete mixtures containing only one type of SCMs (i.e., mixtures using binary systems) were designated as M-X, where M represents the type of SCM (i.e., FA, RFA, GBA, or MK) and X represents mass % of cement replaced with the SCM. For concrete mixtures using ternary systems, concrete mixtures were designated as M-MK-X, where M represents the type of coal ash (i.e., RFA or GBA), MK represents metakaolin, and X represents mass % of cement replaced with SCMs. The percentages of cement replacement (by mass) evaluated for both binary and ternary mixtures were 10%, 20%, and 30%. It is important to mention that for the ternary mixtures only the maximum replacement of coal ash (i.e., GBA or RFA) with MK (i.e., 30% by mass) were evaluated. For all concrete mixtures, the water to binder ratio (w/b) and binder content was kept constant at 0.45 and 344 kg/m<sup>3</sup> (i.e., 580 lb/yd<sup>3</sup>), respectively. Furthermore, all concrete mixtures were produced using AEA and HRWR. A constant AEA dosage of 1.1 mL per kg of binder was used for all mixtures. On the other hand, a constant HRWR dosage of 1.2 ml per kg of binder was used for all mixtures, excepting mixtures using MK. MK significantly reduced the workability of concrete, and therefore a higher dosage of HRWR was required for MK admixed concrete mixtures at 20 and 30% cement replacement levels. The mixture proportions of all binary and ternary concrete mixtures are summarized in Table 7 and <sup>a</sup> % replacement of cement with SCMs

Table 8, respectively.

**Table 7. Binary system concrete mixture proportions.**

ID	Cement (kg/m <sup>3</sup> )	SCM (kg/m <sup>3</sup> )	SCM (%) <sup>a</sup>	Coarse Aggregate (kg/m <sup>3</sup> )	Fine Aggregate (kg/m <sup>3</sup> )	Water (kg/m <sup>3</sup> )	HRWR (L/m <sup>3</sup> )	AEA (L/m <sup>3</sup> )
CO	344.1	0	0	1058.2	743.7	154.2	0.42	0.36
FA-10	309.7	34.4	10	1058.2	734.0	154.2	0.42	0.36
RFA-10	309.7	34.4	10	1058.2	738.5	154.2	0.42	0.36
GBA-10	309.7	34.4	10	1058.2	732.4	154.2	0.42	0.36
MK-10	309.7	34.4	10	1058.2	736.2	154.2	0.43	0.36
FA-20	275.2	68.8	20	1058.2	724.3	154.2	0.42	0.36
RFA-20	275.2	68.8	20	1058.2	719.1	154.2	0.42	0.36
GBA-20	275.2	68.8	20	1058.2	733.3	154.2	0.42	0.36
MK-20	275.2	68.8	20	1058.2	728.6	154.2	0.84	0.36
FA-30	240.8	103.2	30	1058.2	714.7	154.2	0.42	0.36
RFA-30	240.8	103.2	30	1058.2	706.7	154.2	0.42	0.36
GBA-30	240.8	103.2	30	1058.2	728.1	154.2	0.42	0.36
MK-30	240.8	103.2	30	1058.2	721.1	154.2	1.26	0.36

<sup>a</sup> % replacement of cement with SCMs

**Table 8. Ternary system concrete mixture proportions.**

ID	Cement (kg/m <sup>3</sup> )	Coal Ash (kg/m <sup>3</sup> )	MK (kg/m <sup>3</sup> )	SCMs (%) <sup>a</sup>	Coarse Aggregate (kg/m <sup>3</sup> )	Fine Aggregate (kg/m <sup>3</sup> )	Water (kg/m <sup>3</sup> )	HRWR (L/m <sup>3</sup> )	AEA (L/m <sup>3</sup> )
CO	344.1	0	0	0	1058.2	743.7	154.2	0.42	0.36
RFA-MK-10	309.7	24.1	10.3	10	1058.2	738.5	154.2	0.42	0.36
GBA-MK-10	309.7	24.1	10.3	10	1058.2	732.4	154.2	0.42	0.36
RFA-MK-20	275.2	48.2	20.6	20	1058.2	719.1	154.2	0.42	0.36
GBA-MK-20	275.2	48.2	20.6	20	1058.2	733.3	154.2	0.42	0.36
RFA-MK-30	240.8	72.2	31.0	30	1058.2	706.7	154.2	0.42	0.36
GBA-MK-30	240.8	72.2	31.0	30	1058.2	728.1	154.2	0.43	0.36

<sup>a</sup> % replacement of cement with SCMs

### 4.3.2. Specimen Preparation

To prepare the concrete mixtures, initially 2/3 of the mixing water, the coarse aggregate, and the AEA were mixed for one minute in a 1ft<sup>3</sup> capacity drum mixer. Subsequently, all the remaining components (i.e., cement, SCMs, fine aggregate, and HRWR) were added and mixed for another three minutes. Next, the mixtures were kept at rest for three minutes. Finally, the concrete mixtures were mixed for three additional minutes. After the mixing process was completed, the slump and air content of the fresh concrete mixtures (as shown in Figure 8) were determined according to ASTM C143 and ASTM C231, respectively [77,78]. In addition, the unit weight of the fresh concrete was also determined as per ASTM C138 [79]. Subsequently, to measure compressive strength and surface resistivity at 28 and 90 days of curing, six 101.2 mm x 202.4 mm (4 in x 8 in) cylinders were cast (i.e., three cylinders for each curing age). After 24 hours, cylindrical specimens were demolded and allowed to cure in a saturated lime water tank as per ASTM C511 [73].

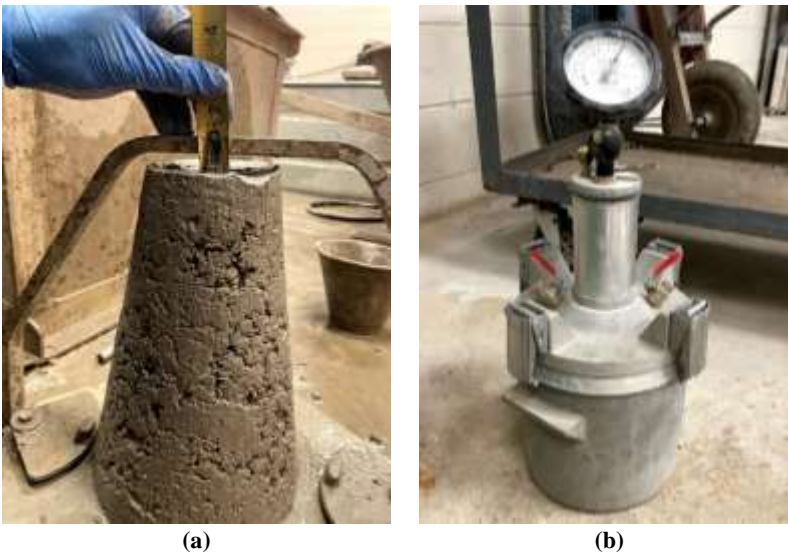


**Figure 8. Fresh properties testing: (a) slump and (b) air content**

### 4.3.3. *Compressive Strength Test*

The compressive strength of the different concrete materials produced in this study was evaluated after 28 and 90 days of curing as per ASTM C39 [80]. A total of three replicas were evaluated at each curing age. The compressive strength tests were performed with a constant loading rate of 0.25 MPa/s under hydraulic pressure (Forney LT-8031-FTS). Figure 9 presents the test setup for compressive strength.



Figure 9. Compression test setup.

### 4.3.4. *Surface Resistivity*

The durability of concrete is largely dependent on the pore size distribution and the interconnectivity of these pores [81–83]. A permeable concrete can accelerate the deterioration of concrete as it allows the ingress of deleterious substances into the material, such as chloride ions. The electrical resistivity of concrete is a measure of concrete’s ability to withstand the transfer of ions when subjected to an electrical field [84]. As such, the measurement of resistivity provides insight into the size and extent of the interconnectivity of pores in concrete. The higher the electrical resistivity of concrete, the lower the probability of chloride ion penetration should be.

Various methods have been developed to evaluate hardened concrete durability in terms of electrical resistivity. In this study, chloride ion penetrability of concrete mixtures was investigated by AASTHO T358 “Standard Method of Test for Surface Resistivity Indication of Concrete’s Ability to Resist Chloride Ion Penetration.” It is worth mentioning that this test is non-destructive, and therefore the same specimens are used for both the surface resistivity test and compressive strength test. A four-point Wenner probe with 1.5-inch (38 mm) probe spacing was used to measure the electrical resistivity of the concrete cylinders. The SR reading was taken after removing the excess water from the surface. A total of eight readings per specimen were taken

(i.e., two sets of reading at the center of the longitudinal axis of the cylinders at 0°, 90°, 180°, and 270°), as shown in Figure 10. A correction factor of 1.1 was applied to the average surface resistivity values obtained to account for the lime water curing condition according to AASTHO T358.



Figure 10. Surface resistivity setup.

According to AASTHO T358, the qualitative chloride-ion penetrability category of each concrete mixture is reported based on the surface resistivity ranges presented in Table 9.

Table 9. Chloride ion penetrability based.

Chloride Ion Penetrability	4 in. X 8 in. Cylinder (kΩ-cm), a=1.5" (38 mm)*	6 in. X 12 in. Cylinder (kΩOhm-cm), a=1.5" (38 mm)*
High	<12.0	<9.5
Moderate	12.0-21.0	9.5-16.5
Low	21.0-37.0	16.5-29.0
Very Low	37.0-254.0	29.0-199.0
Negligible	>254.0	>199

\*Note: a= Wenner probe spacing

#### 4.3.5. *Drying Shrinkage*

ASTM C157 was followed to conduct the shrinkage test. In this test, concrete bars were cast in the laboratory in a prism mold of 3" x 3" x 10" (75mm x 75mm x 250mm) [85]. All the aggregates were sieved so that they passed through a 1-in sieve (25.4 mm) before adding them to the mix. A laboratory mixer was used for mixing following ASTM C192 [86]. It is important to mention that the drying shrinkage concrete mixtures were also designed as per LaDOTD specifications for type A1 structural class concrete as mentioned in section 4.3.1 (i.e., w/b ratio of 0.45 and cement content of 344 kg/m<sup>3</sup>) [76]. However, these mixtures utilized different source of coarse and fine aggregates than the mixtures used for slump, air content, and cylinders. For the manufacture of drying shrinkage samples, the coarse aggregate (i.e., limestone) had a maximum nominal particle size of 25.4 mm, the fine aggregate had a maximum nominal particle size of 4.75 mm. The specific gravity

and absorption for coarse aggregate were 2.77 and 0.75%, respectively. Similarly, for fine aggregate the specific gravity and absorption were 2.62 and 0.76%, respectively. Three specimens were made for each test condition. The concrete specimens were demolded after  $23.5 \pm 0.5$  h since the addition of water to the cement and left for 23 minutes at a 95% humidity. After that, the specimens were placed in lime-saturated water maintained at  $73 \pm 1^\circ\text{F}$  [ $23 \pm 0.5^\circ\text{C}$ ]. After 30 min, the specimens were removed from the lime saturated water and the initial comparator reading was taken using a length comparator. After the initial comparator reading, the specimens were stored in lime-saturated water until they have reached an age of 28 days. During this wet curing, intermediate readings were taken at 3, 7, 14, and 28 days. To measure the drying shrinkage, the specimens were removed from lime water and stored in a drying room upon completion of the 28 days of curing. Comparator readings of each specimen were taken at the periods of air storage after curing of 4, 7, 14, and 28 days.

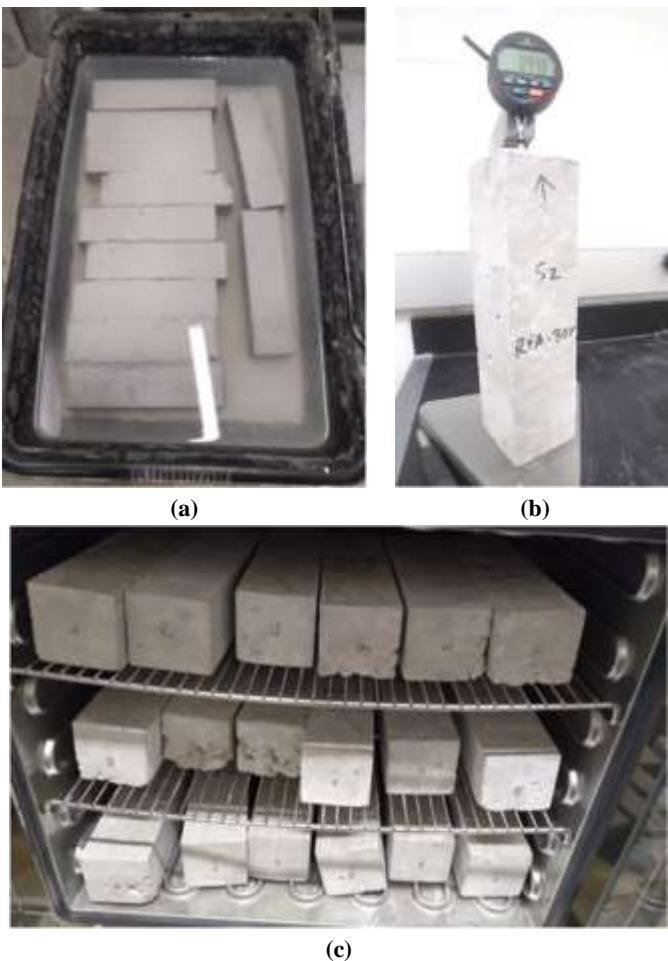


**Figure 11. Drying shrinkage test: (a) lime-saturated water curing of the specimens, (b) taking of reading, and (c) specimens in air storage**



#### 4.3.6. *Alkali-Silica Reactivity*

The ASR tests were conducted in the laboratory as per ASTM C1567 to determine the expansion of concrete in alkaline water [87]. In this test, mortar bars of 285 mm X 25 mm X 25 mm were prepared. The ratio of the cementitious material and aggregate was chosen as 1:2.25. Before adding to the mixture, the aggregates (sandstone, received from Texas) were crushed and sieved using a No.8 sieve size to achieve the required size according to the specification. The water-cement ratio was 0.47 for all the mixtures. The mixing was done as per ASTM C305, and the mortar bars were molded within 2 minutes and 15 seconds [88]. The mixture was loaded in two equal layers, and a tamper was used to compact each layer until a homogenous mix was obtained. For each test condition, two specimens were prepared. The mortar bars were then kept in the moist room after casting and demolded after 24 hours. The initial reading was taken after removing specimens from the mold. The bars were immersed in water at 80°C for another 24 hours. Zero reading was taken after the completion of 24 hours in the water bath and then a solution of 1N NaOH was prepared, and the mortar bars were placed in that solution at 80°C. This submerge condition was maintained until the final reading was taken. To determine the expansion, intermediate readings were taken on the 4<sup>th</sup>, 8<sup>th</sup>, 12<sup>th</sup>, 16<sup>th</sup>, and 20<sup>th</sup> days. A linear variable differential transformer (LVDT) sensor of an ELE Data System Unit (DSU) was used to measure the length changes.

The expansion rate was calculated by determining the difference between the zero reading and the reading at each period by using the following formula:

$$\Delta L = \frac{(L_x - L_0)}{G} \times 100$$

Where:

$\Delta L$  = change in length at x days of age (%),

$L_x$  = comparator reading of specimen at x age minus comparator reading of reference bar at x age,

$L_0$  = zero comparator reading of specimen minus comparator reading of reference bar at that same time, and

G = nominal gauge length.



(a)



(b)



(c)

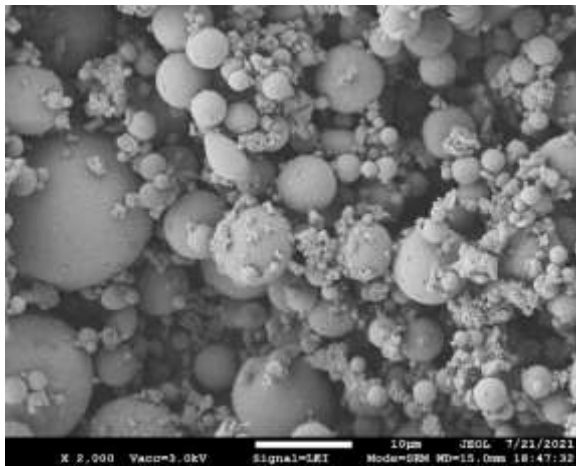
**Figure 12. ASR test: (a) crushed and sieved aggregates, (b) casting of mortar bar, (c) curing of specimen at 1N NaOH solution at 80°C**

## 5. ANALYSIS AND FINDINGS

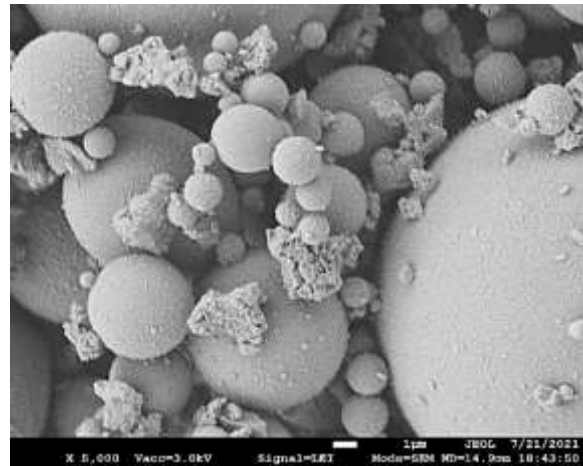
### 5.1. Characterization and Pozzolanic Activity of SCMs

#### 5.1.1. *Microstructure*

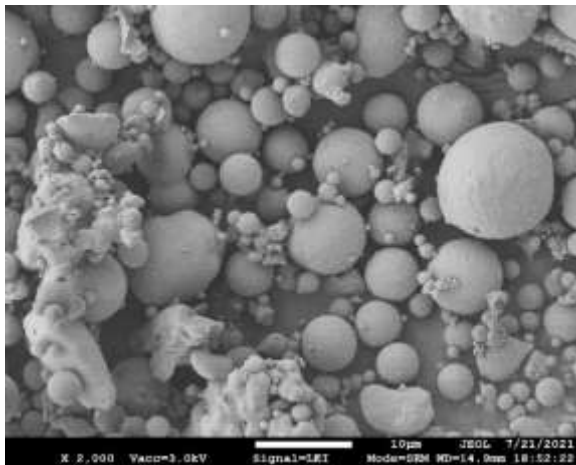
The microstructure of SCMs can significantly influence both the fresh and hardened properties of concrete materials. The SEM micrographs of all coal ashes and metakaolin, at 2000x and 5000x magnification, are presented in Figure 13. As it can be observed, FA and RFA (Figure 13a and Figure 13b) primarily consist of spherical particles. It should be noted that RFA has coarser impurities (i.e., irregular-shaped particles) compared to FA. This is likely because RFA is obtained by reclamation of old FA from landfills; thus, some coarse impurities were present. On the other hand, GBA (Figure 13c) mainly consists of prismatic particles with many sharp edges. Lastly, MK (Figure 13d) consists of plate-like particles that are much smaller than all three coal ashes. From these observations, FA and RFA have the potential to improve the workability of concrete materials due to their predominantly sphere-like shaped particles, which can produce a lubricant effect [19]. On the other hand, RFA and MK are likely to negatively impact the workability of concrete materials, given their irregular and angular shape. The loss in workability may be particularly exacerbated when using MK, given that it also exhibited markedly smaller particles, which increase the specific surface area. Nonetheless, the increase in surface area can enhance the reactivity of the SCM, thus producing positive impacts on concrete's hardened properties [89].



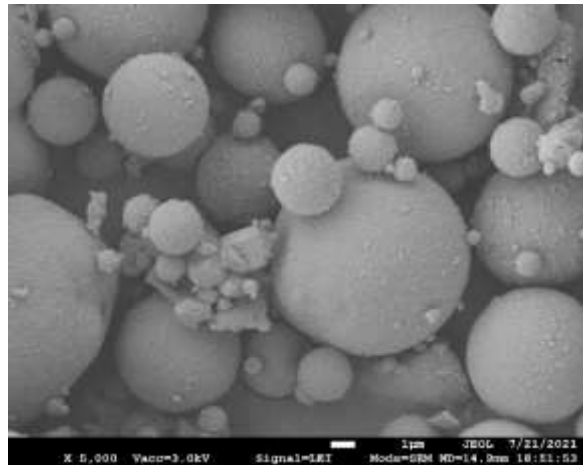
(a)



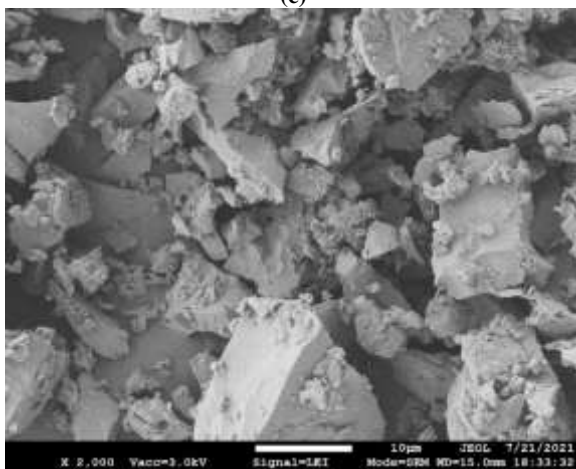
(b)



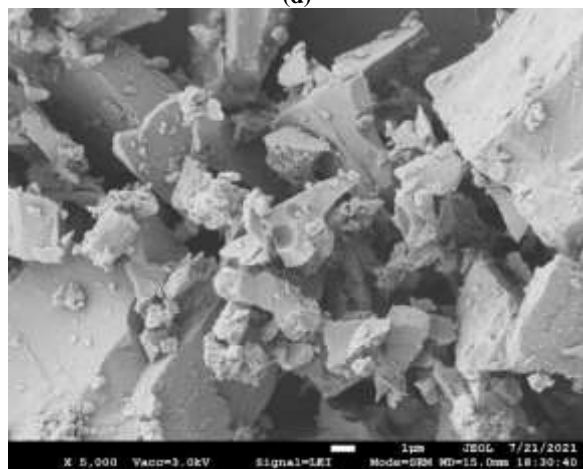
(c)



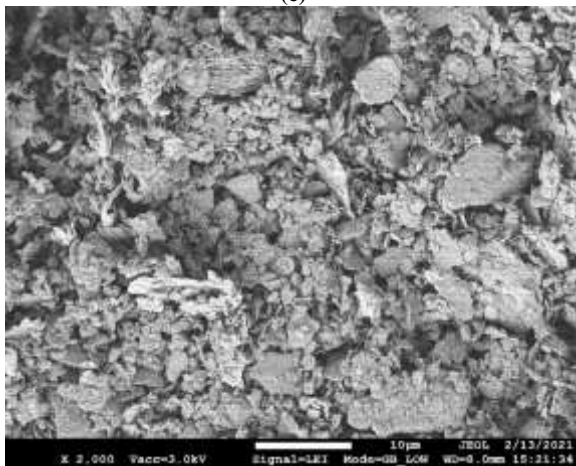
(d)



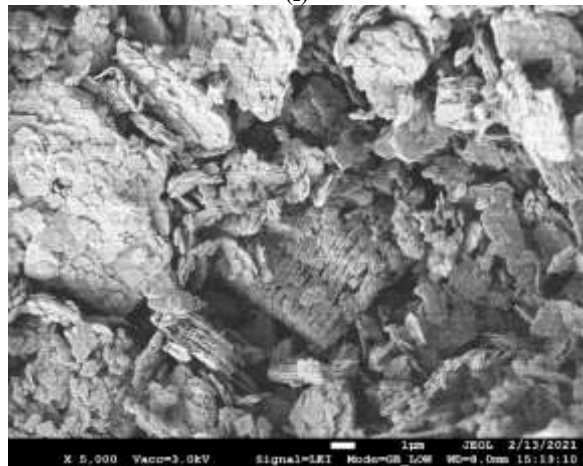
(e)



(f)



(g)



(h)

Figure 13. SEM images: a) FA at 2000x, b) FA at 5000x, (c) RFA at 2000x, (d) RFA at 5000x, (e) GBA at 2000x, (f) GBA at 5000x, (g) MK at 2000x, and (h) MK at 5000x

### 5.1.2. X-ray Diffraction (XRD) and X-ray Fluorescence (XRF)

The chemical oxide and phase composition of the coal ashes and metakaolin are presented in Table 10 and Figure 14, respectively. The chemical composition information from XRF is used to assist in identifying phases from XRD spectra. For FA, XRF shows that it is mainly composed of SiO<sub>2</sub>, Al<sub>2</sub>O<sub>3</sub>, Fe<sub>2</sub>O<sub>3</sub>, and CaO. Furthermore, from XRD, FA was identified to contain quartz (SiO<sub>2</sub>), portlandite (Ca(OH)<sub>2</sub>), and maghemite (Fe<sub>2</sub>O<sub>3</sub>) crystalline phases. Similarly, RFA is mainly composed of SiO<sub>2</sub>, Al<sub>2</sub>O<sub>3</sub>, Fe<sub>2</sub>O<sub>3</sub>, and CaO, and the crystalline phases identified were quartz (SiO<sub>2</sub>) and mullite (Al<sub>6</sub>Si<sub>2</sub>O<sub>13</sub>). In the case of GBA, it is primarily composed of SiO<sub>2</sub>, Al<sub>2</sub>O<sub>3</sub>, CaO, and Fe<sub>2</sub>O<sub>3</sub>, and crystalline phases identified were quartz (SiO<sub>2</sub>) and plagioclase feldspar ((NaAlSi<sub>3</sub>O<sub>8</sub>)<sub>n</sub>(CaAl<sub>2</sub>Si<sub>2</sub>O<sub>8</sub>)<sub>(1-n)</sub>). Lastly, MK is mainly composed of SiO<sub>2</sub>, Al<sub>2</sub>O<sub>3</sub>, and TiO<sub>2</sub>, and the only identified crystalline phase was anatase (TiO<sub>2</sub>). It is important to note that amorphous phases were present in the SCMs evaluated as indicated by the humps observed at around 18-28° 2θ. Notably, the amorphous hump for MK was the most pronounced; thus, signaling a larger amorphous content in contrast to the coal ashes. Moreover, among the coal ashes, FA and RFA displayed a more significant amorphous hump relative to GBA, which is indicative of a greater amorphous phase for FA and RFA relative to GBA.

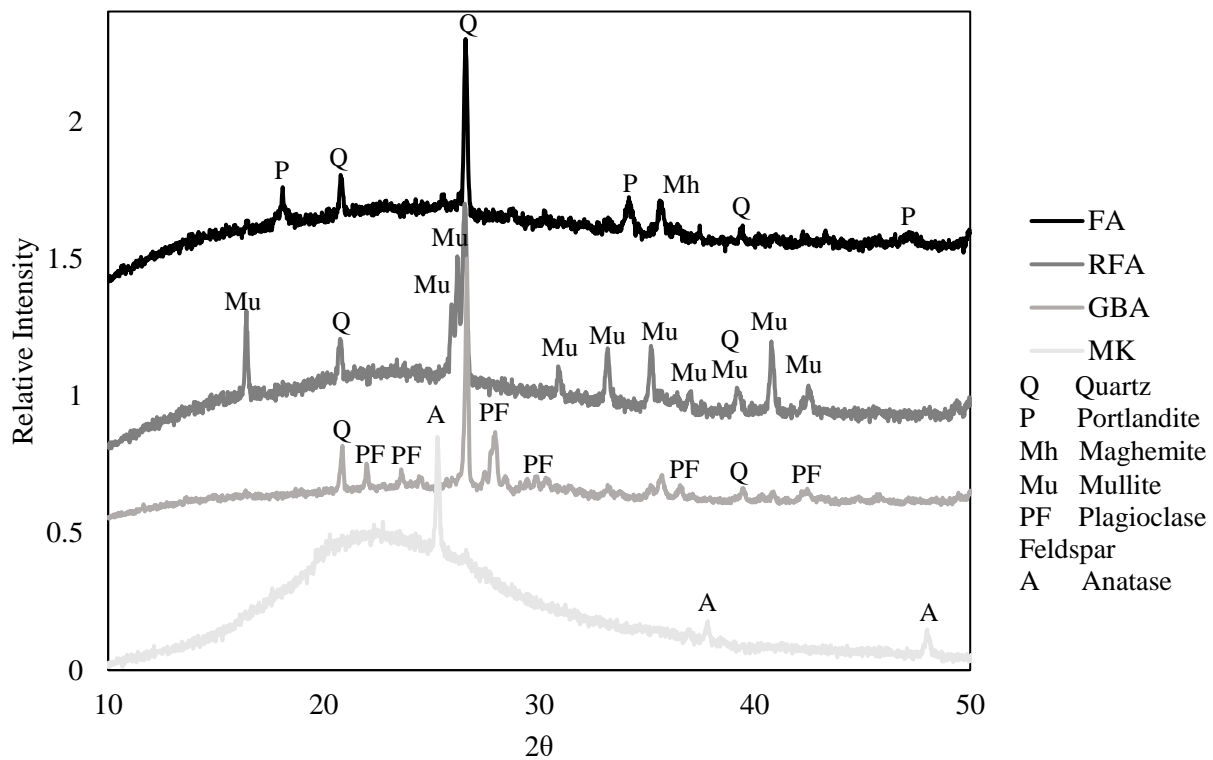


Figure 14. XRD spectra of SCMs.

From the oxide composition presented in Table 10, it can be observed that all the SCMs consist of silica (SiO<sub>2</sub>) and alumina (Al<sub>2</sub>O<sub>3</sub>) as their main constituents; however, MK presents the highest pozzolanic component among all materials evaluated in this study. Among the coal ashes, GBA

exhibited the highest calcium oxide (CaO) content, and RFA presented the lowest CaO content. Yet, GBA did not exceed the threshold to be classified as Class C fly ash as per ASTM C618 (i.e., >18% CaO) [90]. Furthermore, all coal ashes presented a similar pozzolanic component (i.e., the sum of SiO<sub>2</sub>, Al<sub>2</sub>O<sub>3</sub>, and Fe<sub>2</sub>O<sub>3</sub>), i.e., in the range from 87.6% to 89.8%. Relatively, MK has a much higher pozzolanic content (i.e., 96.8%) but mostly consists of silica and alumina. Nevertheless, all the coal ashes and MK presented a higher pozzolanic component than the minimum requirement of 70% to be classified as Class F pozzolan according to ASTM C618 [90]. Furthermore, the sulfur trioxide (SO<sub>3</sub>) content of all the coal ashes and MK was lower than the maximum limit of 5% as per ASTM C618 for Class F pozzolans [90].

**Table 10. Chemical composition of SCM from XRF.**

Material	CaO	SiO <sub>2</sub>	Al <sub>2</sub> O <sub>3</sub>	Fe <sub>2</sub> O <sub>3</sub>	SO <sub>3</sub>	MgO	K <sub>2</sub> O	Na <sub>2</sub> O	TiO <sub>2</sub>	SiO <sub>2</sub> +Al <sub>2</sub> O <sub>3</sub> +Fe <sub>2</sub> O <sub>3</sub> (%)
FA	8.42	57.19	20.21	10.18	1.18	1.58	2.68	1.15	-	87.58
RFA	1.85	53.39	28.01	7.72	0.09	1.00	2.24	0.33	-	89.12
GBA	11.04	62.05	20.83	6.96	0.49	2.82	0.88	0.32	-	89.84
MK	0.02	50.10	46.22	0.46	0.04	0.00	0.14	0.31	2.71	96.78

### 5.1.3. Particle Size Analysis

The particle size distribution of the different SCMs is plotted in volume % vs. particle size in Figure 15. Overall, the results agree with the SEM observations where MK has significantly finer particles than the other three SCMs with most particles ranging between ~2-11 μm. Furthermore, RFA exhibited the largest particles of all the SCMs evaluated, with most of them in the order of ~3-120 μm. In the cases of FA and GBA, both SCMs exhibited similar particle sizes with most of their particles ranging between ~4-47 and ~7-40 μm, respectively. In addition, from Figure 15, it is observed that the mean particle size of RFA was 64.5 μm, whereas for GBA, FA, and MK the mean particle size was 23.2 μm, 19.2 μm, and 6.0 μm respectively.

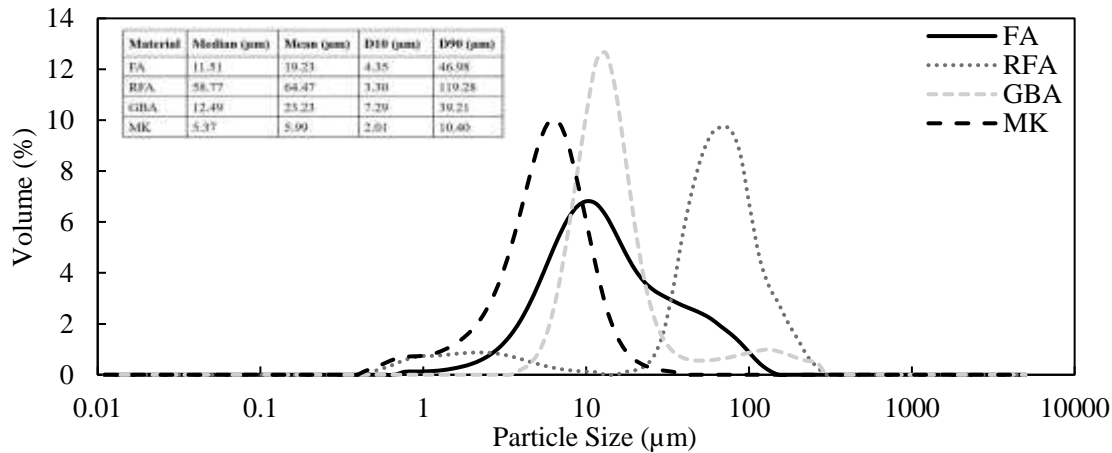


**Figure 15. Particle size distribution of SCMs.**

#### 5.1.4. Moisture Content (MC) and Loss on Ignition (LOI)

As per ASTM C618, the materials should meet the requirement for LOI (i.e., maximum limit of 6%) and moisture content (i.e., maximum limit of 3%) to be classified as a Class F pozzolan. From the data presented in Table 11, all four materials evaluated in this study meet the ASTM C618 requirements for LOI and moisture content. Interestingly, RFA presented the highest LOI, followed by FA, GBA, and finally by MK.

Table 11. Moisture content and LOI of coal ashes and MK.

Materials	Moisture Content (%)	LOI (%)
FA	0.4	1.42
RFA	0.1	2.95
GBA	0.3	0.92
MK	0.0	0.28

#### 5.1.5. Thermogravimetric Analysis

**Error! Reference source not found.** presents the thermogravimeter (TG) and differential thermogravimeter (DTG) curves after 240 hours (i.e., 10 days) of heat treatment for all coal ashes and MK that were mixed with calcium oxide and potassium hydroxide solution. DTG curves for all materials consist of two distinct peaks: (1) the first DTG peak occurring at the temperature range from 25 to 100°C indicates the loss of evaporable water, and (2) a less pronounced second peak occurring in the temperature range from 350°C to 550°C presents a mass loss of the decomposition of calcium hydroxide, Ca(OH)<sub>2</sub>. The mass of free calcium hydroxide (CH) was calculated by using Equation 2. The difference in mass of initial CH and the mass of free CH (obtained from Equation 2) is divided by the amount of SCMs to obtain the CH consumption for each SCM. Figure 17 presents the CH consumption for all coal ashes and MK. The CH consumption for FA, RFA, GBA, and MK is 81.1, 124.0, 91.4, and 219.6 g/100g of SCM, respectively. Among all the materials evaluated in this study, MK presented the highest CH consumption, and FA presented the lowest CH consumption. In addition, both RFA and GBA exhibited higher CH consumption than class F fly ash, signifying a greater pozzolanic reactivity. The higher CH consumption of MK is attributed to different properties, including its very fine particle size (i.e., high surface area), high amorphous content, and high content of silica and alumina. It is important to mention that SCMs exhibiting Ca(OH)<sub>2</sub> consumption higher than 50 g/100 g of SCM are classified as pozzolanic as per Suraneni et al. [75]. As such, all materials evaluated in this study met the criteria to be classified as pozzolans.

$$\text{Mass of free CH} = \text{Mass loss in the second steps of TG curve} * \frac{\text{Molar mass of Ca(OH)}_2 \text{ (i.e.,74.1)}}{\text{Molar mass of H}_2\text{O (i.e.,18)}} [2]$$

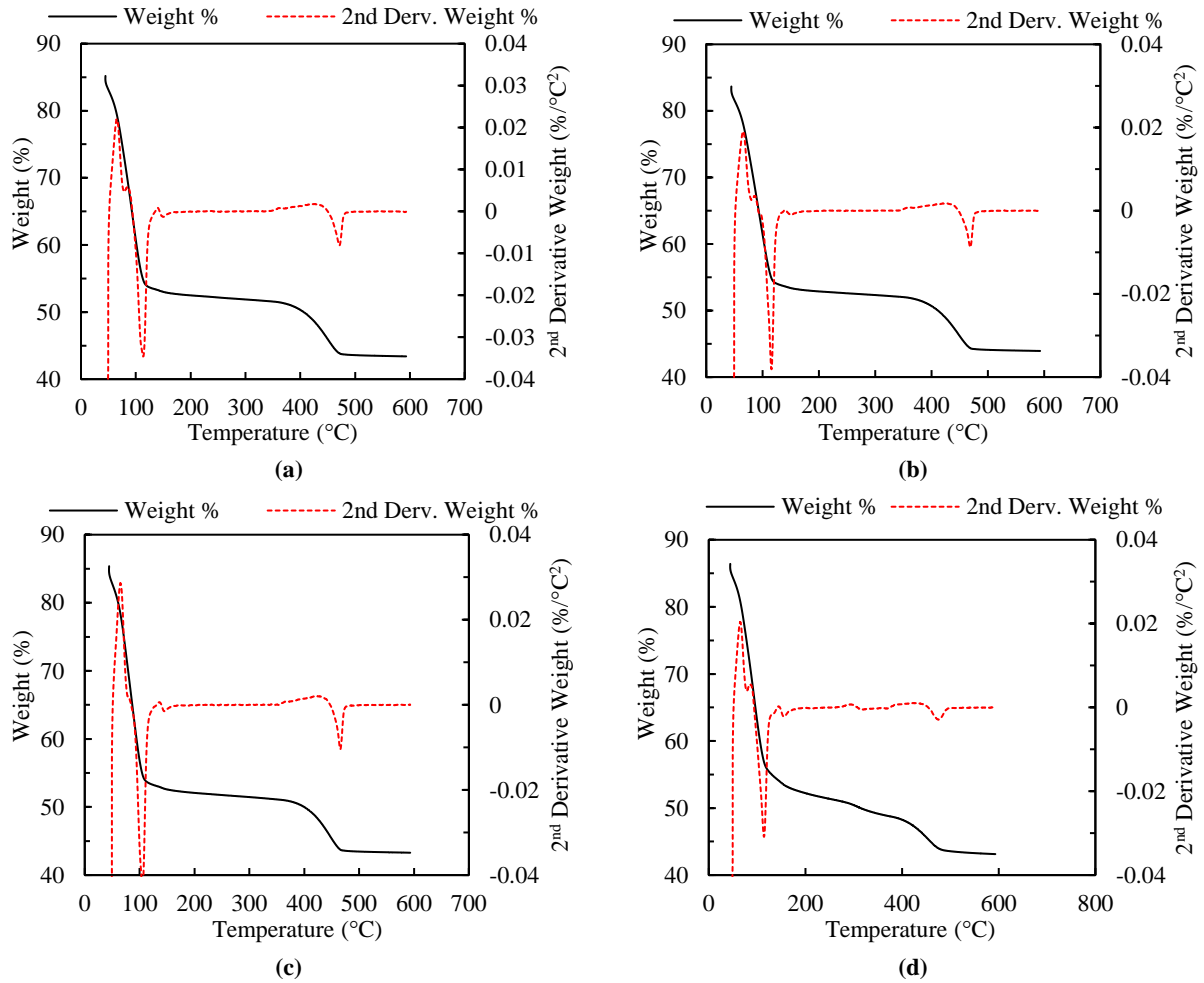


Figure 16. TGA curves: (a) FA, (b) RFA, (c) GBA, and (d) MK

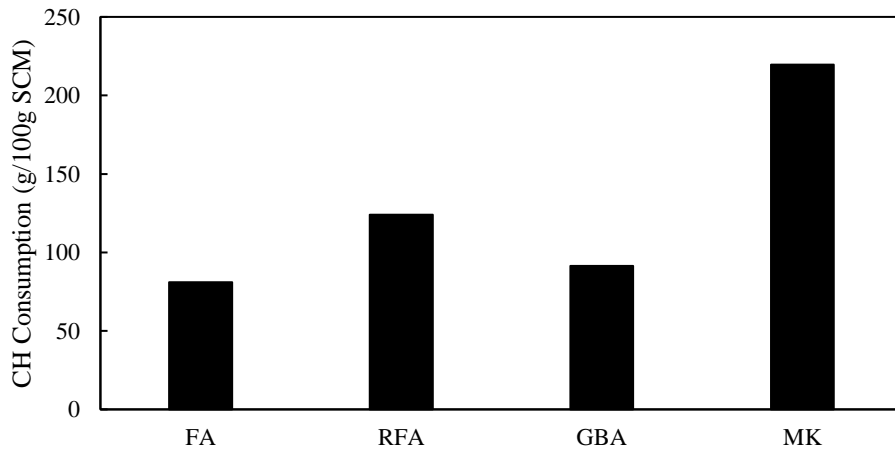


Figure 17. CH consumption of SCMs



### 5.1.6. *Strength Activity Index (SAI)*

The water requirement of the different SCMs as well as that of the combined systems of RFA-MK and GBA-MK (i.e., ternary systems), are presented in Table 12. From Table 12, it is clear that none of the coal ashes increased water requirement; instead, minor reductions are observed for RFA and GBA, i.e., 4.9% and 3.7%, respectively. In comparison to RFA and GBA, FA significantly reduced the water demand to achieve the same workability (i.e., 10.8%). In contrast to coal ashes, MK significantly increased water demand (i.e., by 18.6%). Among all materials evaluated in this study, FA is the most efficient material to reduce water demand, followed by RFA, GBA, and MK. It is worth mentioning that MK did not meet the ASTM C618 water requirement to be classified as a pozzolan (i.e., a maximum limit of 105% compared to the control mixture to be classified as class F or C pozzolan). The higher water requirement of RFA compared to FA is attributed to the presence of the mullite particles as observed by the XRD spectra in Figure 14. Similarly, for GBA, the higher water requirement than FA is due to irregular angular particles observed in SEM imaging (i.e., Figure 13). Likewise, the irregular and plate-shaped particles, in tandem with the very small particle size of MK, led to a significant increase in water requirement. For ternary mixtures, a progressive increase in water requirement with the increase in the MK content is observed. Nevertheless, even at the highest replacement level of RFA or GBA with MK (i.e., 30% by mass), the water requirement did not exceed that of the control mixture without SCMs (i.e., CO). As such, 30% of RFA or GBA can be replaced with MK without producing an increase in water demand.

**Table 12. Water requirement for binary and ternary mortar mixtures**

Mix ID	Water Requirement (%)	W/C Ratio
CO	100.0	0.48
FA	89.2	0.43
RFA	95.1	0.46
GBA	96.3	0.47
MK	118.6	0.57
90RFA+10MK	96.9	0.47
80RFA+20MK	98.4	0.48
70RFA+30MK	100.0	0.48
90GBA+10MK	99.2	0.48
80GBA+20MK	99.6	0.48
70GBA+30MK	100.0	0.48

The 7- and 28-day compressive strength results and corresponding SAI for 50-mm mortar cubes for all binary mixtures are presented in Figure 18. The SAI for FA, RFA, GBA, and MK after 7 days of curing was 92.2%, 87.1%, 101.0%, and 101.0%, respectively. It is important to note that both GBA and MK presented the same and highest SAI at 7 days of curing. On the other hand, RFA presented the lowest SAI at 7 days of curing. At 28 days of curing, the SAI for FA, RFA, GBA, and MK was 92.7%, 94.0%, 91.6%, and 112.9%, respectively. As such, at 28 days of curing, MK and GBA exhibited the highest and lowest SAI, respectively. Furthermore, among the coal ashes, RFA presented the highest SAI at 28 days of curing. Importantly, all coal ashes and MK

exhibited higher SAI than the minimum requirement of 75% (for both 7 and 28 days of curing) as per ASTM C618 to be classified as a pozzolan [90].

Even though GBA and MK exhibited the same SAI at 7 days of curing, the lower SAI for GBA at 28 days is likely attributed to its lower amorphous content, lower pozzolanic component, and larger particle size than MK, resulting in slower pozzolanic reactivity and weaker filler effect in comparison to MK. In contrast, the higher 7-day SAI for GBA, compared to FA or RFA, may be attributed to the higher CaO content (as observed from XRF in Table 10). The outperformance of MK compared to FA and RFA at both curing ages is likely attributed to its smaller particle size, higher pozzolanic content, and amorphous content, allowing it to react more rapidly and exhibit a stronger filler effect; thus, resulting in higher strength. The substantial increase in the SAI of RFA from 7 days to 28 days of curing compared to FA and GBA is attributed to the higher pozzolanic activity of RFA as indicated by the greater CH consumption of RFA in contrast to GBA and FA from TGA analysis.

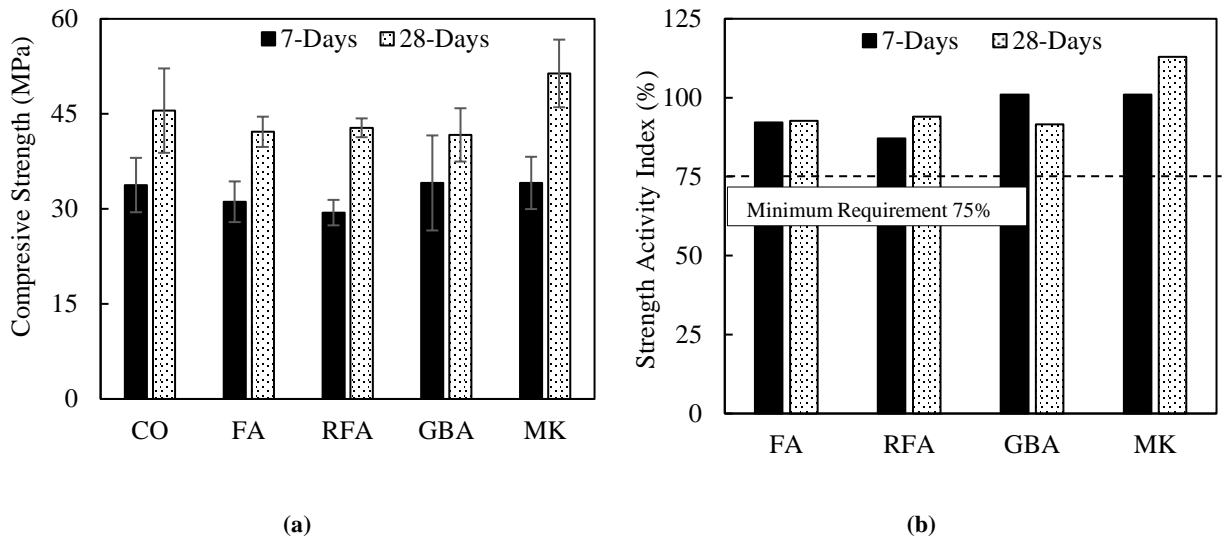
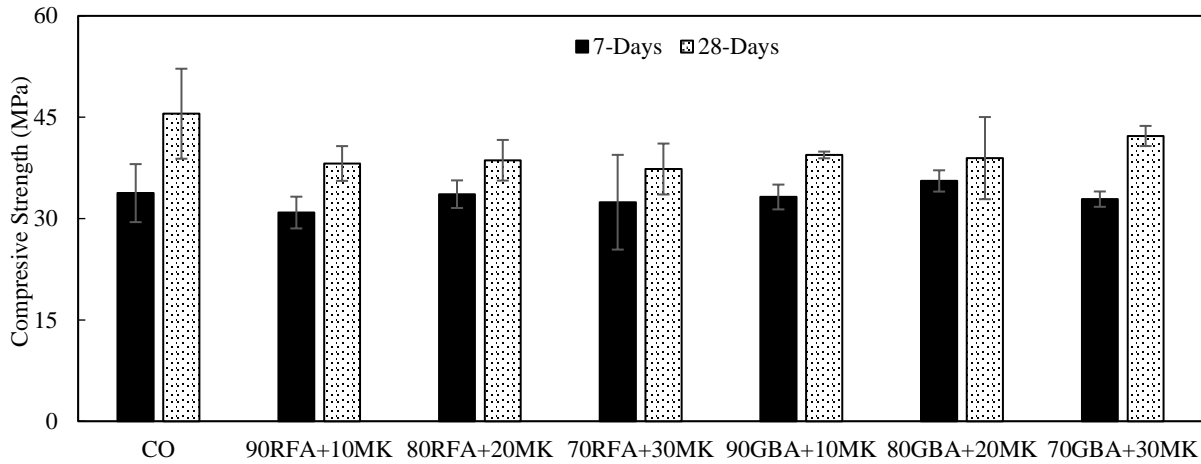


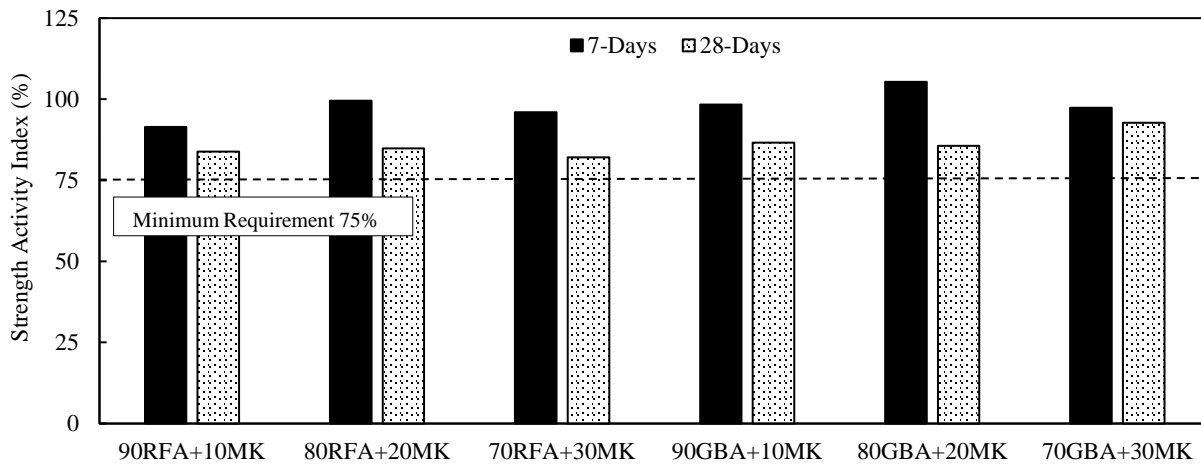
Figure 18. 7- and 28-day SAI results for binary mixtures: (a) compressive strength and (b) SAI

The 7- and 28-day compressive strength results and corresponding SAI for 50-mm mortar cubes for all ternary mixtures are presented in Figure 19. The 7-day SAI for the RFA-MK combined systems are 91.5%, 99.5%, and 96.0% at 10, 20, and 30% replacement of RFA with MK, respectively, which reduced to 83.8%, 84.9%, and 82% at 28 days, respectively. Likewise, for the GBA-MK combined systems, the 7-day SAI for 10, 20, and 30% replacement of RFA with MK was 98.3%, 105.3%, and 97.3%, respectively, which reduced to 86.5%, 85.5%, and 92.7% at 28 days of curing, respectively. Comparatively, the GBA-MK systems exhibited higher SAI than the RFA-MK systems at both curing ages. Nevertheless, at all replacement levels, both combined systems met the minimum requirement of 75% for SAI to be classified as a pozzolan. Relative to GBA alone (i.e., binary system), the GBA-MK systems (i.e., ternary systems) outperformed the binary systems at 20% replacement of GBA with MK for 7 days and 30% replacement of GBA with MK for 28 days. On the other hand, relative to RFA alone, all RFA-MK systems exhibited higher SAI at 7 days, yet none of the RFA-MK systems outperformed RFA alone at 28 days. Even

though MK admixed binary mixtures generally exhibited higher strength than the RFA-MK or GBA-MK combined systems, the combined systems are considered more sustainable than MK alone as these systems use waste and in-expensive materials (i.e., RFA and GBA), thus making concrete more environment-friendly and economical. From the present experimental results, ternary systems of RFA-MK and GBA-MK at 30% replacement level of coal ash with MK were selected for further evaluation in concrete.



(a)



(b)

Figure 19. 7- and 28-day SAI results for ternary mixtures: (a) compressive strength and (b) SAI

The summary of the experimental results of ASTM C618 tests conducted, along with the limits for each test, are presented in Table 14. From Table 14, it is evident that all the SCMs met the different ASTM C618 requirements evaluated to be classified as Class F pozzolan, excepting MK for water requirement.

**Table 13. Summary of alternative SCMs properties**

SCM	Chemical Requirement		Moisture Content (Max. 3%)	LOI (Max. 6.0%)	Strength Activity Index (Min. 75%)		Water Requirement (Max. 105%)
	SiO <sub>2</sub> +Fe <sub>2</sub> O <sub>3</sub> +Al <sub>2</sub> O <sub>3</sub> (Min. 70%)	SO <sub>3</sub> (Max. 5%)			7 Days	28 Days	
RFA	89.12 ✓	0.09 ✓	0.1 ✓	2.95 ✓	87.1 ✓	94.0 ✓	95.1 ✓
GBA	89.84 ✓	0.49 ✓	0.3 ✓	0.92 ✓	101.0 ✓	91.6 ✓	96.3 ✓
MK	96.78 ✓	0.04 ✓	0.0 ✓	0.28 ✓	101.0 ✓	112.9 ✓	118.6 X

(✓) Met the requirement, (X) Did not meet the requirement

## 5.2. Testing of SCMs Admixed Concrete Mixtures

### 5.2.1. Slump

The workability of fresh concrete mixtures was evaluated using the slump test as per ASTM C143 (42). The slump test results for all binary concrete mixtures are presented in Figure 20. The effect of each of the evaluated SCMs on the workability of concrete mixtures is observed in Figure 20. Except for FA, all other SCMs (i.e., RFA, GBA, and MK) exhibited a progressive decrease in the workability of concrete mixtures with the increase in cement replacement levels. For instance, the slump value for the control mixture was 3.5 inches, which decreases in the range from 3.25 to 2.31 inches, 1.75 to 1.13 inches, and 0.50 to 0.10 inches for RFA, GBA, and MK admixed concrete mixtures, respectively. It is important to mention that the use of MK resulted in a dramatic decrease in the workability of the fresh concrete mixtures to the extent that the materials could not be properly mixed. As such, that the HRWR dosage had to be increased to produce a workable mixture. The increased dosage of MK admixed mixtures is presented in Table 7. In contrast, FA noticeably increased the workability of concrete mixtures at both 20 and 30% cement replacement levels, while at 10% replacement, it exhibited comparable workability to the control mixture (i.e., 3.5 inches). Among the coal ashes, GBA admixed concrete mixtures exhibited evident decrements in workability relative to the control mixture at all cement replacement levels evaluated. On the other hand, RFA did only produce noticeable decrements in workability relative to control at 20 and 30% cement replacement levels. Nevertheless, mixtures using GBA or RFA showed a significantly higher slump than those implementing MK. The decrease in workability observed for mixtures using RFA, GBA, and MK suggest that all SCMs admixed concrete mixture, excepting those using FA, require more water than the control mixture to achieve similar workability. The workability exhibited by concrete mixtures using SCMs was consistent with the water requirement test, where FA revealed the lowest water demand, followed by RFA, GBA, and MK. The enhancements in slump observed for FA admixed concrete mixtures are attributed to the sphere-like particle morphology of FA [19]. It is interesting to note that RFA did also exhibit similar morphology as FA, but it did not enhance the workability of the mixture. As such, the mullite impurities present in RFA likely led to the decreased workability. On the other hand, the noticeable increase in the water demand for GBA is credited to its irregular and angular-shaped particles, as observed in Figure 13 (14). Likewise, the irregular and plate-shaped particles of MK also resulted in the reduced workability of concrete mixtures. In addition, from particle size analysis, it was observed that MK has very fine particles; thus, resulting in high surface area and lower workability.

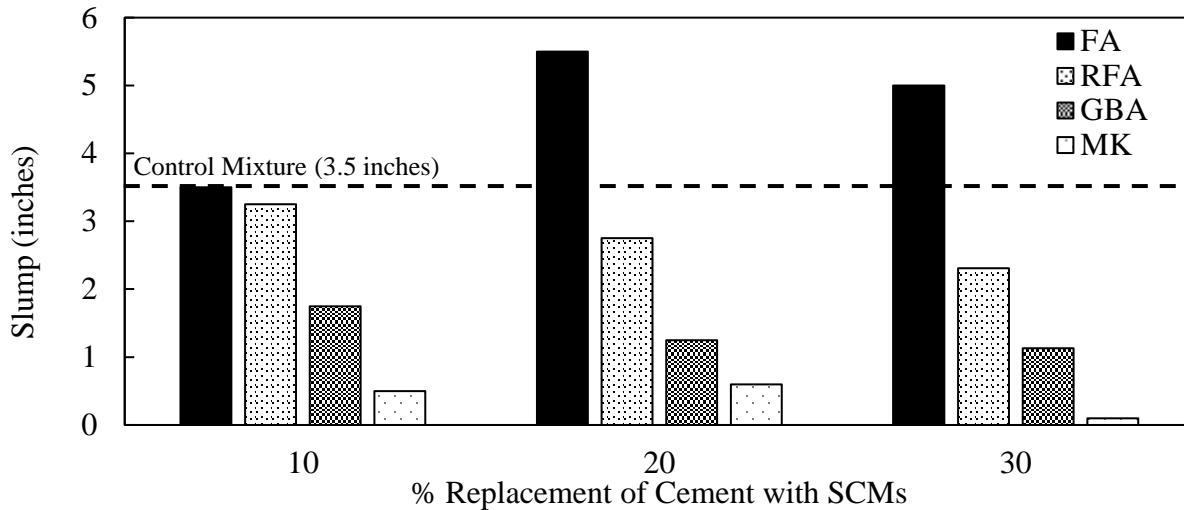


Figure 20. Slump of fresh concrete mixtures (binary systems)

The slump of all ternary mixtures produced in this study is presented in Figure 21. It is observed that all ternary mixtures exhibited a lower slump value than the control mixture. Specifically, concrete mixtures using GBA-MK presented a higher decrease in a slump than mixtures using RFA-MK as SCMs. For instance, RFA-MK and GBA-MK combined system presented slump values ranging from 2.5 to 0.75 and 1.5 to 0.13 inches, respectively. From binary mixtures slump results (i.e., Figure 20), it is observed that GBA and MK produced a lower slump than RFA. As such, a similar trend was observed in ternary mixtures, where the GBA-MK combined system exhibited a lower slump than the RFA-MK combined system.

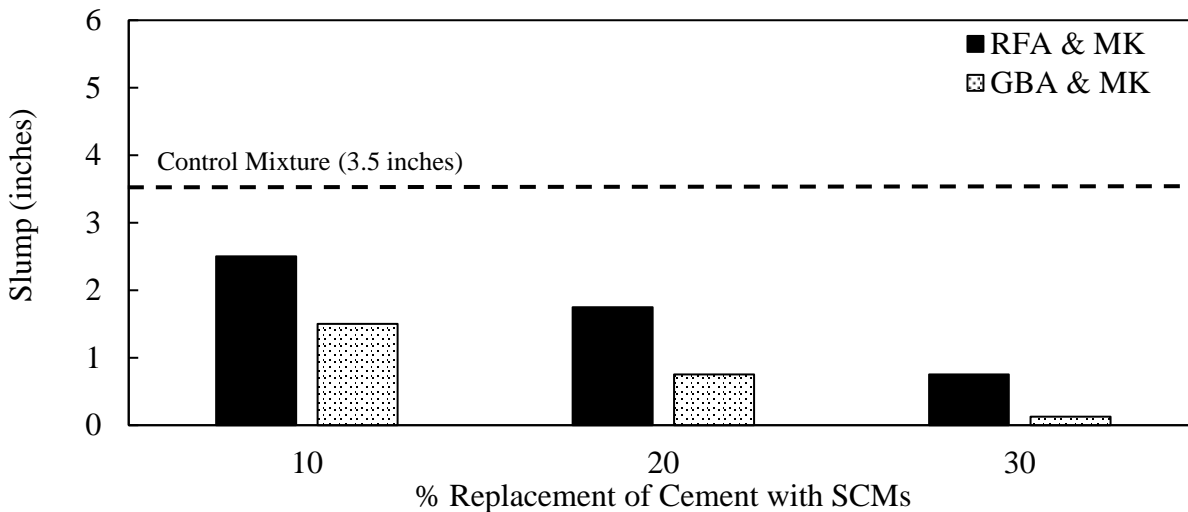


Figure 21. Slump of fresh concrete mixtures (ternary systems)

### 5.2.2. Air Content and Unit Weight

The air content and unit weight of the fresh concrete mixtures were evaluated as per ASTM C231 and ASTM C138, respectively (42). Air content results for all binary concrete mixtures produced in this study are presented in Figure 22. It is observed that concrete mixtures utilizing any of the SCMs exhibited lower air content than the control mixture (i.e., 5.5%), except for FA-20. For instance, FA, RFA, GBA, and MK admixed concrete mixtures exhibited air content in the range of 3.5% to 5.6%, 4.5% to 4.8%, 2.8% to 3.6%, and 3.2% to 3.8%, respectively. At 10% cement replacement level, the mixture using RFA presented the lowest decrease in air content relative to control, whereas the mixture using MK presented the highest decrease in air content. Furthermore, at 20% cement replacement level, the FA admixed concrete mixture exhibited the lowest decrease in air content while the mixture using GBA produced the lowest air content decrease. Finally, at 30% cement replacement level, the mixture using RFA produced the lowest decrease in air content, whereas the mixture using GBA produced the largest decrease. From the experimental results, generally, RFA produced the lowest decrease in air content while GBA tended to produce the highest decrease. The air content of the fresh concrete mixture is influenced by different characteristics of the SCMs, including the nature and content of organic coal residues as well as the fineness of the SCMs (a decrease in carbon content and increase in fineness of SCMs generally decreases the air content of concrete mixtures) [69]. MK exhibited the smallest average particle size among all SCMs evaluated in this study, while RFA exhibited the largest (i.e.,  $\approx 10$  times that of MK and  $\approx 3$  times that of GBA and FA). As such, the decrease in air content for mixtures using GBA and FA relative to those using RFA is likely attributed to their smaller particle size. Interestingly, MK admixed concrete mixtures did not exhibit the lowest air content among all mixtures even though MK exhibited the smallest particle size among all SCMs evaluated. This is likely due to the higher content of HRWR required for MK admixed concrete mixtures at 20 and 30% cement replacement levels. As reported in Table 7. Binary system concrete mixture proportions., MK mixtures used higher HRWR dosage to produce a workable mixture. The existing literature shows that the increase in the dosage of polycarboxylate-based HRWR increases the air content [91]. Consequently, the higher air content of mixtures implementing MK compared to those using GBA at 20 and 30% cement replacement levels is likely credited to the higher dosage of HRWR used in MK mixtures. Besides the effect of particle size of SCMs, the content and properties of carbon in the SCMs also influence concrete mixtures' air content. It is important to note that RFA exhibited the highest LOI among all SCMs evaluated in this study, yet the replacement of cement with RFA did not result in the highest decrease in air content; rather, it generally presented the lowest decrease in air content among all concrete mixtures. This is likely attributed to the influence of other factors, such as carbon surface polarity, pore size, and surface area on the air content of concrete mixtures. Nonetheless, these factors were not investigated for the SCMs evaluated in the present study, and therefore the interaction mechanism between the carbon present in the different SCMs and air in concrete cannot be fully elucidated.

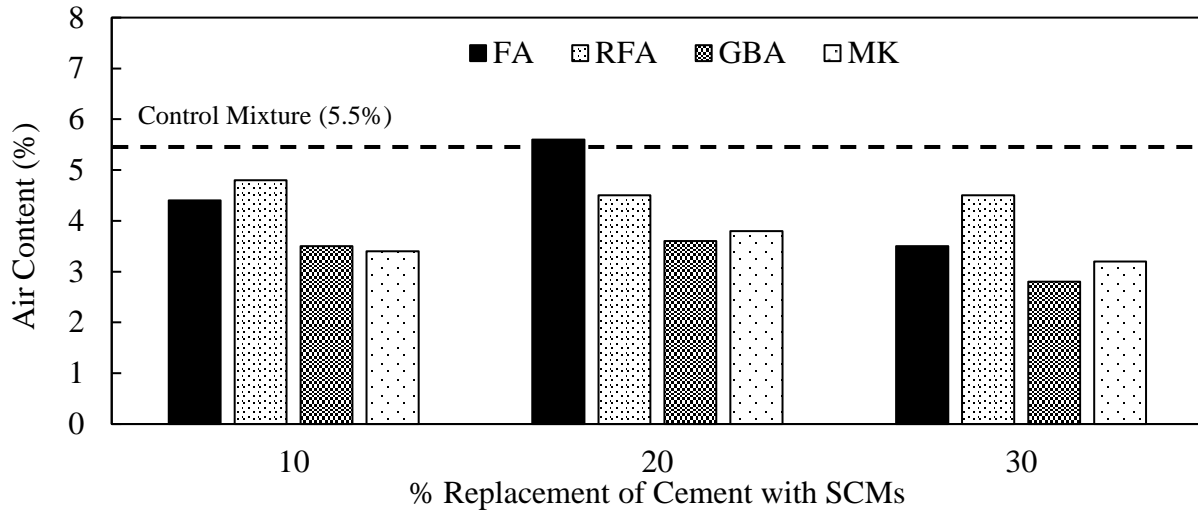


Figure 22. Air content for of fresh concrete mixtures (binary systems)

Figure 23 presents the air content of all ternary mixtures produced in this study. Three clear tendencies are observed, (1) all ternary mixtures produced lower air content than the control mixture, (2) the increase in cement replacement with SCMs produced a more significant decrease in air content relative to control, and (3) RFA-MK mixtures exhibited higher air content than GBA-MK mixtures. Relative to the binary RFA mixtures, the RFA-MK ternary mixtures produced lower air contents. Furthermore, in the case of the GBA-MK ternary mixtures, air content remained comparable to that of the GBA binary mixtures.

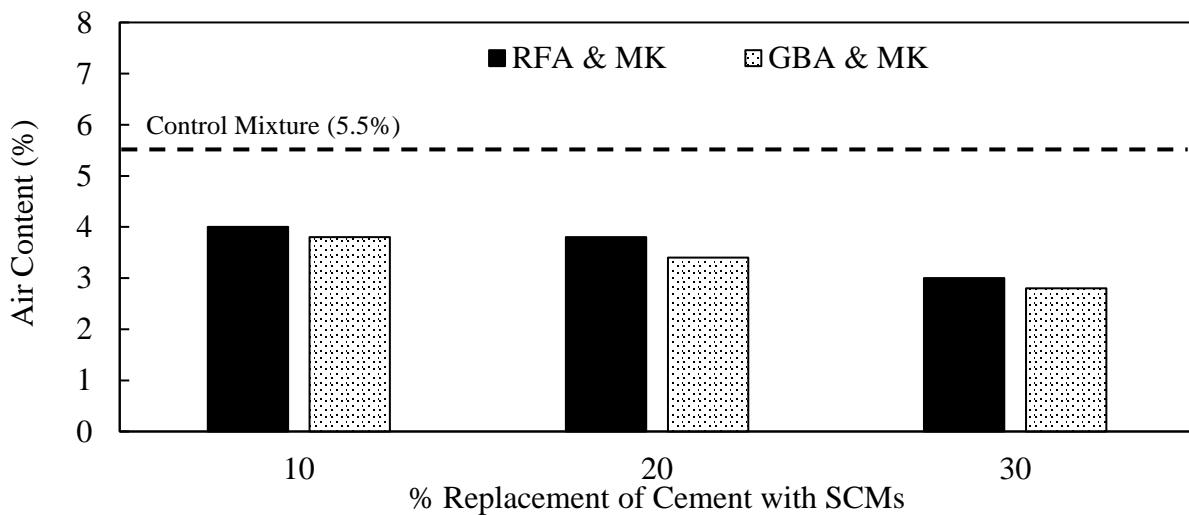


Figure 23. Air Content of fresh concrete mixtures (ternary systems)

The unit weight of all fresh binary mixtures is presented in Figure 24. It is observed that the control mixture exhibited a unit weight of  $2410 \text{ kg/m}^3$ , which decreases marginally for all other SCMs admixed concrete mixtures (i.e., a maximum decrease of 5.7% in comparison to the control mix is observed for FA-30). Among all SCMs admixed concrete mixtures, FA mixtures present the lowest unit weight, which is likely attributed to the low specific gravity of fly ash (i.e., 2.36) relative to

the cement (i.e., 3.15) as well as high air content when compared to other SCMs admixed concrete mixtures. In contrast, GBA presented the highest unit weight among all SCMs admixed concrete mixtures at 10% cement replacement level, and MK presented the highest unit weight at 20 and 30% cement replacement levels. This is likely attributed to the lower air content of MK and GBA admixed concrete mixtures and the higher specific gravity of GBA (i.e., 2.67) and MK (i.e., 2.5) relative to FA (i.e., 2.36) and RFA (i.e., 2.21).

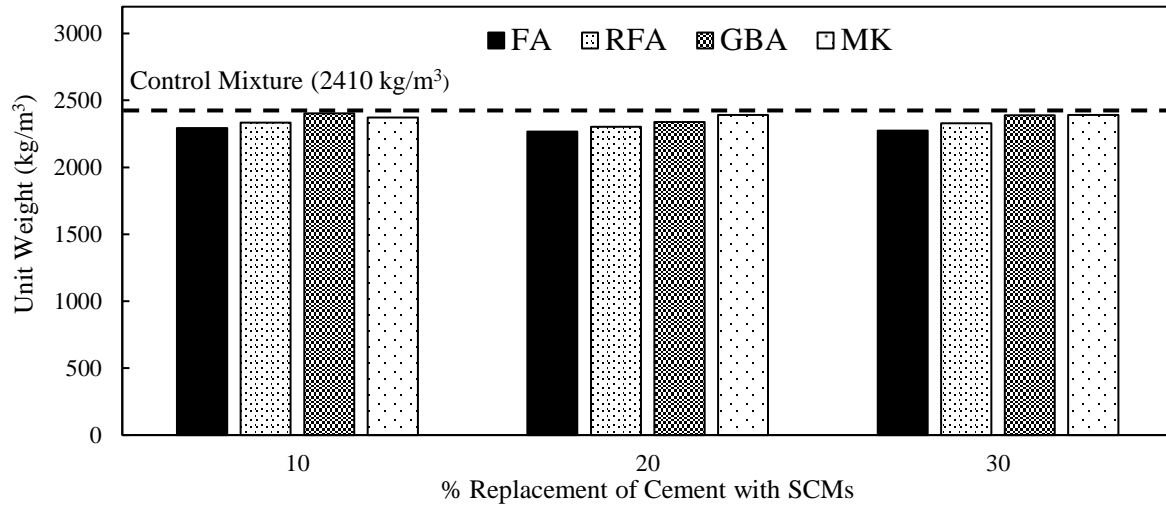


Figure 24. Unit Weight of fresh concrete mixtures (binary systems)

The unit weight of all fresh ternary mixtures is presented in Figure 25. It is observed that the control mixture exhibited the highest unit weight, which decreases marginally for both RFA-MK and GBA-MK combined systems (i.e., a maximum decrease of 3.4% in comparison to the control mixture is observed for RFA-MK-20). Relatively, GBA-MK admixed concrete mixtures exhibited slightly higher unit weight than RFA-MK mixtures. This is likely attributed to the higher specific gravity of GBA (i.e., 2.67) in comparison to RFA (i.e., 2.21) and the lower air content of GBA-MK mixtures in comparison to the RFA-MK mixtures. Nevertheless, the difference in air content between these two ternary mixtures is negligible.



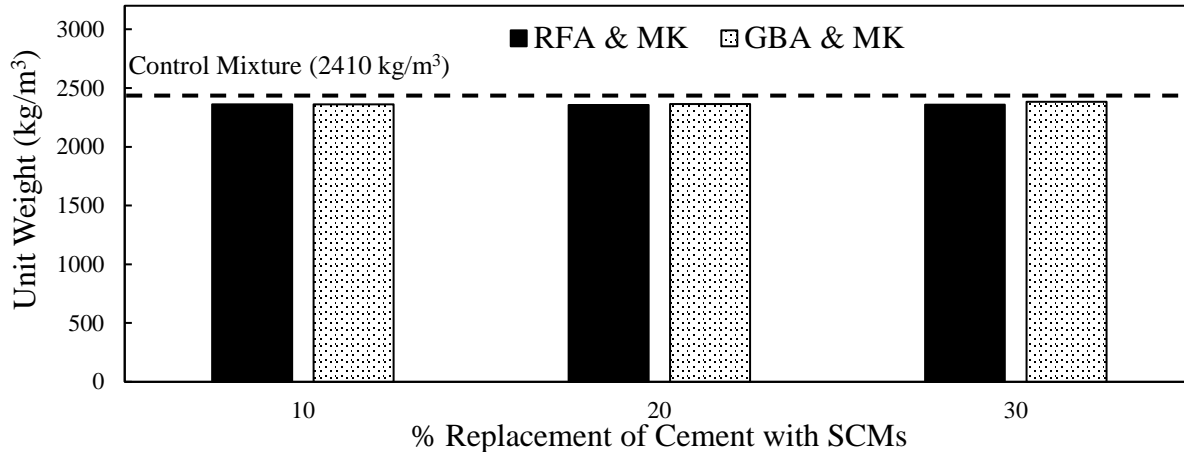
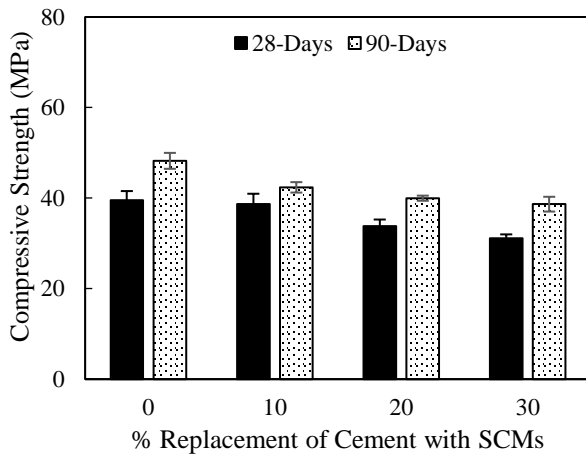


Figure 25. Unit Weight of fresh concrete mixtures (ternary systems)

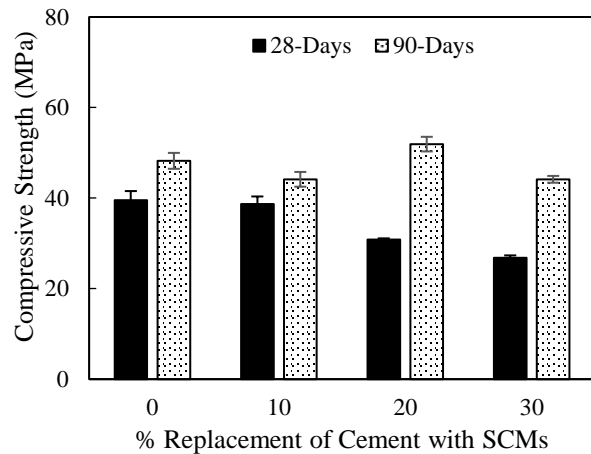
### 5.2.3. Compressive Strength

The 28- and 90-day compressive strength for all binary concrete mixtures are presented in Figure 26. As shown, the control mixture exhibited a compressive strength of 39.5 MPa and 48.2 MPa after 28 and 90 days of curing, respectively. As such, the specified 28-day compressive strength of 31 MPa as per LaDOTD for type A1 structural class concrete was exceeded by the control mixture [76]. From Figure 26a, it is observed that all FA admixed concrete mixtures exhibited a progressive decrement in compressive strength with the increase in cement replacement at both curing ages. Furthermore, from Figure 26b, RFA admixed concrete mixtures did also present a decrease in compressive strength with the increase in cement replacement at 28 days of curing. However, after 90 days of curing, decrements in strength relative to the control mixture were only observed at 10 and 30% cement replacement levels, whereas an increase in compressive strength was observed at 20% cement replacement level. In the case of GBA mixtures, only 30% cement replacement after 28 days of curing produced a decrement in strength relative to control. All other GBA admixed concrete mixtures exhibited higher compressive strength than the control mixture at both 28 and 90 days of curing. For MK admixed concrete mixtures, a notable increase in compressive strength was observed relative to the control mixture at all cement replacement levels after both 28 and 90 days of curing. After 28 days of curing, the compressive strength of mixtures implementing FA, RFA, GBA and MK ranged from 31.2 to 38.7 MPa, 26.8 to 38.7 MPa, 36.1 to 40.94 MPa, and 52.1 to 67.8 MPa, respectively. Moreover, after 90 days of curing, the compressive strength of mixtures implementing FA, RFA, GBA and MK ranged from 38.7 to 42.4 MPa, 44.1 to 51.9 MPa, 48.8 to 54.8 MPa, and 50.5 to 68.2 MPa, respectively. Generally, in terms of compressive strength, the best SCM among the coal ashes was GBA, while MK was the best performing SCM among all the SCMs evaluated. Between FA and RFA mixtures, FA mixtures tended to perform better than RFA mixtures after 28 days of curing (except for 10% cement replacement level); however, after 90 days of curing, RFA mixtures outperformed FA mixtures at all cement replacement levels. This is attributed to the inferior pozzolanic activity of FA relative to RFA, as indicated by its lower CH consumption from TGA analysis.

An analysis of variance (ANOVA) conducted at a 5% confidence level showed statistically significant differences in the average compressive strength among the concrete mixtures at both curing ages (i.e., at both curing ages  $p\text{-value} < 0.0001$ ). As such, to identify the mixtures that were statistically different, Tukey's honest significance difference (HSD) test was performed on all possible combinations. The ANOVA and Tukey's HSD test results for compressive strength are presented in Appendix A. From the results of the statistical analysis, it is observed that FA produced statistically significant differences relative to the control mixture at 20 and 30% cement replacement levels after 28 days of curing and at 30% cement replacement level after 90 days. Furthermore, for mixtures implementing RFA statistically significant differences relative to control were observed at 20 and 30% cement replacement levels after 28 days of curing, whereas no statistically significant differences were encountered after 90 days of curing. Notably, in the case of GBA mixtures, no statistically significant differences relative to control were observed after both 28 and 90 days of curing at any of the cement replacement levels evaluated. In turn, this indicates that GBA is the best performing SCM among the coal ashes evaluated and that GBA can perform similarly to the control mixture at cement replacement levels ranging from 10 to 30%. From the air content results reported in Figure 22, GBA exhibited the lowest air content among all concrete mixtures. Since it is documented that a 1% increase in the air content can decrease compressive strength by ~5%, the strength decrease of RFA and FA mixtures relative to GBA mixtures is likely attributed to the higher air content produced by RFA and FA [79]. Finally, for mixtures incorporating MK, statistically significant differences relative to control were observed for all mixtures but MK-10 after 90 days of curing. The significantly higher compressive strengths displayed by MK mixtures are attributed to MK's fine particles (Figure 15), high content of pozzolanic component (Table 10), and significant amorphous phase (Figure 14) in contrast to the coal ashes.



(a)



(b)

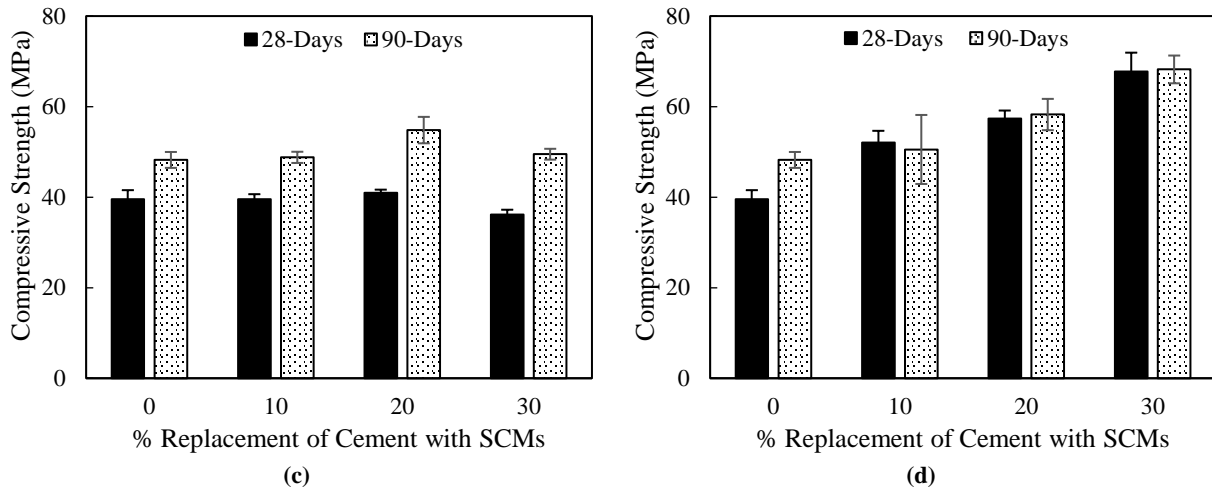
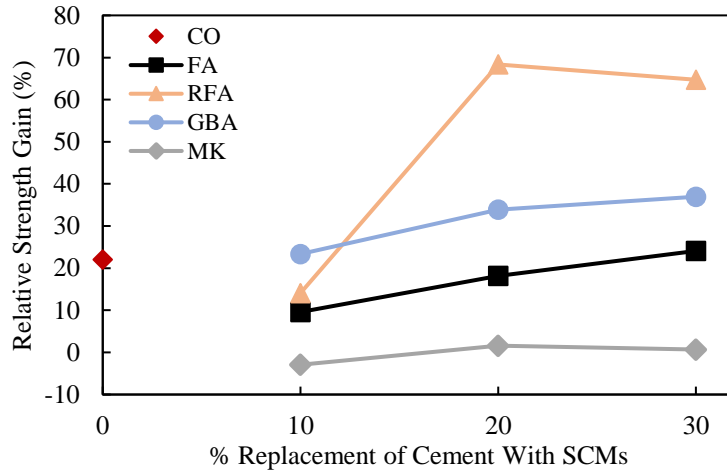


Figure 26. Compressive strength of binary concrete mixtures after 28 and 90 days: (a) FA, (b) RFA, (c) GBA, and (d) MK

The relative strength gain of all the concrete mixtures from 28 to 90 days was computed and is presented in Figure 27. For all coal ashes, the relative strength gains generally increased with the increase in cement replacement level. However, MK admixed concrete mixtures did not exhibit an increasing trend in strength gain. At 10% cement replacement level, the strength gain of the MK mixture was slightly negative (i.e., meaning that the 90-day strength is lower than the 28-day strength), and at 20 and 30% cement replacement levels, the strength gain was negligible (i.e., 1.6% and 0.7%, respectively), signaling a limited reaction beyond 28 days. Since MK is highly reactive, it is hypothesized that most of the MK reacted within 28 days of curing, thus limiting further strength gain beyond 28 days [92,93]. Relative to MK, all coal ashes produced significantly higher relative strength gains at all cement replacement levels. However, relative to control, at 10% cement replacement level, only GBA presented higher relative strength gain. At 20% cement replacement level GBA and RFA exceeded the relative strength gain of control. Finally, at 30% cement replacement, all coal ashes outperformed control in terms of relative strength gain. Generally, RFA produced higher relative strength gains followed by GBA and FA. This is likely attributed to the higher pozzolanic activity of RFA indicated by the high CH consumption from TGA analysis.



**Figure 27. Relative strength gain (%) of binary concrete mixtures**

The 28-day and 90-day compressive strength for ternary mixtures is presented in Figure 28. It is observed that both combined systems (i.e., RFA-MK and GBA-MK) at all cement replacement levels and at both curing ages presented higher compressive strength than the control mixture, except for RFA-MK at 30% cement replacement level at 90 days of curing. For RFA-MK mixtures, the 28-day compressive strength ranged from 42.5 MPa to 45.8 MPa, whereas the 90-day compressive strength ranged from 47.3 MPa to 50.0 MPa. The highest strength for RFA-MK mixtures at 28 and 90 days of curing occurred at 20% and 10% cement replacement levels, respectively. Interestingly, relative to the binary RFA mixtures, the implementation of MK in the RFA-MK ternary mixtures mitigated the strength reduction observed for RFA binary mixtures at 28-days. This is highly relevant as RFA binary mixtures did not meet the minimum specified 28-day compressive strength of 31 MPa at 20 and 30% cement replacement levels, whereas all RFA-MK ternary mixtures did. In turn, this highlights the benefit of incorporating MK in a blended system with RFA. Regarding the GBA-MK mixtures, a progressive increase in the 28-day compressive strength is observed with the increase in cement replacement level. The 28-day compressive strength of GBA-MK mixtures ranged from 44.9 MPa to 49.8 MPa, whereas the 90-day compressive strength ranged from 50.0 MPa to 52.9 MPa. For GBA-MK mixtures, the highest strength reported occurred at the 30% cement replacement level at both curing ages. Relatively, GBA-MK mixtures generally showed higher strength than the RFA-MK mixtures after 28 and 90 days of curing. This result was expected as GBA outperformed RFA in binary mixtures. Furthermore, relative to the binary GBA mixtures, GBA-MK ternary mixtures produced higher compressive strength at all cement replacement levels at 28 days of curing, and at 10 and 30% cement replacement levels at 90 days of curing.

An ANOVA conducted at a 5% confidence level showed statistically significant differences in the average compressive strength of ternary mixtures after 28 days of curing ( $p$ -value $<0.0001$ ) and after 90 days of curing ( $p$ -value  $<0.017$ ). Consequently, a Tukey's HSD test was performed on all possible combinations to identify the mixtures that were statistically different. The ANOVA and Tukey's HSD test results for ternary mixtures are presented in Appendix B. At 28-days of curing, the statistical analysis shows that only the RFA-MK mixture at 20% cement replacement level encountered a statistically significant difference with respect to the control mixture. Furthermore,

the increase in 28-day compressive strength reported for GBA-MK mixtures relative to the control mixture was statistically significant at all cement replacement levels. At 90-days of curing, the statistical analysis showed that none of the ternary mixtures encountered statistically significant differences with respect to the control mixture. Since no statistically significant decrement in compressive strength was reported for the ternary systems (relative to the control mixtures) at both curing ages, results indicate that RFA-MK and GBA-MK combined systems can be used to replace up to 30% of cement without compromising the strength of the concrete mixture. While MK binary mixtures presented higher strength than ternary mixtures, the ternary systems provide environmental benefits as these use waste materials and are more cost-effective, thus making concrete more environmentally friendly and economical.

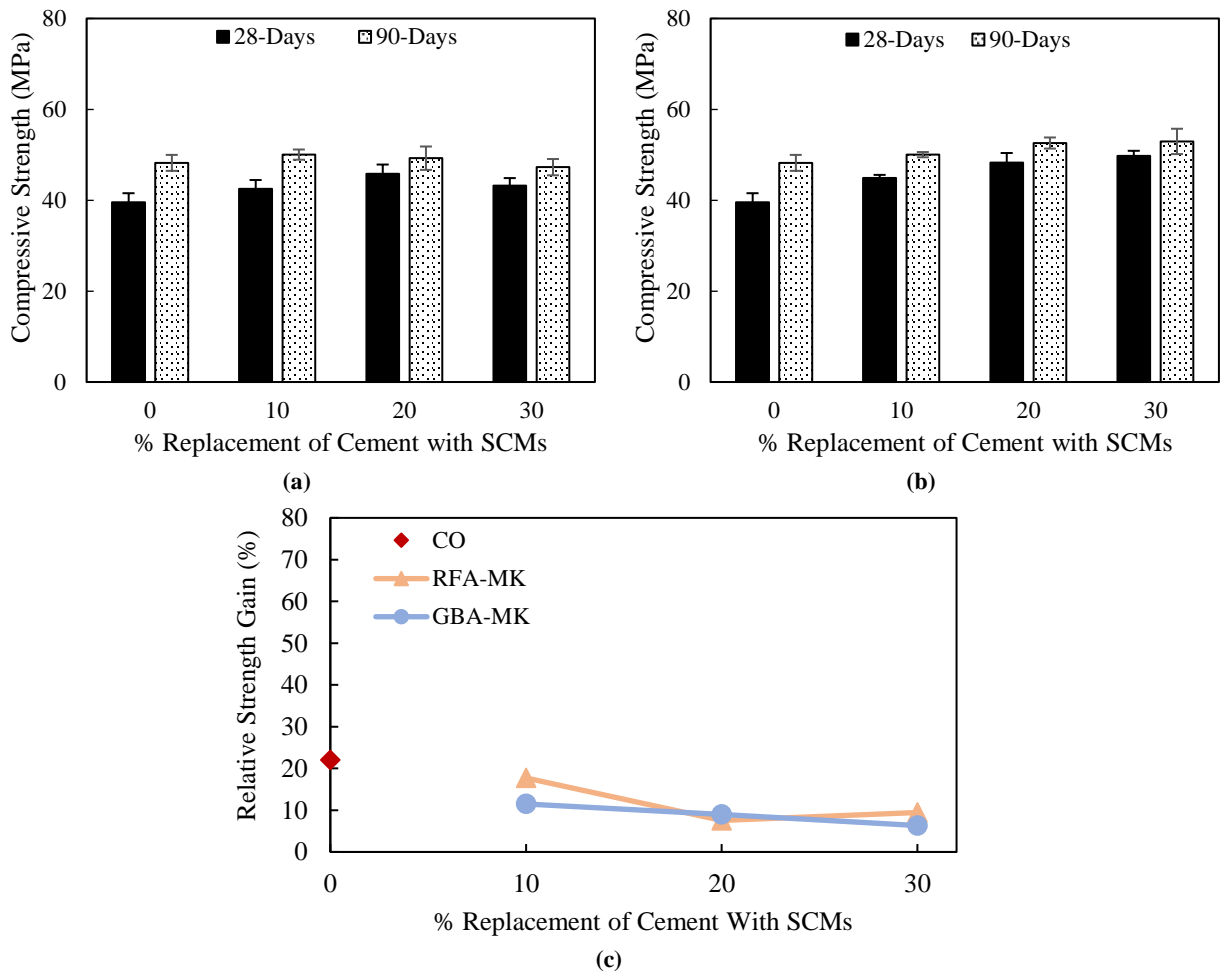


Figure 28. Compressive strength for ternary concrete mixtures: (a) RFA-MK, (b) GBA-MK, and (c) Relative strength gain

The relative strength gain from 28 to 90 days of all the ternary concrete mixtures was computed and is presented in Figure 28. Compressive strength for ternary concrete mixtures: (a) RFA-MK, (b) GBA-MK, and (c) Relative strength gain. In comparison to the control mixture, all ternary concrete mixtures exhibited lower relative strength gain. Furthermore, the ternary mixtures generally exhibited lower relative strength gain than the respective binary mixtures (i.e., RFA and

GBA) at the same cement replacement level. This is likely the case due to the addition of MK in ternary mixtures, which accelerates strength development. For both RFA-MK and GBA-MK ternary mixtures, the maximum relative strength gain was observed at 10% cement replacement level.

#### 5.2.4. *Surface Resistivity*

The 28- and 90-day surface resistivity for all binary concrete mixtures are presented in Figure 29. The control mixture exhibited a surface resistivity of 11.9 k $\Omega$ -cm and 17.0 k $\Omega$ -cm after 28 and 90 days of curing, respectively. The chloride ion penetrability (CIP) classification of the control mixture after 28 days of curing was high CIP, while after 90 days it was moderate CIP. It is important to mention that the control mixture did not meet the 28-day surface resistivity requirement specified by LaDOTD for class A1 concrete (i.e., >22 k $\Omega$ -cm). All SCMs admixed concrete mixtures exhibited higher surface resistivity than the control mixture at both curing ages. Furthermore, all SCMs admixed concrete mixtures exhibited increments in surface resistivity with the increase in cement replacement with SCMs. Importantly, the increment in surface resistivity of the mixtures using SCMs was much more markedly after 90 days of curing. FA admixed concrete mixtures exhibited surface resistivity values in the range of 12.2 to 12.8 k $\Omega$ -cm and 19.7 to 46.7 k $\Omega$ -cm after 28 and 90 days of curing, respectively. Furthermore, RFA admixed concrete mixtures presented surface resistivity values ranging from 12.1 to 15.0 k $\Omega$ -cm and from 24.9 to 49.4 k $\Omega$ -cm after 28 and 90 days of curing, respectively. The surface resistivity values for GBA admixed concrete mixtures ranged from 12.4 to 17.6 k $\Omega$ -cm and from 31.1 to 60.5 k $\Omega$ -cm after 28 and 90 days of curing, respectively. From these results, it is observed that mixtures implementing GBA exhibited relatively higher surface resistivity values than those using FA or RFA, thus indicating that GBA is the best-performing SCM in terms of surface resistivity among the coal ashes evaluated. In the case of MK admixed concrete mixtures, compared to the control mixture and mixtures using coal ashes, a dramatic increase in surface resistivity is observed at all cement replacement levels for both curing ages. For instance, the surface resistivity of MK admixed concrete mixture ranged from 66.8 to 111.5 k $\Omega$ -cm and from 91.5 to 212.8 k $\Omega$ -cm at 28 and 90 days of curing.

An Analysis of variance (ANOVA), conducted at 5% confidence level, showed statistically significant differences in the average surface resistivity among the concrete mixtures at both curing ages (i.e., p-value<0.0001 at both curing ages). Subsequently, a Tukey's HSD test was conducted. The ANOVA and Tukey's HSD test results are presented in Appendix C. According to the statistical analysis, after 28 days of curing, no statistically significant differences were encountered between the control mixture and mixtures implementing coal ashes. In contrast, all MK mixtures exhibited statistically significant differences with respect to the control mixture as well as mixtures implementing coal ashes after 28 days of curing. At 10% cement replacement level, RFA mixtures exhibited the lowest surface resistivity, while at 20 and 30% replacement level FA showed the lowest surface resistivity among all concrete mixtures after 28 days of curing. Conversely, MK exhibited the highest surface resistivity at all cement replacement levels.

After 90 days of curing, statistically significant differences with respect to the control mixture were encountered for all mixtures utilizing SCMs at all cement replacement levels, except FA-10 and RFA-10. In addition, MK admixed concrete mixture also presented statistically significant

differences with all other mixtures. Generally, GBA mixtures exhibited the highest 90-day surface resistivity among coal ashes, followed by RFA and then FA (except RFA and FA at 20% cement replacement level, where they presented the same values). However, in comparison to the MK mixtures, mixtures implementing coal ashes exhibited lower SR values. The higher SR values for MK admixed mixtures are attributed to high amorphous silica content and very fine particles of MK. Amorphous silica and alumina in MK react with calcium hydroxide (CH) from cement hydration to form calcium-silicate-hydrate (CSH) and calcium-aluminate-hydrate (CAH), respectively [94,95]. This pozzolanic reaction results in a denser microstructure, which ultimately lowers the concrete permeability [94–96]. In addition, MK can also act as a mineral filler in concrete mixtures due to its very fine size, improving particle packing; and thus, leading to lower permeability (i.e., higher SR) [96,97]. Since all mixtures showed the highest surface resistivity at 30% replacement level, 30% is the optimum cement replacement level for all SCMs in terms of surface resistivity.

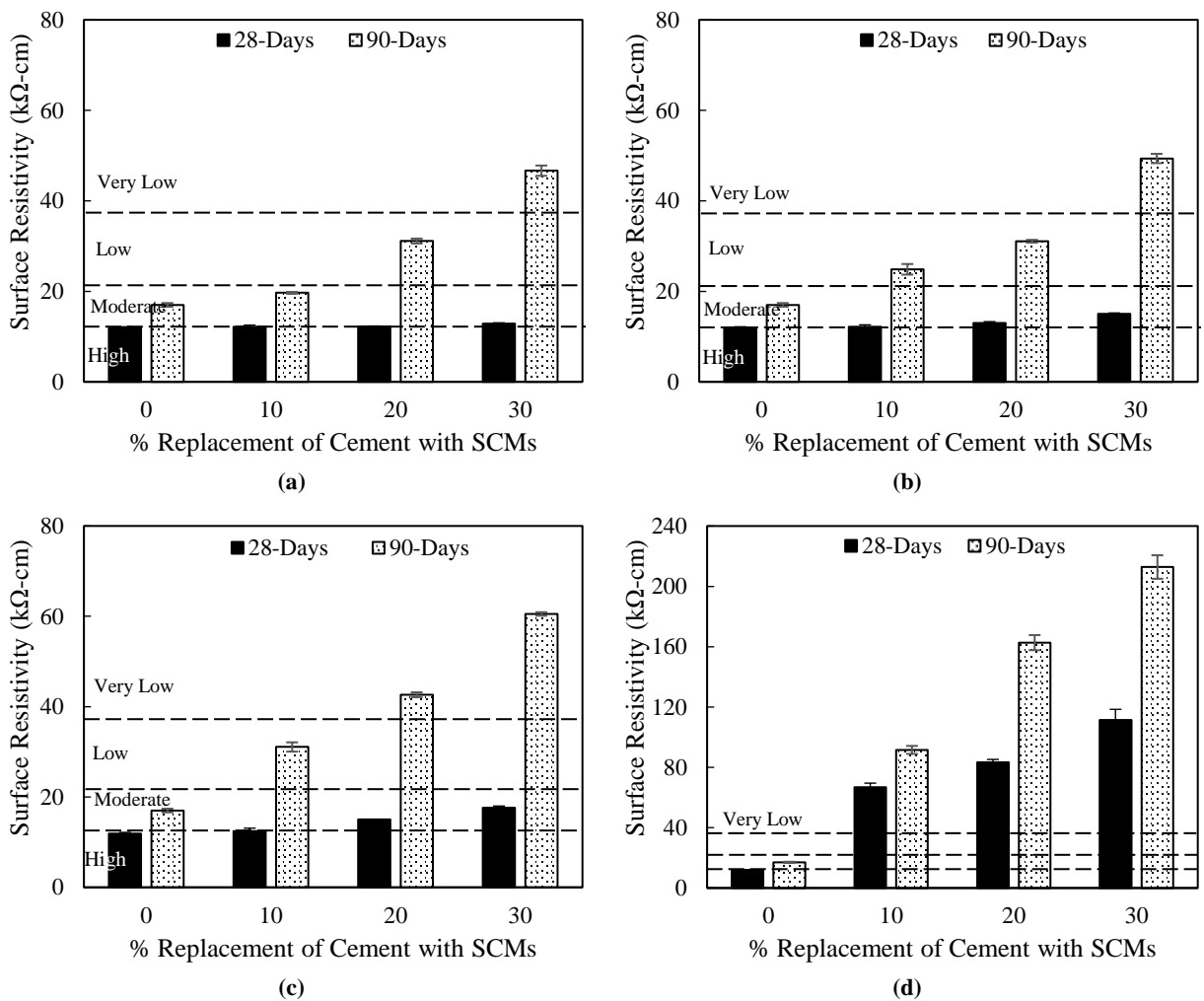
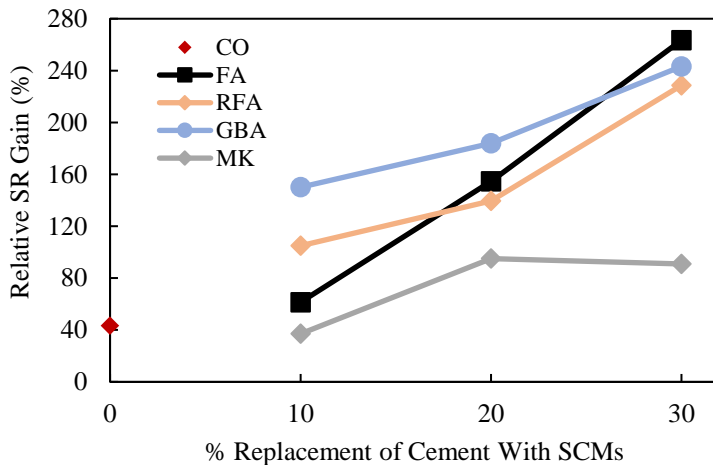


Figure 29. 28- and 90-day surface resistivity of binary concrete mixtures: (a) FA, (b) RFA, (c) GBA, and (d) MK

The relative surface resistivity gain from 28 to 90 days for all binary mixtures is presented in Figure 30. For all mixtures implementing coal ashes, the relative surface resistivity gain is higher at all cement replacement levels than that of the control mixture. Furthermore, with the increase in cement replacement level, mixtures implementing coal ashes presented increments in surface resistivity gain. The higher surface resistivity gain for mixtures with coal ashes is attributed to the pozzolanic reaction, which led to the further significant formation of CSH gel and the densification of the concrete microstructure at later ages. For coal ashes, at 10% and 20% cement replacement level, GBA exhibited higher surface resistivity gain. However, at 30% cement replacement level, all coal ashes exhibited a similar surface resistivity gain, yet FA slightly outperformed RFA and GBA. Interestingly, while MK admixed concrete mixtures presented the highest surface resistivity values, the relative surface resistivity gain from 28 to 90 days was lower for MK mixtures than that of mixtures implementing coal ashes at all cement replacement levels. This is likely attributed to MK's highly reactive nature, which likely resulted in a dense microstructure at 28 days of curing, and only minimal pozzolanic effect at later curing ages. Nonetheless, the surface resistivity gain of MK mixtures was higher than that of the control mixtures at 20 and 30% cement replacement levels. For MK mixtures, the surface resistivity gain increased with the increase in cement replacement level from 10 to 20%. Yet, at the 30% cement replacement level, a similar value to that of the 20% cement replacement level was observed.



**Figure 30. Relative SR Gain (%) of binary concrete mixtures**

The 28-day and 90-day surface resistivity results for all ternary mixtures are presented in Figure 31. It is observed that both combined systems (i.e., RFA-MK and GBA-MK) presented higher surface resistivity than the control mixture at all cement replacement levels at both 28 and 90 days. Furthermore, for both RFA-MK and GBA-MK mixtures the increase in cement replacement level increased the surface resistivity at both curing ages. For RFA-MK mixtures, the 28-day surface resistivity ranged from 21.2 to 55.6 kΩ-cm, whereas the 90-day surface resistivity ranged from 34.2 to 85.9 kΩ-cm. In the case of GBA-MK mixtures, the surface resistivity ranged from 22.0 to 68.0 kΩ-cm and from 43.0 kΩ-cm to 115.7 kΩ-cm after 28 and 90 days of curing, respectively. It is worth noticing that the binary systems using only RFA or GBA presented lower surface resistivity than those of the RFA-MK and GBA-MK ternary mixtures at both curing ages for the



same replacement level, respectively. This is attributed to the effect of MK in enhancing the microstructure of the concrete mixtures. Importantly, while mixtures implementing coal ash binary systems (i.e., FA, RFA, and GBA) did not meet the minimum 28-day surface resistivity requirement of LaDOTD for class A1 concrete (i.e., >22 k $\Omega$ -cm), mixtures implementing ternary systems (i.e., RFA-MK and GBA-MK) did, excepting the RFA-MK mixture at 10% cement replacement level.

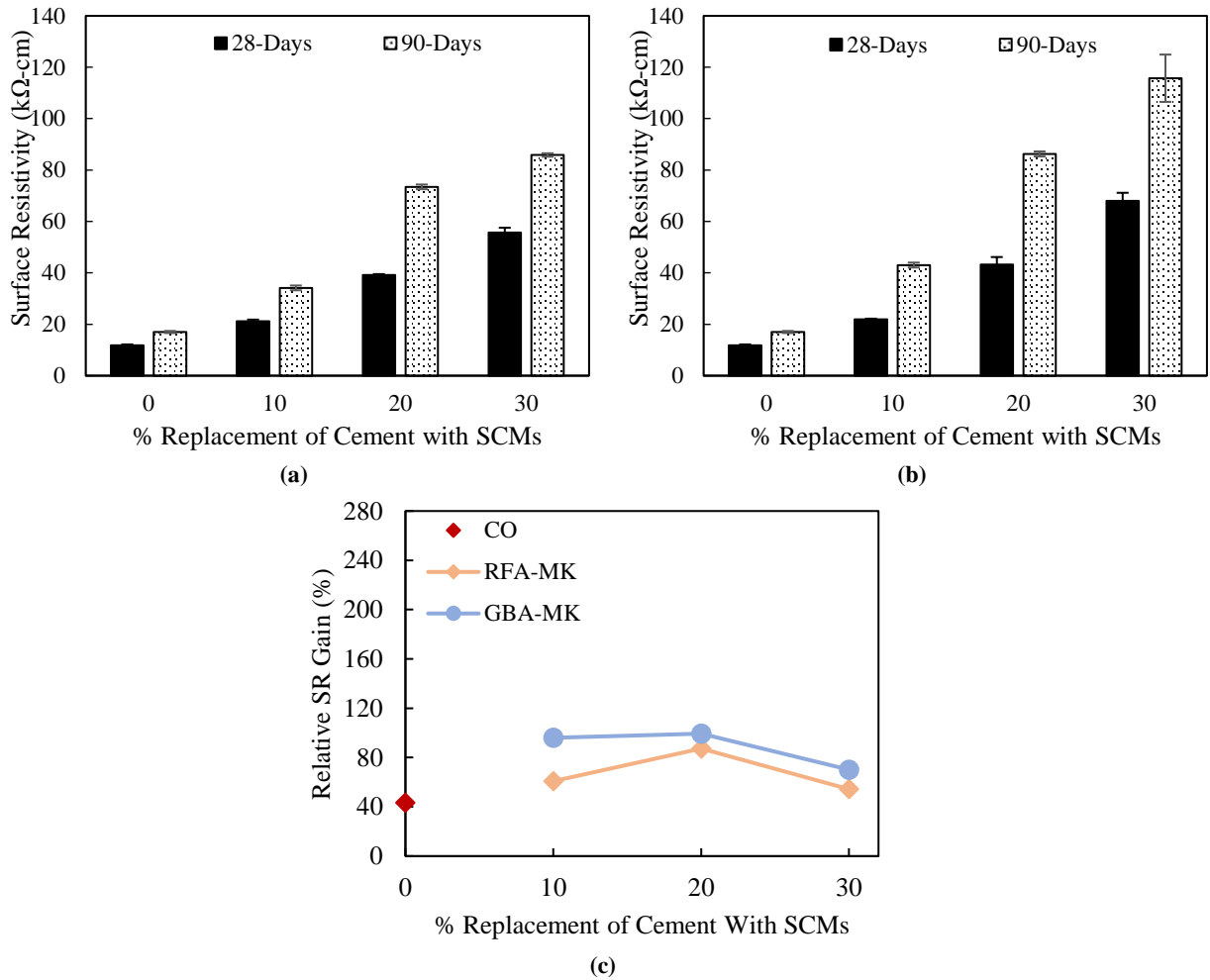


**Figure 31. Surface resistivity of ternary concrete mixtures: (a) RFA and MK, (b) GBA and MK, and (c) relative surface resistivity gain**

An ANOVA conducted at a 5% confidence level showed statistically significant differences in the average surface resistivity among the mixtures after 28 and 90 days of curing (p-value<0.0001 for both curing ages). To identify the mixtures that were statistically different, Tukey’s HSD test was performed on all possible combinations. The ANOVA and Tukey test results are presented in Appendix D. Relative to the control mixture, the analysis showed statistically significant differences in SR values for all ternary concrete mixtures at both curing ages. Furthermore, at 28 days of curing, for the same SCM dosage, statistically significant differences among the RFA-MK and GBA-MK concrete mixtures were only encountered at 30% cement replacement level. In

contrast, at 90 days of curing, statistically significant differences among the RFA-MK and GBA-MK mixtures were encountered at 20 and 30% cement replacement levels.

The relative surface resistivity gain from 28 to 90 days of all the ternary concrete mixtures was computed and is presented in Figure 28. Compressive strength for ternary concrete mixtures: (a) RFA-MK, (b) GBA-MK, and (c) Relative strength gain. It is noticed that, for the same cement replacement level, the binary systems using only RFA or GBA presented higher relative SR gain than those of the RFA-MK and GBA-MK ternary mixtures, respectively. This might be attributed to the higher reactivity of MK. It is also noticed that relative to binary mixtures, which presented an increasing trend in relative SR gain with the increase in the cement replacement level, ternary mixtures, presented increases in relative SR gain only up to 20% cement replacement level. Finally, it was observed that GBA-MK ternary mixtures exhibited higher relative SR gain than RFA-MK ternary mixtures at all cement replacement levels.

### 5.2.1. *Drying Shrinkage*

Drying shrinkage after curing (i.e., after 28 days wet curing) up to 28 days in air storage of the binary and ternary mixtures is presented in Figure 32 and Figure 33, respectively. Generally, it is observed that the concrete mixture without SCMs showed the highest drying shrinkage compared to the mixtures modified with any SCM. Furthermore, it shows that the inclusion of SCMs for binary mixtures reduced the drying shrinkage from 24.2 to 69.1% relative to control. In the case of ternary mixtures, drying shrinkage relative to control reduced by 55.2 to 75.3%.

As shown in Figure 32a, after 28 days of drying, minor differences were observed in the drying shrinkage of mixtures implementing FA at different cement replacement levels. Nonetheless, all mixtures implementing FA presented a significantly lower drying shrinkage than the control mixture, i.e., ranging from 42.1 to 44.3%. In the case of RFA mixtures as shown in Figure 32b, a benefit of increasing cement replacement level from 10% to 20% was observed by producing a reduction in 28-day drying shrinkage. However, further increments in cement replacement level from 20 to 30% did not provide further decrements in shrinkage. Relative to the control mixture, RFA mixtures produced decrements in 28-day drying shrinkage ranging from 36.6 to 49.0%. As shown in Figure 32c, the 28-day drying shrinkage for GBA mixtures was the lowest at 10% cement replacement level and increased slightly for higher cement replacement levels (i.e., 20 and 30%). As such, higher cement replacement levels with GBA did not provide additional benefits in terms of drying shrinkage. Relative to the control mixture, GBA mixtures produced a decrease in 28-day drying shrinkage ranging from 24.2 to 36.6%. Drying shrinkage of MK mixtures is presented in Figure 32d. As shown, MK mixtures with 20% cement replacement level produced the lowest 28-day drying shrinkage among MK mixtures whereas mixtures using 10 and 30% cement replacement level presented similar drying shrinkage. Compared to the control mixture, MK mixtures presented a decrease in 28-day drying shrinkage ranging from 51.0 to 69.1%. From the presented results, MK was generally the best SCM in terms of drying shrinkage reduction followed by FA and RFA (which performed similarly), and finally GBA. Moreover, generally 10 and 20% cement replacement levels produced the lowest drying shrinkage. Importantly, all SCMs evaluated were highly effective in reducing drying shrinkage relative to the control mixture.

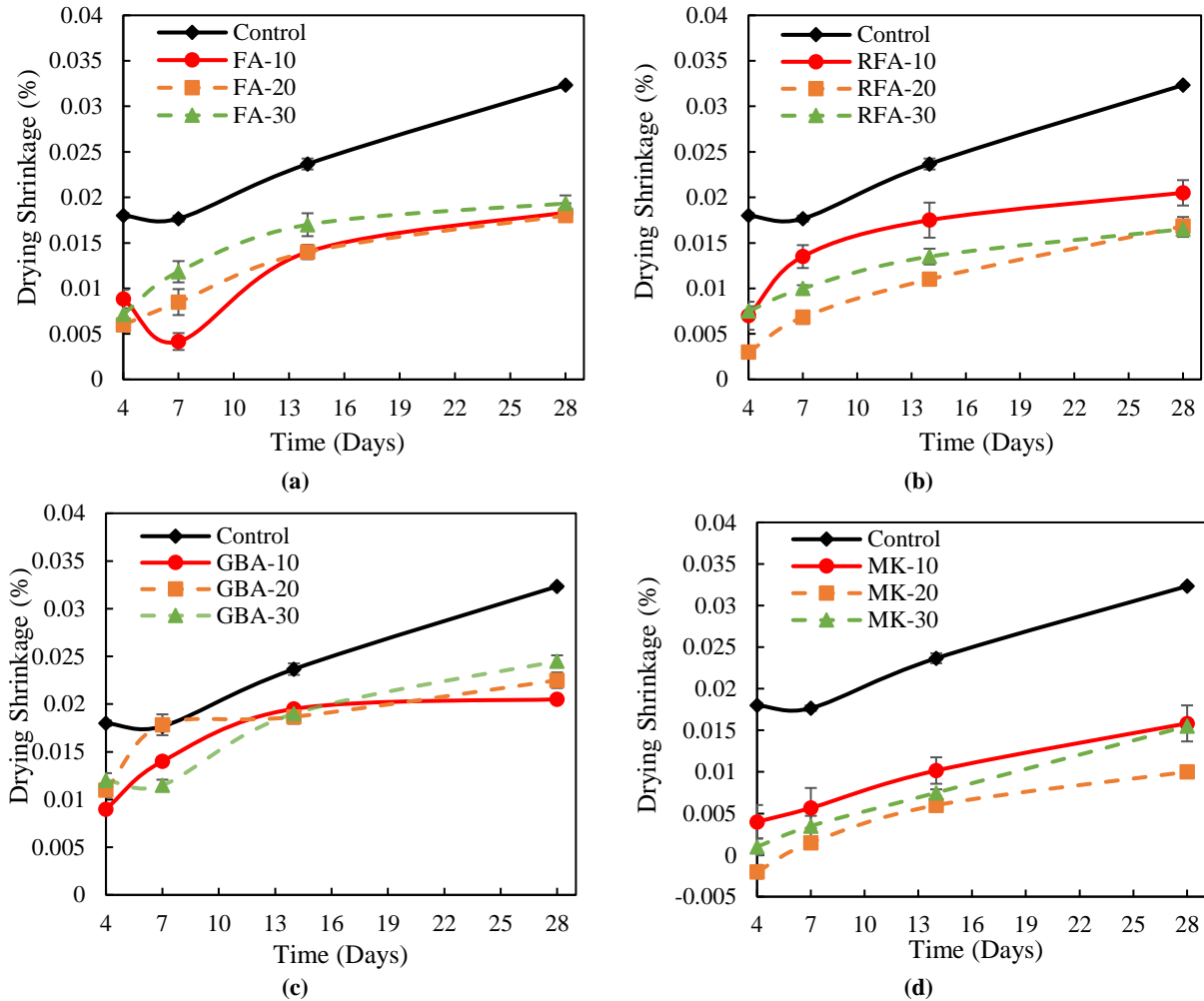


Figure 32. Drying shrinkage of binary concrete mixtures: (a) FA, (b) RFA, (c) GBA, and (d) MK

The drying shrinkage results for mixtures implementing combined SCM systems (i.e., ternary systems) are presented individually in Figure 33. As it can be observed in Figure 33a, RFA-MK mixtures produced decrements in the 28-day drying shrinkage relative to the control mixture ranging from 55.2 to 69.6% with 10% cement replacement level presenting the lowest drying shrinkage, followed by 20% and 30% cement replacement levels. In the case of GBA-MK mixtures shown in Figure 33b, 28-day drying shrinkage decrements relative to the control mixture ranged from 56.2 to 75.3% with 30% cement replacement level presenting the lowest drying shrinkage followed by 10 and 20% cement replacement levels, which presented similar values. From the ternary systems, the use of the GBA-MK system as SCM generally produced the lowest 28-day drying shrinkage, yet the RFA-MK system exhibited a similar performance. Interestingly, both ternary systems were generally better than any of the binary systems in terms of 28-day drying shrinkage reduction. In turn, this suggests a potential synergistic effect between the coal ashes and MK in terms of drying shrinkage reduction.

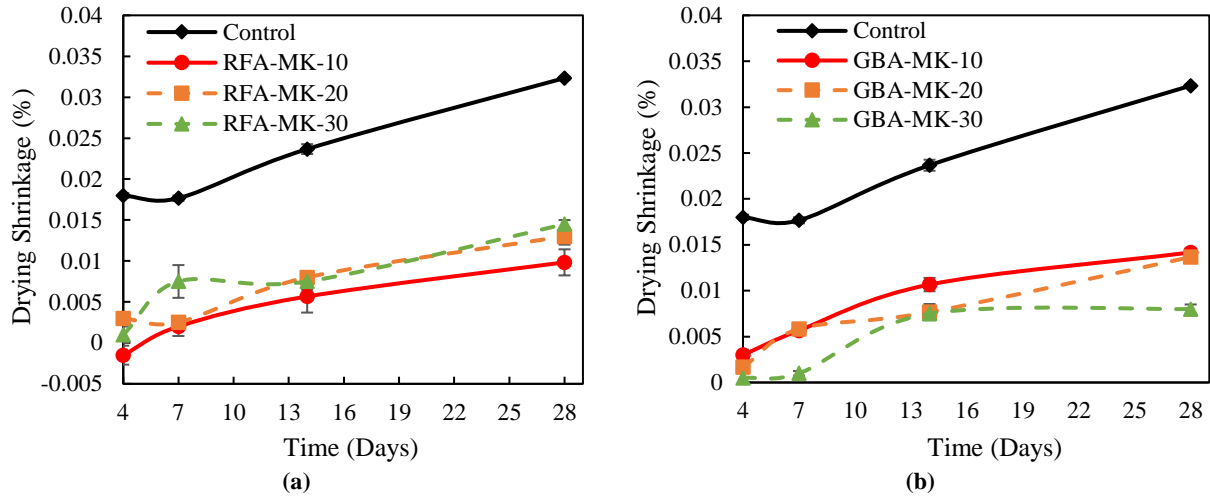
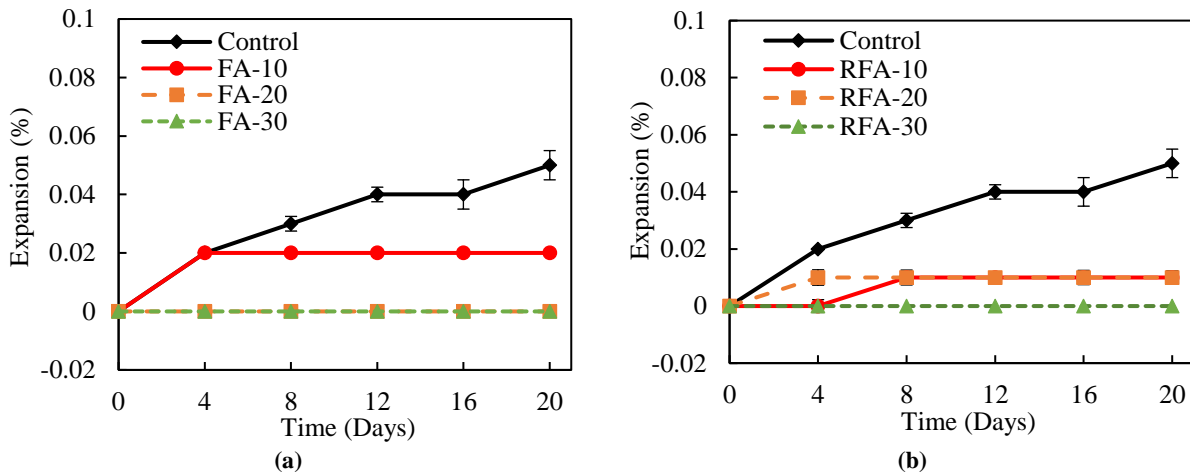


Figure 33. Drying shrinkage of ternary concrete mixtures: (a) RFA and MK, and (b) GBA and MK

### 5.2.2. Alkali-Silica Reactivity

The data obtained from the ASR tests for all mixtures is shown graphically in Figure 34 and Figure 35. It can be noticed that the mortar bars exhibited less than 0.10% expansion after 16 days in all cases, which is the permissible limit according to ASTM C1567. This low expansion indicates that the aggregate (sandstone) used in this study exhibited low reactivity. Importantly, in all cases, mortar bars implementing SCMs presented significantly lower expansion than those without SCMs (i.e., control). Furthermore, generally, the increase in cement replacement with SCMs reduced the expansion. These observations suggest that the SCMs evaluated in this study can be effective in mitigating the expansion associated with ASR, specially at high cement replacement levels (i.e., 20 to 30% cement replacement level). Interestingly, for specimens using GBA and combined systems of GBA-MK and RFA-MK at high cement replacement levels (i.e., 20 to 30% cement replacement by mass) some shrinkage instead of expansion was measured. A similar trend has been noticed in research with silica fume that showed negative expansion over a long time [100].



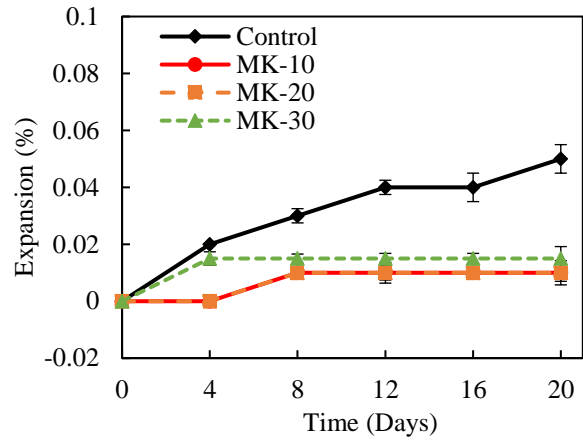
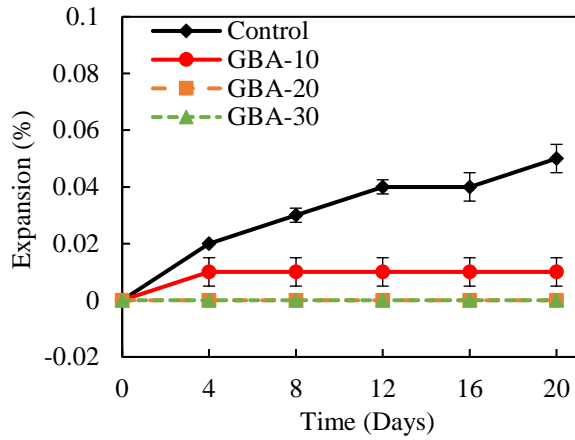


Figure 34. ASR with sandstone for binary mortar mixtures: (a) FA, (b) RFA, (c) GBA, and (d) MK

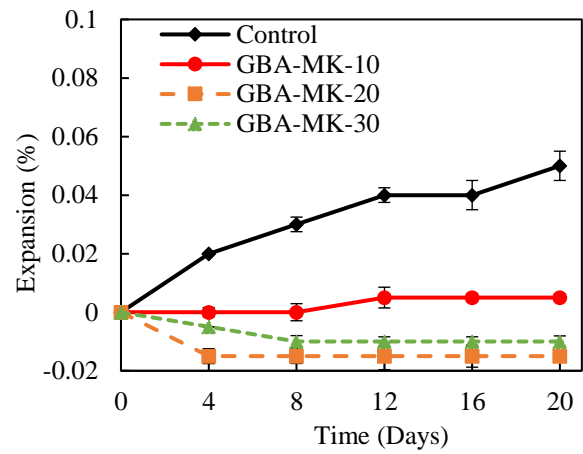
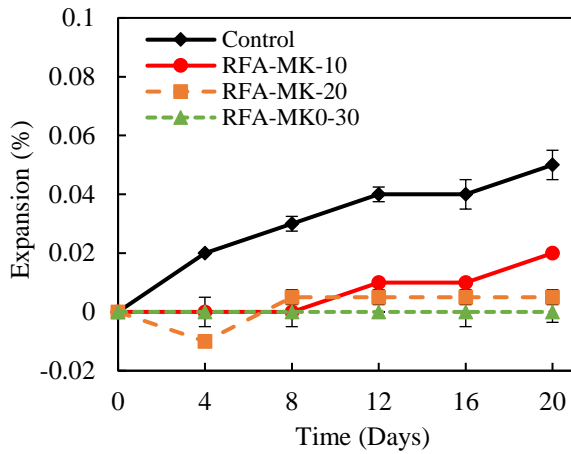


Figure 35. ASR with sandstone for ternary mortar mixtures: (a) RFA and MK, and (b) GBA and MK

## 6. CONCLUSIONS

The present study evaluated the use of alternative sources of SCMs for the manufacture of concrete for transportation infrastructure in Region 6. SCMs evaluated included: (1) reclaimed fly ash (RFA), (2) reclaimed ground bottom ash (GBA), (3) metakaolin (MK), and (4) conventional Class F fly ash (FA) as a reference. The microstructure, mineralogical composition, and physical and chemical properties of the SCMs were evaluated. Furthermore, the fresh and hardened properties of concrete implementing different dosages of each SCM (i.e., 10, 20, and 30% cement replacement by mass) were evaluated. In addition, this study also investigated the feasibility of using blended systems of unconventional coal ashes (i.e., RFA and GBA) and MK (i.e., ternary systems) as SCMs for concrete mixtures. The blend proportion evaluated for the ternary systems was 70% coal ash (i.e., RFA or GBA) and 30% MK by mass. Based on the experimental results, the following conclusions can be drawn:

- **SCMs Characterization:** FA and RFA consisted of mostly spherical particles with RFA presenting coarser impurities (i.e., irregular-shaped particles). On the other hand, GBA exhibited a prismatic morphology with many sharp edges while MK consisted of plate-like particles. MK presented the smallest particles among all the SCMs evaluated with a mean particle size of 6.0  $\mu\text{m}$ . Furthermore, among the coal ashes, RFA exhibited the largest particles (i.e., mean particle size of 64.4  $\mu\text{m}$ ), followed by GBA (i.e., mean particle size of 23.2  $\mu\text{m}$ ) and FA (i.e., mean particle size of 19.2  $\mu\text{m}$ ), which exhibited similar particle size. The main constituents of all the SCMs evaluated were silica ( $\text{SiO}_2$ ) and alumina ( $\text{Al}_2\text{O}_3$ ). However, MK presented the highest content of alumina among all the SCMs evaluated. Among the coal ashes, GBA exhibited the highest calcium oxide ( $\text{CaO}$ ) content while RFA presented the lowest  $\text{CaO}$  content. In terms of mineralogical composition, FA was identified to contain quartz, portlandite, and maghemite crystalline phases. In the case of RFA, quartz and mullite crystalline phases were identified, whereas for GBA quartz and plagioclase feldspar crystalline phases were recognized. In MK, only one crystalline phase was identified, which was anatase. Importantly, all SCMs presented amorphous humps in the XRD spectra signaling the presence of amorphous phases. In particular, MK presented a noticeably large amorphous hump, whereas GBA presented the smallest amorphous hump from all the SCMs evaluated. The calcium hydroxide (CH) consumption (determined through TGA analysis) of all the SCMs evaluated in this study exceeded the threshold to be classified as pozzolanic materials. Furthermore, MK presented the highest CH consumption followed by RFA, GBA, and finally FA. All the SCMs met the requirements for pozzolanic component (i.e., the sum of  $\text{SiO}_2$ ,  $\text{Al}_2\text{O}_3$ , and  $\text{Fe}_2\text{O}_3$ ),  $\text{CaO}$ ,  $\text{SO}_3$ , moisture content, LOI, and 7-day and 28-day SAI to be classified as Class F pozzolan according to ASTM C618. GBA and MK presented the same and highest SAI after 7 days of curing, whereas after 28 days, MK exhibited the highest SAI among all the SCMs, followed by RFA, FA, and GBA. In terms of water requirement according to ASTM C618, all SCMs but MK met this requirement.
- **Concrete Fresh Properties:** Concrete implementing RFA, GBA, and MK presented a progressive decrease in workability (i.e., slump) with the increase in cement replacement when compared to the control concrete mixture (i.e., without SCMs). Among these SCMs,

MK produced by far the largest decrease in workability followed by GBA and finally RFA, which produced generally mild decrements in workability. The decrement in workability observed for concrete implementing MK and GBA was attributed to their particle micro-morphology, yet in the case of MK the markedly small size of the particles also played an important role in decreasing workability. In the case of RFA, the mild reduction in workability was credited to mullite impurities. Importantly, concrete using FA exhibited similar or better workability than the control mixture. For mixtures implementing ternary systems of RFA-MK and GBA-MK, workability reduced with the increment in cement replacement in contrast to the control mixture. Furthermore, GBA-MK systems produced the largest decrements in workability. All SCMs produced a decrease in the air content of fresh concrete compared to the control mixture (except for FA at 20% cement replacement). Among the coal ashes, RFA generally produced the lowest decrease in air content, followed by FA and GBA. Interestingly, despite exhibiting the highest LOI of among all SCMs evaluated, the air content reduction observed in mixtures implementing RFA was small at all cement replacement levels evaluated. Mixtures implementing ternary systems also exhibited a decrease in air content relative to the control mixture and air content reduced with the increase in cement replacement. RFA-MK systems produced lower decrements in air content relative to GBA-MK systems.

- **Concrete Hardened Properties:** Generally, the 28-day compressive strength of concrete implementing FA and RFA decreased (relative to the control mixture) and the strength decrease augmented with the increase in cement replacement. Nonetheless, decrements in 28-day compressive strength observed at the 10% cement replacement level for FA and RFA were negligible and not statistically significant. After 90 days of curing, a similar tendency was observed for FA admixed concrete (i.e., strength decrease with increments in cement replacement), yet decrements in 90-day compressive strength relative to the control mixture were only statistically significant at the 30% cement replacement level. In the case of concrete implementing RFA, no statistically significant differences were observed (relative to the control mixture) in the 90-day compressive strength at any of the cement replacement levels evaluated. Notably, in the case of GBA admixed concrete, no statistically significant differences were observed in both the 28-day and 90-day compressive strength (relative to the control mixture) at any of the cement replacement levels evaluated. Generally, concrete mixtures implementing MK presented statistically significant increments in the 28-day and 90-day compressive strength (relative to the control mixture) at all cement replacement levels evaluated. The only exception observed was for the mixture using 10% cement replacement with MK, which did not exhibit a statistically significant difference in the 90-day compressive strength relative to the control mixture. In the case of concrete mixtures implementing ternary systems of RFA-MK and GBA-MK, the 28-day compressive strength generally increased with the increase in cement replacement level. However, for RFA-MK mixtures, statistically significant differences in the 28-day compressive strength (relative to control) were only encountered at 20% cement replacement, whereas for GBA-MK mixtures increments in strength reported were statistically significant at all cement replacement levels evaluated. After 90 of curing no statistically significant difference in strength was encountered for ternary mixtures relative to the control mixture.

After 28-days of curing, concrete mixtures implementing coal ashes (i.e., FA, RFA, and GBA) did not produce statistically significant differences in surface resistivity relative to the control mixture at any of the cement replacement levels evaluated. Conversely, after 90-days of curing, excepting FA-10 and RFA-10, all mixtures implementing coal ashes produced statistically significant increments in surface resistivity (relative to the control mixture), where the surface resistivity increased with the increase in cement replacement. Among the coal ashes, GBA mixtures generally presented the highest surface resistivity values, followed by RFA and FA mixtures. Importantly, for cement replacement levels above 10%, all mixtures implementing coal ashes fell in the categories of low or very low CIP after 90 days of curing, whereas the control mixture fell in the category of moderate CIP. Mixtures implementing MK presented statistically significant improvements in 28-day and 90-day surface resistivity relative to the control mixture and mixtures implementing coal ashes. Furthermore, increments in MK content increased the 28-day and 90-day surface resistivity. All MK admixed mixtures met the minimum 28-day surface resistivity requirement for class A1 concrete according to LaDOTD. In the case of mixtures implementing ternary systems (i.e., RFA-MK and GBA-MK), statistically significant improvements in 28- and 90-day surface resistivity were observed (relative to the control mixture) at all cement replacement levels and surface resistivity increased with the increase in cement replacement level. Importantly, while mixtures implementing coal ashes binary systems did not meet the minimum 28-day surface resistivity requirement for class A1 concrete according to LaDOTD, mixtures implementing ternary systems did, excepting the RFA-MK mixture at 10% cement replacement level.

- **Drying Shrinkage:** Overall, all SCMs evaluated were highly effective in reducing drying shrinkage relative to the control mixture. Drying shrinkage reduction for concrete mixtures implementing binary SCM systems (i.e., FA, RFA, GBA, and MK) ranged from 24.2 to 69.1% (relative to the control mixture). Generally, MK was the best performing SCM in terms of drying shrinkage reduction, followed by FA and RFA (which performed similarly), and finally GBA. In the case of mixtures implementing ternary systems, the reductions in drying shrinkage reported ranged from 55.2 to 75.3%.
- **Alkali-Silica Reaction (ASR):** All mortar mixtures evaluated (i.e., with and without SCMs) exhibited a lower expansion than the permissible limit according to ASTM C1567 after 16 days. Nonetheless, mixtures implementing SCMs presented significantly lower expansion than that of the control mixture. Moreover, the increase in cement replacement with SCMs further reduced the expansion. Results suggest that the SCMs evaluated may be effective at suppressing ASR related expansion, particularly at high cement replacement levels (i.e., 20 to 30%).

Table 14 below presents a general qualitative summary of the effects of the different SCMs and blended SCM systems evaluated on the properties of concrete. Based on the experimental results, all SCMs evaluated are promising for their use in concrete materials. However, depending on the SCM selected and cement replacement level, slight adjustments in the concrete mixture design and/or admixture dosage may be necessary to meet specified fresh and hardened properties. For the concrete mixture evaluated, generally, up to 20% cement replacement with RFA and GBA, and up to 30% of cement with MK, RFA-MK, or GBA-MK can be used without compromising



concrete’s long-term mechanical and durability properties. Importantly, while the alternative SCMs evaluated in this study mostly presented a satisfactory performance, verification of SCMs’ performance should be conducted on a supplier and source basis prior to implementation in concrete mixtures.

**Table 14. Summary of SCMs effect on concrete properties**

Materials	Fresh Properties		Hardened Properties				Shrinkage	ASR
	Slump	Air Content	28-Day f'c	90-Day f'c	28-Day Surface Resistivity	90-Day Surface Resistivity		
FA	✓	X	X	X	--	✓	✓	✓
RFA	X	X	X	--	--	✓	✓	✓
GBA	X	X	--	--	--	✓	✓	✓
MK	X	X	✓	✓	✓	✓	✓	✓
RFA-MK	X	X	✓	--	✓	✓	✓	✓
GBA-MK	X	X	✓	--	✓	✓	✓	✓

(✓) Performed favorably, (X) Did not perform well, (--) Impact is neutral

## 7. REFERENCES

- [1] Statista, Apparent cement consumption in the U.S. from 2004 to 2020 (in 1,000 metric tons), (n.d.). <https://www.statista.com/statistics/273367/consumption-of-cement-in-the-us/>.
- [2] ASTM Standard C618, Standard Specification for Coal Fly Ash and Raw or Calcined Natural Pozzolan for Use in Concrete, 2017. <https://doi.org/10.1520/C0618>.
- [3] I. Diaz-Loya, M. Juenger, S. Seraj, R. Minkara, Extending supplementary cementitious material resources: Reclaimed and remediated fly ash and natural pozzolans, *Cement and Concrete Composites*. 101 (2019) 44–51. <https://doi.org/10.1016/j.cemconcomp.2017.06.011>.
- [4] P.J. Tikalsky, M. V. Huffman, G.M. Barger, Use of Raw or Processed Natural Pozzolans in Concrete, *American Concrete Institute*. (2001) 1–24.
- [5] AASHTO Subcommittee on Materials, AASHTO Subcommittee on Materials (SOM) 2016 Fly Ash Task Force Report, (2016) 1–22.
- [6] American Coal Ash Association, Production and Use Reports, American Coal Ash Association. (2018). <https://www.aaa-usa.org/publications/productionuserreports.aspx> (accessed April 8, 2020).
- [7] E. Sugawara, H. Nikaido, EIA energy outlook 2020, *Antimicrobial Agents and Chemotherapy*. 58 (2019) 7250–7257.
- [8] A.P. Black, Production and Use of Coal Combustion Products in the US, *American Road and Transportation Builders Association*, Washington, DC. (2015).
- [9] H. Toutanji, N. Delatte, S. Aggoun, R. Duval, A. Danson, Effect of supplementary cementitious materials on the compressive strength and durability of short-term cured concrete, *Cement and Concrete Research*. 34 (2004) 311–319. <https://doi.org/10.1016/j.cemconres.2003.08.017>.
- [10] B. Lothenbach, K. Scrivener, R.D. Hooton, Supplementary cementitious materials, *Cement and Concrete Research*. 41 (2011) 1244–1256. <https://doi.org/10.1016/j.cemconres.2010.12.001>.
- [11] M.C.G. Juenger, R. Siddique, Recent advances in understanding the role of supplementary cementitious materials in concrete, *Cement and Concrete Research*. 78 (2015) 71–80. <https://doi.org/10.1016/j.cemconres.2015.03.018>.
- [12] R. Snellings, G. Mertens, J. Elsen, Supplementary cementitious materials, *Reviews in Mineralogy and Geochemistry*. 74 (2012) 211–278. <https://doi.org/10.2138/rmg.2012.74.6>.
- [13] S.C. Association, Slag Cement Shipping, (n.d.). <https://www.slagcement.org/resources/shipments.aspx> (accessed February 1, 2020).
- [14] S. Al-Shmaisani, R. Kalina, M. Rung, R. Ferron, M. Juenger, Implementation of a Testing Protocol for Approving Alternative Supplementary Cementitious Materials (SCMs):

- Natural Minerals and Reclaimed and Remediated Fly Ashes, University of Texas at Austin. Center for Transportation Research, 2018.
- [15] S. Al-Shmaisani, R.D. Kalina, R.D. Ferron, M.C.G. Juenger, Evaluation of Beneficiated and Reclaimed Fly Ashes in Concrete, *ACI Materials Journal*. 116 (2019) 79–87.
- [16] Boral Resources, Fly Ash Reclaimed From Landfill, 2018.
- [17] K. Bergson, Fly ash: the “poor man’s portland cement,” (2000) 3–4. [www.ncgia.ucsb.edu/ncrst/](http://www.ncgia.ucsb.edu/ncrst/).
- [18] Federal Highway Administration, SUPPLEMENTARY CEMENTITIOUS Best Practices for Concrete Pavements, (2016) 1–7.
- [19] American Coal Ash Association, Fly Ash Facts for Highway Engineers, *Journal of Chemical Information and Modeling*. 53 (2013) 1689–1699. <https://doi.org/10.1017/CBO9781107415324.004>.
- [20] C. Argiz, A. Moragues, Use of ground coal bottom ash as cement constituent in concretes exposed to chloride environments, 170 (2018) 25–33. <https://doi.org/10.1016/j.jclepro.2017.09.117>.
- [21] S.A. Mangi, M.H. Wan Ibrahim, N. Jamaluddin, M.F. Arshad, P.J. Ramadhansyah, Effects of ground coal bottom ash on the properties of concrete, *Journal of Engineering Science and Technology*. 14 (2019) 338–350.
- [22] M. Rafieizonooz, J. Mirza, M.R. Salim, M.W. Hussin, E. Khankhaje, Investigation of coal bottom ash and fly ash in concrete as replacement for sand and cement, *Construction and Building Materials*. 116 (2016) 15–24. <https://doi.org/10.1016/j.conbuildmat.2016.04.080>.
- [23] P. Pormmoon, A. Abdulmatin, C. Charoenwaiyachet, W. Tangchirapat, C. Jaturapitakkul, Effect of cut-size particles on the pozzolanic property of bottom ash, *Journal of Materials Research and Technology*. 10 (2021) 240–249. <https://doi.org/10.1016/j.jmrt.2020.12.017>.
- [24] M. Singh, R. Siddique, Resources , Conservation and Recycling Effect of coal bottom ash as partial replacement of sand on properties of concrete, “Resources, Conservation & Recycling.” 72 (2013) 20–32. <https://doi.org/10.1016/j.resconrec.2012.12.006>.
- [25] H.K. Kim, H.K. Lee, Use of power plant bottom ash as fine and coarse aggregates in high-strength concrete, *Construction and Building Materials*. 25 (2011) 1115–1122. <https://doi.org/10.1016/j.conbuildmat.2010.06.065>.
- [26] M. Singh, R. Siddique, Properties of concrete containing high volumes of coal bottom ash as fine aggregate, 91 (2015). <https://doi.org/10.1016/j.jclepro.2014.12.026>.
- [27] J. Pera, L. Coutaz, J. Ambroise, M.Chababbet, USE OF INCINERATOR BOTTOM ASH IN CONCRETE, *Cement and Concrete Research*. 27 (1997) 1–5.
- [28] M. Singh, R. Siddique, Strength properties and micro-structural properties of concrete containing coal bottom ash as partial replacement of fine aggregate, *Construction and*

- Building Materials. 50 (2014) 246–256.  
<https://doi.org/10.1016/j.conbuildmat.2013.09.026>.
- [29] L.B. Andrade, J.C. Rocha, M. Cheriaf, Influence of coal bottom ash as fine aggregate on fresh properties of concrete, *Construction and Building Materials*. 23 (2009) 609–614.  
<https://doi.org/10.1016/j.conbuildmat.2008.05.003>.
- [30] M. Rafieizonooz, J. Mirza, M. Razman, M. Warid, E. Khankhaje, Investigation of coal bottom ash and fly ash in concrete as replacement for sand and cement, *Construction and Building Materials*. 116 (2016) 15–24. <https://doi.org/10.1016/j.conbuildmat.2016.04.080>.
- [31] P. Aggarwal, Y. Aggarwal, S.M. Gupta, EFFECT OF BOTTOM ASH AS REPLACEMENT OF FINE AGGREGATES IN CONCRETE, *ASIAN JOURNAL OF CIVIL ENGINEERING (BUILDING AND HOUSING)*. 8 (2007) 49–62.
- [32] S. Ali, M. Haziman, W. Ibrahim, N. Jamaluddin, M. Fadzil, Engineering Science and Technology , an International Journal Performances of concrete containing coal bottom ash with different fineness as a supplementary cementitious material exposed to seawater, *Engineering Science and Technology, an International Journal*. 22 (2019) 929–938.  
<https://doi.org/10.1016/j.jestch.2019.01.011>.
- [33] C. Argiz, M.Á. Sanjuán, E. Menéndez, Coal Bottom Ash for Portland Cement Production, 2017 (2017).
- [34] S. Oruji, N.A. Brake, R.K. Guduru, L. Nalluri, Ö. Günaydın-s, K. Kharel, S. Rabbanifar, S. Hosseini, E. Ingram, Mitigation of ASR expansion in concrete using ultra-fine coal bottom ash, 202 (2019) 814–824. <https://doi.org/10.1016/j.conbuildmat.2019.01.013>.
- [35] H. Kurama, M. Kaya, Usage of coal combustion bottom ash in concrete mixture, *Construction and Building Materials*. 22 (2008) 1922–1928.  
<https://doi.org/10.1016/j.conbuildmat.2007.07.008>.
- [36] M. Singh, R. Siddique, Strength properties and micro-structural properties of concrete containing coal bottom ash as partial replacement of fine aggregate, *Construction and Building Materials*. 50 (2014) 246–256.  
<https://doi.org/10.1016/j.conbuildmat.2013.09.026>.
- [37] G. Sua-Iam, N. Makul, Utilization of high volumes of unprocessed lignite-coal fly ash and rice husk ash in self-consolidating concrete, *Journal of Cleaner Production*. 78 (2014) 184–194. <https://doi.org/10.1016/j.jclepro.2014.04.060>.
- [38] B. Sabir, S. Wild, J. Bai, Metakaolin and calcined clays as pozzolans for concrete: A review, *Cement and Concrete Composites*. 23 (2001) 441–454. [https://doi.org/10.1016/S0958-9465\(00\)00092-5](https://doi.org/10.1016/S0958-9465(00)00092-5).
- [39] R. Siddique, J. Klaus, Influence of metakaolin on the properties of mortar and concrete: A review, *Applied Clay Science*. 43 (2009) 392–400.  
<https://doi.org/10.1016/j.clay.2008.11.007>.

- [40] N.J. Coleman, W.R. Mcwhinnie, The solid state chemistry of metakaolin-blended ordinary Portland cement, *Journal of Materials Science*. 35 (2000) 2701–2710. <https://doi.org/10.1023/A:1004753926277>.
- [41] P. Dinakar, P.K. Sahoo, G. Sriram, Effect of Metakaolin Content on the Properties of High Strength Concrete, *International Journal of Concrete Structures and Materials*. 7 (2013) 215–223. <https://doi.org/10.1007/s40069-013-0045-0>.
- [42] V. Kannan, K. Ganesan, Mechanical and transport properties in ternary blended self compacting concrete with metakaolin and fly ash, *IOSR Journal of Mechanical and Civil Engineering (IOSRJMCE)*, ISBN. (2012) 1684–2278.
- [43] R.D. Moser, A.R. Jayapalan, V.Y. Garas, K.E. Kurtis, Assessment of binary and ternary blends of metakaolin and Class C fly ash for alkali-silica reaction mitigation in concrete, *Cement and Concrete Research*. 40 (2010) 1664–1672. <https://doi.org/10.1016/j.cemconres.2010.08.006>.
- [44] V.Y. Garas, K.E. Kurtis, Assessment of methods for optimising ternary blended concrete containing metakaolin, *Magazine of Concrete Research*. 60 (2008) 499–510. <https://doi.org/10.1680/macrc.2007.00095>.
- [45] S. Sujjavanich, P. Suwanvitaya, D. Chaysuwan, G. Heness, Synergistic effect of metakaolin and fly ash on properties of concrete, *Construction and Building Materials*. 155 (2017) 830–837. <https://doi.org/10.1016/j.conbuildmat.2017.08.072>.
- [46] E. Güneyisi, M. Gesoğlu, Properties of self-compacting mortars with binary and ternary cementitious blends of fly ash and metakaolin, *Materials and Structures/Materiaux et Constructions*. 41 (2008) 1519–1531. <https://doi.org/10.1617/s11527-007-9345-7>.
- [47] Z. Li, Drying shrinkage prediction of paste containing meta-kaolin and ultrafine fly ash for developing ultra-high performance concrete, *Materials Today Communications*. 6 (2016) 74–80. <https://doi.org/10.1016/j.mtcomm.2016.01.001>.
- [48] D. Zhang, P. Han, Q. Yang, M. Mao, Shrinkage Effects of Using Fly Ash instead of Fine Aggregate in Concrete Mixtures, *Advances in Materials Science and Engineering*. 2020 (2020). <https://doi.org/10.1155/2020/2109093>.
- [49] L. Wu, N. Farzadnia, C. Shi, Z. Zhang, H. Wang, Autogenous shrinkage of high performance concrete: A review, *Construction and Building Materials*. 149 (2017) 62–75. <https://doi.org/10.1016/j.conbuildmat.2017.05.064>.
- [50] S.A. Kristiawan, M.T.M. Aditya, Effect of high volume fly ash on shrinkage of self-compacting concrete, *Procedia Engineering*. 125 (2015) 705–712. <https://doi.org/10.1016/j.proeng.2015.11.110>.
- [51] E. Ghafari, S.A. Ghahari, H. Costa, E. Júlio, A. Portugal, L. Durães, Effect of supplementary cementitious materials on autogenous shrinkage of ultra-high performance concrete, *Construction and Building Materials*. 127 (2016) 43–48. <https://doi.org/10.1016/j.conbuildmat.2016.09.123>.

- [52] S. Cheng, Z. Shui, T. Sun, R. Yu, G. Zhang, Durability and microstructure of coral sand concrete incorporating supplementary cementitious materials, *Construction and Building Materials*. 171 (2018) 44–53. <https://doi.org/10.1016/j.conbuildmat.2018.03.082>.
- [53] Z. Guo, T. Jiang, J. Zhang, X. Kong, C. Chen, D.E. Lehman, Mechanical and durability properties of sustainable self-compacting concrete with recycled concrete aggregate and fly ash, slag and silica fume, *Construction and Building Materials*. 231 (2020) 117115. <https://doi.org/10.1016/j.conbuildmat.2019.117115>.
- [54] X. Hu, C. Shi, Z. Shi, B. Tong, D. Wang, Early age shrinkage and heat of hydration of cement-fly ash-slag ternary blends, *Construction and Building Materials*. 153 (2017) 857–865. <https://doi.org/10.1016/j.conbuildmat.2017.07.138>.
- [55] S. Cheng, Z. Shui, T. Sun, Y. Huang, K. Liu, Effects of seawater and supplementary cementitious materials on the durability and microstructure of lightweight aggregate concrete, *Construction and Building Materials*. 190 (2018) 1081–1090. <https://doi.org/10.1016/j.conbuildmat.2018.09.178>.
- [56] A.K. Saha, M.N.N. Khan, P.K. Sarker, F.A. Shaikh, A. Pramanik, The ASR mechanism of reactive aggregates in concrete and its mitigation by fly ash: A critical review, *Construction and Building Materials*. 171 (2018) 743–758. <https://doi.org/10.1016/j.conbuildmat.2018.03.183>.
- [57] M. Zhang, W. Zhang, F. Xie, Experimental study on ASR performance of concrete with nano-particles, *Journal of Asian Architecture and Building Engineering*. 18 (2019) 3–9. <https://doi.org/10.1080/13467581.2019.1582420>.
- [58] F.L. Costa, A.S. Torres, R.A. Neves, Analysis of concrete structures deteriorated by alkali-aggregate reaction: case study, *Journal of Building Pathology and Rehabilitation*. 1 (2016) 1–8. <https://doi.org/10.1007/s41024-016-0016-3>.
- [59] J. Cassiani, M. Dugarte, G. Martinez-Arguelles, Evaluation of the chemical index model for predicting supplementary cementitious material dosage to prevent the alkali-silica reaction in concrete, *Construction and Building Materials*. 275 (2021) 122158. <https://doi.org/10.1016/j.conbuildmat.2020.122158>.
- [60] D. Xuan, P. Tang, C.S. Poon, Effect of casting methods and SCMs on properties of mortars prepared with fine MSW incineration bottom ash, *Construction and Building Materials*. 167 (2018) 890–898. <https://doi.org/10.1016/j.conbuildmat.2018.02.077>.
- [61] S. Oruji, N.A. Brake, R.K. Guduru, L. Nalluri, Ö. Günaydın-Şen, K. Kharel, S. Rabbanifar, S. Hosseini, E. Ingram, Mitigation of ASR expansion in concrete using ultra-fine coal bottom ash, *Construction and Building Materials*. 202 (2019) 814–824. <https://doi.org/10.1016/j.conbuildmat.2019.01.013>.
- [62] M. Mahyar, S.T. Erdoğan, M. Tokyay, Extension of the chemical index model for estimating Alkali-Silica reaction mitigation efficiency to slags and natural pozzolans, *Construction and Building Materials*. 179 (2018) 587–597. <https://doi.org/10.1016/j.conbuildmat.2018.05.217>.

- [63] J. Wei, B. Gencturk, A. Jain, M. Hanifehzadeh, Mitigating alkali-silica reaction induced concrete degradation through cement substitution by metakaolin and bentonite, *Applied Clay Science*. 182 (2019). <https://doi.org/10.1016/j.clay.2019.105257>.
- [64] S. Seraj, R. Cano, S. Liu, D. Whitney, D. Fowler, R. Ferron, J. Zhu, M. Juenger, Evaluating the performance of alternative supplementary cementing material in concrete, 2014.
- [65] ASTM C 150/ C150M, Standard Specification for Portland Cement, ASTM International, West Conshohocken, PA. (2017) 1–8. <https://doi.org/10.1520/C0150>.
- [66] ASTM C136/C136M, Standard Test Method for Sieve Analysis of Fine and Coarse Aggregates, West Conshohocken, PA, 2019. 10.1520/C0136\_C0136M-19.
- [67] ASTM Standard C127, Standard Test Method for Relative Density (Specific Gravity) and Absorption of Coarse Aggregate, West Conshohocken, PA, 2015.
- [68] ASTM Standard C128, Standard Test Method for Relative Density (Specific Gravity) and Absorption of Fine Aggregate, ASTM International, West Conshohocken, PA, 2015, 2015.
- [69] K. Folliard, Effects of Texas Fly Ash on Air-Entrainment in Concrete: Comprehensive Report (FHWA/TX-08/0-5207-1), (2009).
- [70] N. Doebelin, R. Kleeberg, Profex: A graphical user interface for the Rietveld refinement program BGMN, *Journal of Applied Crystallography*. 48 (2015) 1573–1580. <https://doi.org/10.1107/S1600576715014685>.
- [71] ASTM C311/C311M, Standard Test Methods for Sampling and Testing Fly Ash or Natural Pozzolans for Use in Portland-Cement Concrete., ASTM International, West Conshohocken, PA. 04.02 (2005) 204–212. <https://doi.org/10.1520/C0311-13.2>.
- [72] ASTM C1437, Test method for slump of hydraulic cement concrete, ASTM International, West Conshohocken, PA. (2005) 12–15. <https://doi.org/10.1520/C1437-15.2>.
- [73] ASTM Standard C511, Standard Specification for Mixing Rooms, Moist Cabinets, Moist Rooms, and Water Storage Tanks Used in the Testing of Hydraulic Cements and Concretes, 2019. <https://doi.org/10.1520/C0511-09.2>.
- [74] ASTM C109/109M, Standard Test Method for Compressive Strength of Hydraulic Cement Mortars (Using 2-in. or [50-mm] Cube Specimens)1, ASTM International West Conshohocken, PA. 32 (2016) 1–10. <https://doi.org/10.1520/C0109>.
- [75] P. Suraneni, A. Hajibabae, S. Ramanathan, Y. Wang, J. Weiss, New insights from reactivity testing of supplementary cementitious materials, *Cement and Concrete Composites*. 103 (2019) 331–338. <https://doi.org/10.1016/j.cemconcomp.2019.05.017>.
- [76] Louisiana Department of Transportation and Development, Louisiana Standard Specification for Roads and Bridges, State of Louisiana Department of Transportation and Development, Baton Rouge, Louisiana. (2016).
- [77] ASTM Standard C143/ C143M, Standard Test Method for Slump of Hydraulic-Cement

- Concrete, ASTM International, West Conshohocken, PA. (2015) 12–15. <https://doi.org/10.1520/C0143>.
- [78] ASTM Standard C231 / C231M-17a, Standard Test Method for Air Content of Freshly Mixed Concrete by the Pressure Method, ASTM International, West Conshohocken, PA, 2017.
- [79] ACI Committee 212, ACI 212.3 R-16 Report on Chemical Admixtures for Concrete, 2016.
- [80] ASTM C39/C39M, Standard Test Method for Compressive Strength of Cylindrical Concrete Specimens, ASTM International, West Conshohocken, PA. (2016) 1–7. <https://doi.org/10.1520/C0039>.
- [81] Y.Y. Kim, K.M. Lee, J.W. Bang, S.J. Kwon, Effect of W/C ratio on durability and porosity in cement mortar with constant cement amount, *Advances in Materials Science and Engineering*. 2014 (2014). <https://doi.org/10.1155/2014/273460>.
- [82] T. Ishida, K. Maekawa, Modeling of durability performance of cementitious materials and structures based on thermo-hygro physics, in: *Rilem Proceedings PRO*, 2003: pp. 39–49.
- [83] T. Ishida, K. Maekawa, T. Kishi, Enhanced modeling of moisture equilibrium and transport in cementitious materials under arbitrary temperature and relative humidity history, *Cement and Concrete Research*. 37 (2007) 565–578.
- [84] H. Layssi, P. Ghods, A.R. Alizadeh, M. Salehi, Electrical Resistivity of Concrete: Concepts, applications, and measurement techniques, *Concrete International*. (2015) 41–46.
- [85] ASTM Standard C157/ C157M, Standard Test Method for Length Change of Hardened Hydraulic-Cement Mortar and Concrete, ASTM International, West Conshohocken, PA. (2017) 7. <https://doi.org/10.1520/C0157>.
- [86] ASTM Standard C192/C192M, Standard Practice for Making and Curing Concrete Test Specimens in the Laboratory, 2016. <https://doi.org/10.1520/C0192>.
- [87] ASTM C1567-21, Standard Test Method for Determining the Potential Alkali-Silica Reactivity of Combinations of Cementitious Materials and Aggregate (Accelerated Mortar-Bar Method), West Conshohocken, PA, 2021.
- [88] ASTM 305, Standard Practice for Mechanical Mixing of Hydraulic Cement Pastes and Mortars of Plastic Consistency, West Conshohocken, PA, 2020.
- [89] S.W.M. Supit, F.U.A. Shaikh, P.K. Sarker, Effect of ultrafine fly ash on mechanical properties of high volume fly ash mortar, *Construction and Building Materials*. 51 (2014) 278–286. <https://doi.org/10.1016/j.conbuildmat.2013.11.002>.
- [90] ASTM C618, Standard Specification for Coal Fly Ash and Raw or Calcined Natural Pozzolan for Use in Concrete, ASTM International, West Conshohocken, PA. (2019) 3–6. <https://doi.org/10.1520/C0618>.
- [91] B. Łązniewska-Piekarczyk, The methodology for assessing the impact of new generation



- superplasticizers on air content in self-compacting concrete, *Construction and Building Materials*. 53 (2014) 488–502. <https://doi.org/10.1016/j.conbuildmat.2013.11.092>.
- [92] S. Wild, J.M. Khatib, A. Jones, RELATIVE STRENGTH, POZZOLANIC ACTIVITY AND CEMENT HYDRATION IN SUPERPLASTICIZED METAKAOLIN CONCRETE, *Cement and Concrete Research*. 26 (1996) 1537–1544.
- [93] C.S. Poon, L. Lam, S.C. Kou, Y.L. Wong, R. Wong, Rate of pozzolanic reaction of metakaolin in high-performance cement pastes, *Cement and Concrete Research*. 31 (2001) 1301–1306. [https://doi.org/10.1016/S0008-8846\(01\)00581-6](https://doi.org/10.1016/S0008-8846(01)00581-6).
- [94] A.A. Ramezani-pour, *Cement Replacement Materials: Properties, Durability, Sustainability*, 2014. <https://doi.org/10.1007/978-3-642-36721-2>.
- [95] E. Güneyisi, M. Gesoğlu, S. Karaoğlu, K. Mermerdaş, Strength, permeability and shrinkage cracking of silica fume and metakaolin concretes, *Construction and Building Materials*. 34 (2012) 120–130. <https://doi.org/10.1016/j.conbuildmat.2012.02.017>.
- [96] G.C. Isaia, A.L.G. Gastaldini, R. Moraes, Physical and pozzolanic action of mineral additions on the mechanical strength of high-performance concrete, *Cement and Concrete Composites*. 25 (2003) 69–76. [https://doi.org/10.1016/S0958-9465\(01\)00057-9](https://doi.org/10.1016/S0958-9465(01)00057-9).
- [97] F. Deschner, F. Winnefeld, B. Lothenbach, S. Seufert, P. Schwesig, S. Dittrich, F. Goetz-Neunhoeffler, J. Neubauer, Hydration of Portland cement with high replacement by siliceous fly ash, *Cement and Concrete Research*. 42 (2012) 1389–1400. <https://doi.org/10.1016/j.cemconres.2012.06.009>.

## APPENDIX A: STATISTICAL ANALYSIS OF CONCRETE CYLINDERS COMPRESSIVE STRENGTH (BINARY SYSTEM)

Table A1. Binary concrete mixtures cylinders 28 days compressive strength one-way ANOVA results

Source	DF	Sum of Squares	Mean Square	F Value	Pr > F
Model	12	4789.69	399.14	114.29	<.0001
Error	26	90.80	3.492		
Corrected Total	38	4880.49			

### Compressive\_Strength\_MPa Tukey Grouping for Means of Percent\_Cement\_Replacement (Alpha = 0.05)

Means covered by the same bar are not significantly different.

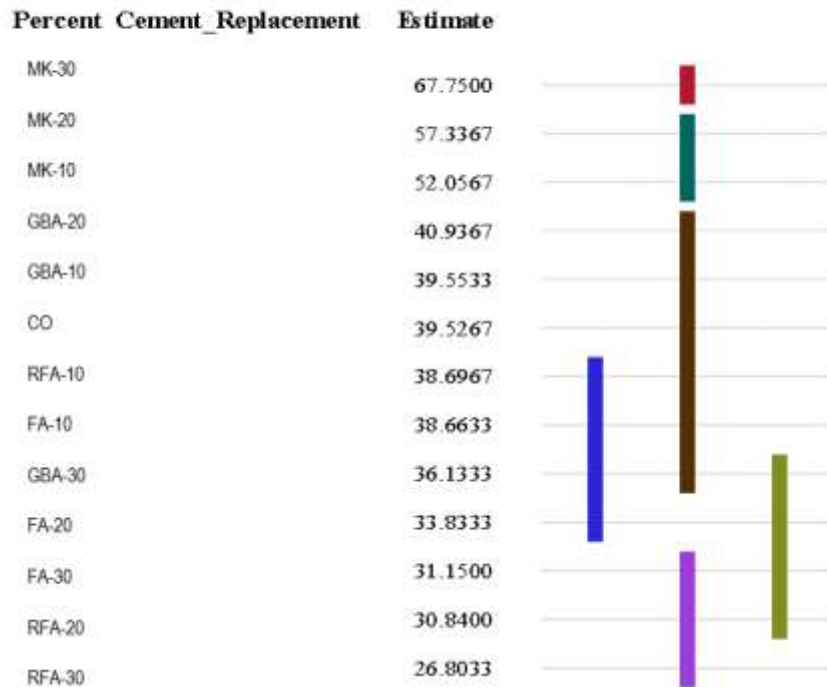


Figure A1. Binary concrete mixtures cylinders 28 days compressive strength Tukey grouping for means of index ( $\alpha=0.05$ )

Table A2. Binary concrete mixtures cylinders 90 days compressive strength one-way ANOVA results

Source	DF	Sum of Squares	Mean Square	F Value	Pr > F
Model	12	2338.40	194.86	24.32	<.0001
Error	26	208.30	8.01		
Corrected Total	38	2546.70			

Compressive\_Strength\_MPa Tukey Grouping for Means of Percent\_Cement\_Replacement (Alpha = 0.05)  
 Means covered by the same bar are not significantly different.

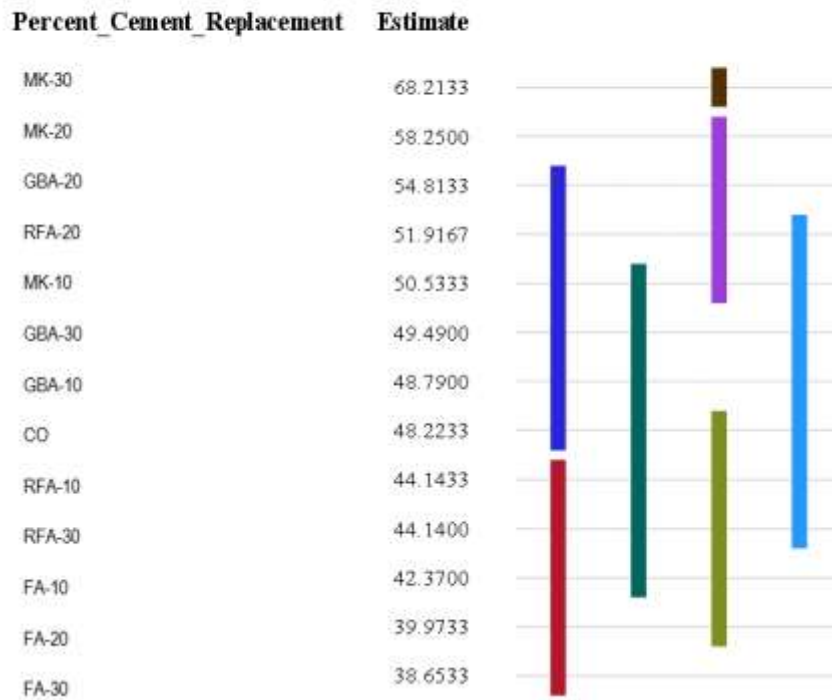


Figure A2. Binary concrete mixtures cylinders 90 days compressive strength Tukey grouping for means of index ( $\alpha=0.05$ )

## APPENDIX B: STATISTICAL ANALYSIS OF CONCRETE CYLINDERS COMPRESSIVE STRENGTH (TERNARY SYSTEM)

Table B1. Ternary concrete mixture cylinders 28 days compressive strength one-way ANOVA results

Source	DF	Sum of Squares	Mean Square	F Value	Pr > F
Model	6	220.66	36.77	12.19	<.0001
Error	14	42.22	3.02		
Corrected Total	20	262.89			

### Compressive\_Strength\_MPa Tukey Grouping for Means of Percent\_Cement\_Replacement (Alpha = 0.05)

Means covered by the same bar are not significantly different.

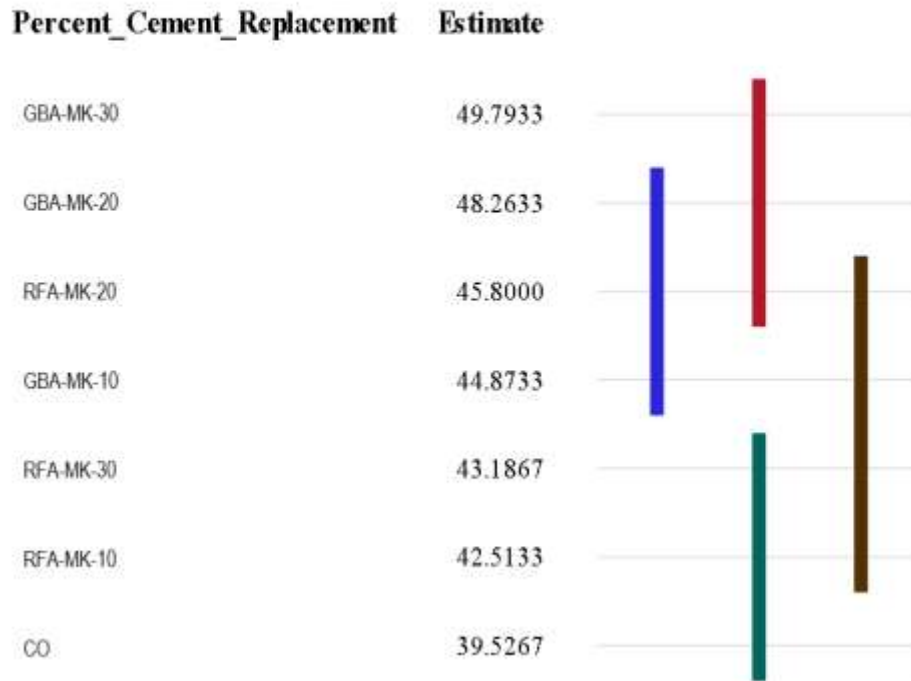


Figure B1. Ternary concrete mixtures cylinders 28 days compressive strength Tukey grouping for means of index ( $\alpha=0.05$ )

Table B2. Ternary concrete mixture cylinders 90 days compressive strength one-way ANOVA results

Source	DF	Sum of Squares	Mean Square	F Value	Pr > F
Model	6	79.36	13.23	3.89	0.0169
Error	14	47.55	3.39		
Corrected Total	20	126.91			

**Compressive\_Strength\_MPa Tukey Grouping for Means of Percent\_Cement\_Replacement (Alpha = 0.05)**

Means covered by the same bar are not significantly different.

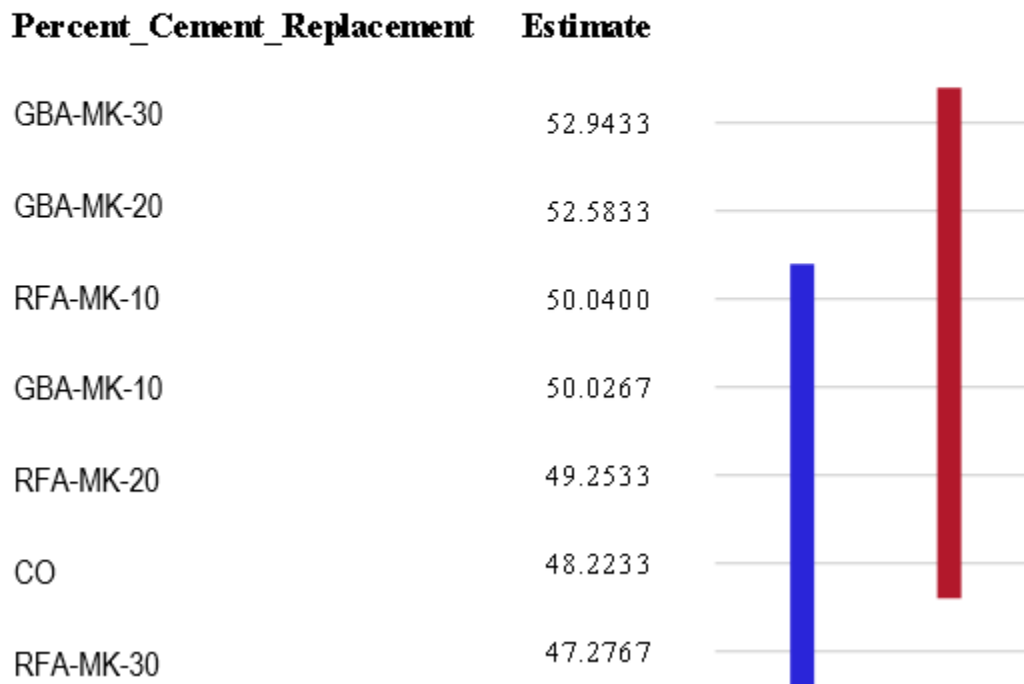


Figure B2. Ternary concrete mixtures cylinders 90 days compressive strength Tukey grouping for means of index ( $\alpha=0.05$ )

## APPENDIX C: STATISTICAL ANALYSIS OF CONCRETE CYLINDERS SURFACE RESISTIVITY (BINARY SYSTEM)

Table C1. Binary concrete mixtures cylinders 28 days surface resistivity one-way ANOVA results

Source	DF	Sum of Squares	Mean Square	F Value	Pr > F
Model	12	32658.65771	2721.55481	574.84	<.0001
Error	26	123.09547	4.73444		
Corrected Total	38	32781.75317			

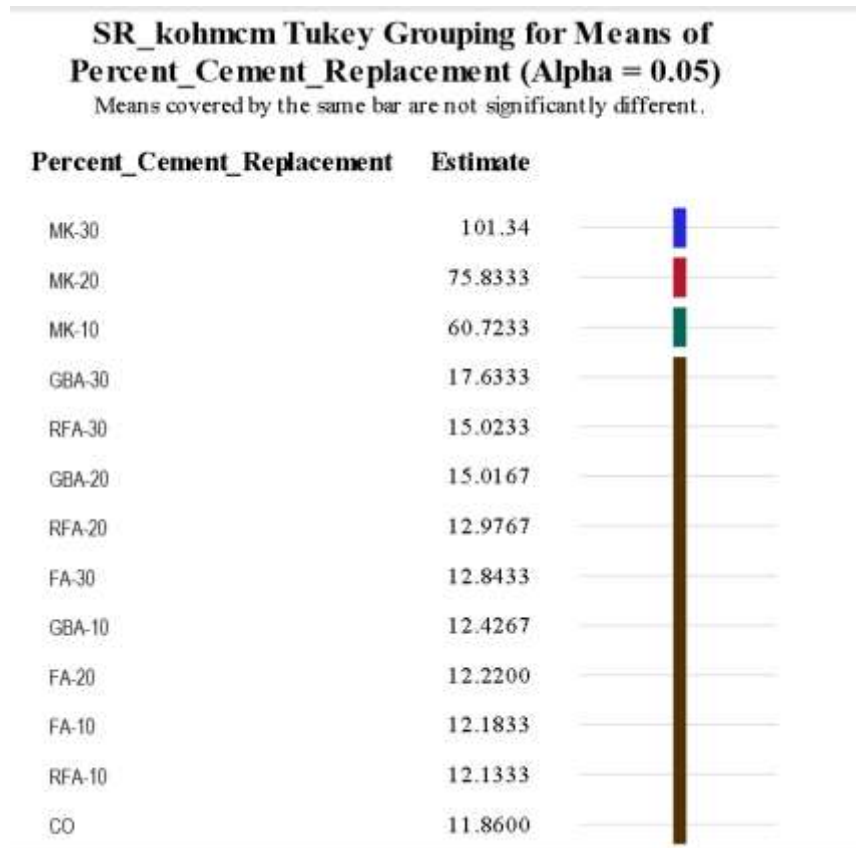


Figure C1. Binary concrete mixtures cylinders 28 days surface resistivity Tukey grouping for means of index ( $\alpha=0.05$ )

Table C2. Binary concrete mixtures cylinders 90 days surface resistivity one-way ANOVA results

Source	DF	Sum of Squares	Mean Square	F Value	Pr > F
Model	12	127714.59	10642.88	1155.82	<.0001
Error	26	239.401	9.21		
Corrected Total	38	127953.99			

**SR\_kohmcm Tukey Grouping for Means of Percent\_Cement\_Replacement (Alpha = 0.05)**

Means covered by the same bar are not significantly different.

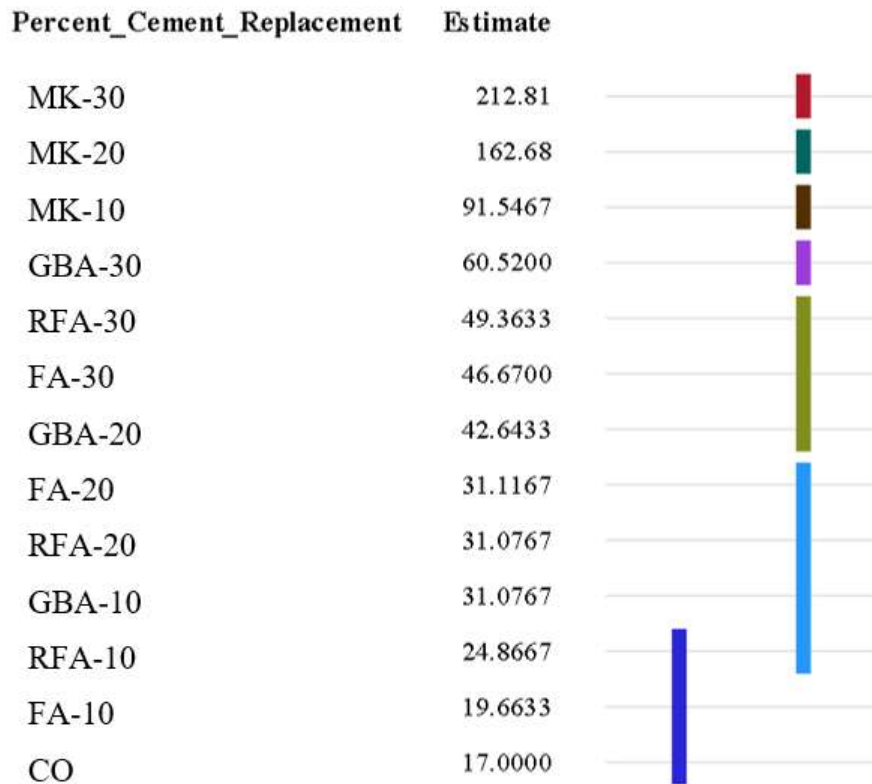


Figure C2. Binary concrete mixtures cylinders 90 days surface resistivity Tukey grouping for means of index ( $\alpha=0.05$ )





## APPENDIX D: STATISTICAL ANALYSIS OF CONCRETE CYLINDERS SURFACE RESISTIVITY (TERNARY SYSTEM)

Table D1. Ternary concrete mixtures cylinders 28 days surface resistivity one-way ANOVA results

Source	DF	Sum of Squares	Mean Square	F Value	Pr > F
Model	6	7381.36	1230.23	317.11	<.0001
Error	14	54.31	3.88		
Corrected Total	20	7435.68			

**SR\_kohmcm Tukey Grouping for Means of Percent\_Cement\_Replacement (Alpha = 0.05)**  
Means covered by the same bar are not significantly different.

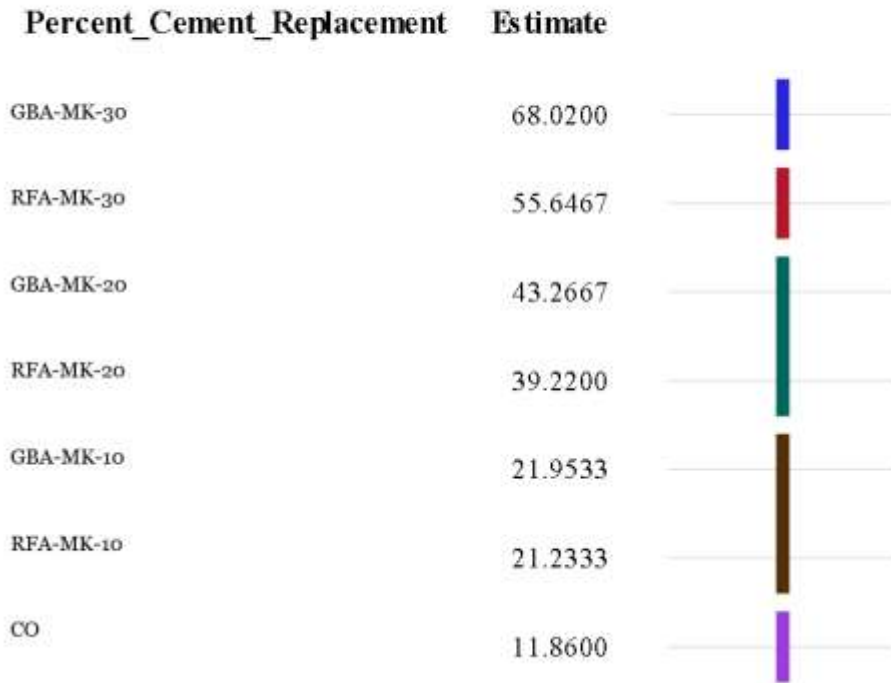


Figure D1. Ternary concrete mixtures cylinders 28 days surface resistivity Tukey grouping for means of index ( $\alpha=0.05$ )

Table D2. Ternary concrete mixtures cylinders 90 days surface resistivity one-way ANOVA results

Source	DF	Sum of Squares	Mean Square	F Value	Pr > F
Model	6	21808.60	3634.77	236.62	<.0001
Error	14	215.06	15.36		
Corrected Total	20	22023.66			

**SR\_kohmcm Tukey Grouping for Means of Percent\_Cement\_Replacement (Alpha = 0.05)**

Means covered by the same bar are not significantly different.

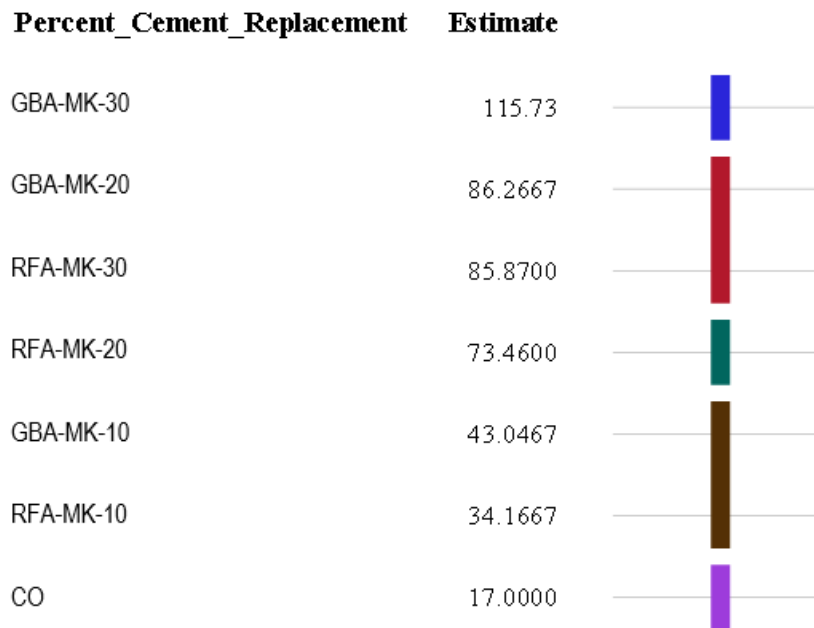


Figure D2. Ternary concrete mixtures cylinders 90 days surface resistivity Tukey grouping for means of index ( $\alpha=0.05$ )